U.S. DEPARTMENT OF COMMERCE
National Technical Information Service

PB-291 314

Combustion Research on Characterization of Particulate Organic Matter from Flames

Massachusetts Inst of Tech, Cambridge

Prepared for

Industrial Environmental Research Lab, Research Triangle Park, NC

Aug 78

United States
Environmental Protection
Agency

Industrial Environmental Research
Laboratory
Research Triangle Park NC 27711

EPA-600/7-78-167
August 1978

EPA

Combustion Research on Characterization of Particulate Organic Matter from Flames

PB 291314

JAN 10 80

Interagency Energy/Environment R&D Program Report

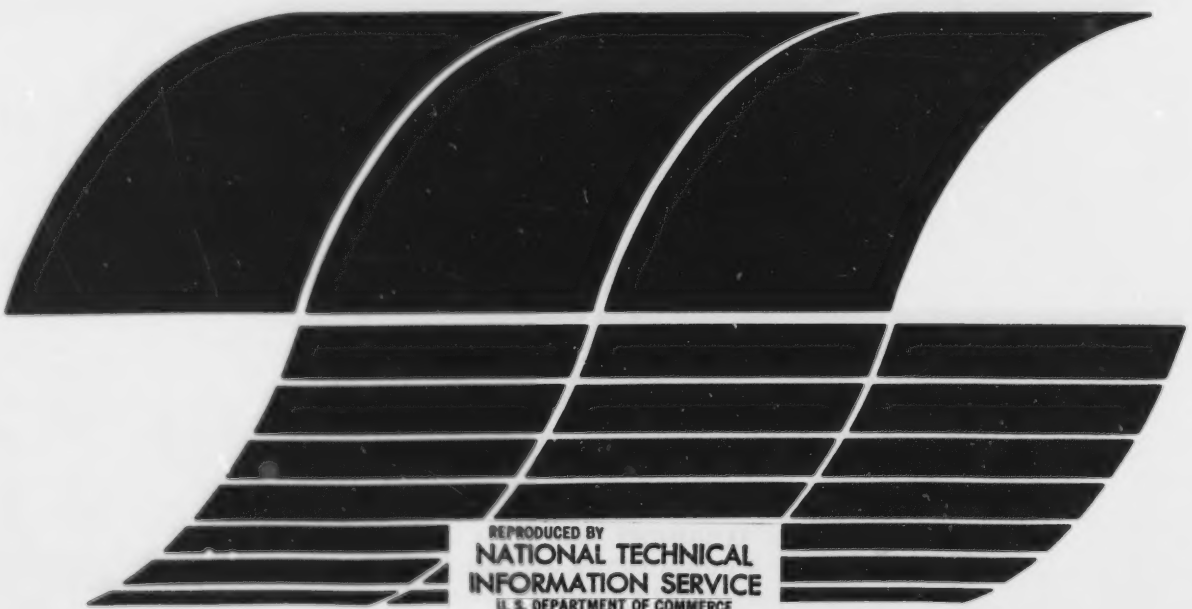

TECHNICAL REPORT DATA (Please read Instructions on the reverse before completing)		
1. REPORT NO. EPA-600/7-78-167	2.	3. RECIPIENT'S ACCESSION NO. PB291314
4. TITLE AND SUBTITLE Combustion Research on Characterization of Particulate Organic Matter from Flames		5. REPORT DATE August 1978 6. PERFORMING ORGANIZATION CODE
7. AUTHOR(S) R. A. Hites and J. B. Howard		8. PERFORMING ORGANIZATION REPORT NO.
9. PERFORMING ORGANIZATION NAME AND ADDRESS Massachusetts Institute of Technology Department of Chemical Engineering Cambridge, Massachusetts 02139		10. PROGRAM ELEMENT NO. EHE624A 11. CONTRACT/GRANT NO. Grant R803242, Task 1
12. SPONSORING AGENCY NAME AND ADDRESS EPA, Office of Research and Development Industrial Environmental Research Laboratory Research Triangle Park, NC 27711		13. TYPE OF REPORT AND PERIOD COVERED Task Final; 8/74-8/77 14. SPONSORING AGENCY CODE EPA/600/13

15. SUPPLEMENTARY NOTES IERL-RTP project officer is John H. Wasser, Mail Drop 65, 919/541-2476.

16. ABSTRACT The report gives results of a study of the formation and emission of soot and polycyclic aromatic hydrocarbons (PAH) from both laminar flames and a turbulent continuous-flow combustor. Decreasing the atomizing pressure decreased the amount of soot and PAH produced in the latter system. Benzene fuel gave more soot and PAH than did kerosene, and the PAH from benzene were more substituted. Nitrogen- and sulfur-doped fuels did not affect total soot production. The distribution of soot and PAH within the flame was consistent with the concept that certain PAH may serve as intermediates in soot formation. The PAH formed during combustion of coal, wood, and kerosene were separated and identified by capillary column gas chromatography and mass spectrometry. The PAH from coal combustion were found to be similar to airborne PAH from Indianapolis, a high coal consumption area; those from kerosene combustion were similar to airborne PAH from Boston, an area of low coal consumption and high consumption of petroleun derived fuels. Nitrogen containing fuels primarily produce polycyclic aromatic compounds in which the nitrogen is in a cyano substituent (approximately 70%). This contrasts with the observation that nitrogen heterocyclic compounds are the major nitrogen containing compounds in airborne particulate matter.

17. KEY WORDS AND DOCUMENT ANALYSIS

a. DESCRIPTORS		b. IDENTIFIERS/OPEN ENDED TERMS	c. COSATI Field/Group
Pollution	Aromatic Polycyclic Hydrocarbons	Pollution Control	13B
Combustion		Stationary Sources	21B
Research	Benzene	Particulate	14B
Flames	Kerosene		21D
Properties	Coal		
Organic Compounds	Wood		07C 11L
Soot	Nitrogen		07B

18. DISTRIBUTION STATEMENT	19. SECURITY CLASS (This Report)	21. NO. OF PAGES
Unlimited	Unclassified	94
	20. SECURITY CLASS (This page) Unclassified	22. PRICE PC A05/MF A01

EPA Form 2220-1 (9-73)

EPA-600/7-78-167
August 1978

Combustion Research on Characterization of Particulate Organic Matter from Flames

by

R.A. Hites and J.B. Howard

Massachusetts Institute of Technology
Department of Chemical Engineering
Cambridge, Massachusetts 02139

Grant No. R803242
Task No. 1
Program Element No. EHE624A

EPA Project Officer: John H. Wasser

Industrial Environmental Research Laboratory
Office of Energy, Minerals, and Industry
Research Triangle Park, NC 27711

Prepared for

U.S. ENVIRONMENTAL PROTECTION AGENCY
Office of Research and Development
Washington, DC 20460

ABSTRACT

The formation and emission of soot and polycyclic aromatic hydrocarbons (PAH) from both laminar flames and a turbulent continuous flow combustor were studied. The amount of soot and PAH produced in the latter system was diminished by a decrease in the atomizing air pressure. Benzene fuel gave more soot and PAH than did kerosene, and the PAH from benzene were more substituted. Nitrogen and sulfur doped fuels did not affect total soot production. The distribution of soot and PAH within the flame was consistant with the concept that certain PAH may serve as intermediates in soot formation.

The PAH formed during combustion of coal, wood, and kerosene were separated and identified by capillary column gas chromatography and mass spectrometry. The PAH from coal combustion were found to be similar to airborne PAH from Indianapolis, a high coal consumption area, while the PAH from kerosene combustion were similar to airborne PAH from Boston, an area of low coal consumption and high consumption of petroleum derived fuels.

Mixed charge exchange chemical ionization mass spectrometry allows the differentiation of PAH isomers on the basis of ionization potential. This method may be able to predict the mass spectra of presently unidentifiable isomers.

GC-MS analysis of carbon blacks found a wide range of PAH including sulfur containing aromatics which had not previously been identified in carbon blacks. The quantity of PAH was somewhat dependent on conditions of formation.

Nitrogen containing fuels primarily produce polycyclic aromatic compounds in which the nitrogen is in a cyano substituent (approximately 70%). This contrasts with the observation that nitrogen heterocyclic compounds are the major nitrogen containing compounds in airborne particulate matter.

This report was submitted in fulfillment of Grant No. R803242 by the Massachusetts Institute of Technology under the sponsorship of the U.S. Environmental Protection Agency. This report covers the period August 1, 1974 to July 31, 1977, and work was completed as of September 30, 1978.

CONTENTS

Abstract ii

Overview 1

Appendices

A. Soot and Hydrocarbon Formation in a Turbulent Diffusion Flame 5

B. Formation of Soot and Polycyclic Aromatic Hydrocarbons in Combustion Systems 19

C. Soot Concentration Measurements in Fuels Doped with Nitrogen and Sulfur Containing Compounds 41

D. Source Identification of Urban Airborne Polycyclic Aromatic Hydrocarbons by Gas Chromatographic Mass Spectrometry and High Resolution Mass Spectrometry 64

E. Mixed Charge Exchange-Chemical Ionization Mass Spectrometry of Polycyclic Aromatic Hydrocarbons 70

F. Charge Exchange-Chemical Ionization of Polycyclic Aromatic Compounds 72

G. Characterization of Sulfur-Containing Polycyclic Aromatic Compounds in Carbon Blacks 76

H. Cyano-Aromatic Compounds Produced by the Combustion of Nitrogen Containing Fuels 81

FIGURES

Number		Page
A-1	Water-flushed soot sampling probe	7
A-2	Influence of atomizing-air pressure on axial profile of soot mass loading (cold gas velocity = 0.96 m/s)	9
A-3	Influence of atomizing-air pressure on axial profile of soot mass loading (cold gas velocity = 2.67 m/s)	9
A-4	Influence of atomizing-air pressure on axial profile of PCAH mass loading	10
A-5	Influence of the type of fuel on axial profile of soot mass loading	10
A-6	Influence of the type of fuel on axial profile of PCAH mass loading	10
B-1	Summary of proposed mechanisms of soot formation	23
B-2	Molecular beam mass spectrometer system	25
B-3	Schematic of mass spectrometer instrumentation	27
B-4	Schematic of gas introduction system for studying mass discrimination	29
B-5	Profiles of signal intensities relative to argon for major stable species in an acetylene-oxygen flame near the sooting limit	34
B-6	Profiles of signal intensities relative to argon for minor species in an acetylene-oxygen flame near the sooting limit	35
C-1	Overall experimental arrangements	44
C-2	Burner details	45
C-3	Water-cooled sampling probe	47
C-4	Variation of soot concentration with height above burner for each of four additives in benzene	48
C-5	Variation of soot concentration with height above burner for pyridine additive in benzene	51
C-6	Variation of soot concentration with height above burner for pyrrole additive in benzene	52
C-7	Variation of soot concentration with height above burner for thiophene additive in benzene	53
C-8	Variation of soot concentration with height above burner for carbon disulfide additive in benzene	54
C-9	Variation of soot concentration with height above burner for pure methane fuel with no additive	56

Figures (Continued)

Number		Page
C-10	Variation of soot concentration with height above burner for thiophene and pyrrole additive in hexane	57
C-11	Variation in soot concentration with height above burner for each of three additives in benzene and a lower equivalence ratio	58
D-1	Capillary-column gas chromatogram of the PAH fraction of coal combustion products	67
D-2	Capillary-column gas chromatogram of the PAH fraction of wood combustion products	67
D-3	Capillary-column gas chromatogram of the PAH fraction of kerosene combustion products	68
D-4	Alkyl homolog distribution plots for several PAH series in coal combustion products	69
D-5	Alkyl homolog distribution plots for the pyrene-type series in the combustion products of coal, wood, and kerosene, and in air particulate matter from Indianapolis and Boston	69
D-6	Composite alkyl homolog distribution plots for PAH in the combustion products of coal, wood, and kerosene, and in air particulate matter from Indianapolis and Boston	69
E-1	Plot of the abundance ratio obtained by CH_4-Ar chemical ionization mass spectrometry as a function of ionization potential for a series of four tetracyclic polycyclic aromatic hydrocarbons	71
G-1	Compounds identified in carbon blacks by GC/MS and HRMS	77
G-2	Packed-column gas chromatograms of furnace black 1 and furnace black 3	79
G-3	Glass capillary-column gas chromatogram of the extract of furnace black 1	80
H-1	Gas chromatograms of fraction 3, isolated from organic compounds produced by combustion of solution of 32% pyridine in o-xylene	84

TABLES

Number		Page
A-I	Effect of Injected Water on Gas Composition	8
A-II	Computed and Experimental Soot Mass Loading	11
A-III	Polycyclic Aromatic Hydrocarbons in the Combustion Products of Kerosene and Benzene	12
A-IV	Distribution of PCAH for Kerosene and Benzene Fuel Along the Burner Axis	13
A-V	Arithmetic Mean Particle Diameter (Kerosene and Benzene; Cold Gas Velocity = 0.96 m/s)	14
A-VI	Arithmetic Mean Particle Diameter (Kerosene; Cold Gas Velocity = 2.67 m/s)	14
B-I	Masses at Which Signals Were Observed but Positive Identifications Were Not Made	37
B-II	Additional Species Near the End of the Reaction Zone in a C_2H_2/O_2 Flame	39
C-1	Information on Benzene and Additives	50
D-1	PAH Identified by G.C.M.S.	68
E-I	Abundance Ratios for Selected PAH Obtained by CH_4-Ar Chemical Ionization Mass Spectrometry	71
F-1	Some of the Polycyclic Aromatic Compounds Investigated	74
G-I	Carbon Black Characteristics	79
H-I	Fractionation of Soot Extracts	83
H-II	Mass Spectra of Peaks 1-7 in EI and CE/CI Modes	84

OVERVIEW

Polycyclic aromatic hydrocarbons (PAH) are ubiquitous in the environment. Many specific PAH have been found to be carcinogenic in animals. Since PAH are present in small particulates, they are potentially extremely dangerous to human health since they can easily be inhaled deep in the respiratory system. Consequently PAH are highly suspect in the relationship of lung cancer and atmospheric pollution.

Since different PAH vary widely in their toxicity and carcinogenic effects, from harmless to extremely hazardous, it is essential to be able to identify the specific PAH in a mixture. Since common sources of PAH contain only minute quantities of many different species, the combination of gas chromatography and mass spectrometry (GC-MS) is extremely well suited to resolving PAH. The mass spectrometer provides identification through empirical formulae and the partial elucidation of major structures. Gas chromatography, since it is very sensitive to shape, allows the separation and quantification of isomers. Unfortunately, one difficulty encountered in exact structure determination is the inability of mass spectrometry to discriminate between isomeric PAH.

Since the major source of airborne PAH is combustion products, variables affecting PAH and soot production in combustion systems may have great effects on airborne pollution. The increased use of aromatic fuels (from coal) and additional controls on NO_x production may result in increased amounts and different distributions of PAH. Knowledge of the variation of PAH production within a flame as well as the mechanism operating in its formation will aid in attempts to limit emission of these compounds.

The general goal of this project has been an improved understanding of the production of soot and PAH in combustion systems. Toward this end, studies on a variety of combustion systems were carried out. The types of combustor were varied as were the fuels; samples were collected and analyzed for PAH. In some cases, improvements in the state-of-the-art analytical tools were required. All of our work has been published in the open literature and these reprints from the body of this report. The following paragraphs are a summary of our work and a guide to the appended reprints.

Soot and PAH formation in a turbulent flame were observed, while parameters such as mixing intensity, fuel equivalence ratio and type of fuel were varied to determine the effects on total mass, composition and size distribution of PAH produced. Lowering the atomizing air pressure resulted in a 10,000 fold increase in soot emission. (Appendix A, Fig. 2). A similar effect was observed in the profile of PAH (Fig. 4). This effect may be attributed to improved mixing of fuel and air with increased pressure. In general, but with some exceptions, more intense mixing and hence increased O_2 consump-

tion in the first section of the flame and decreased combustion in the later portions, results in decreased soot formation.

The presence of anthracene in the fuel has little effect on the amount of soot or PAH formed in the turbulent diffusion flame. (Appendix A, Figs. 5 and 6). However, benzene combustion produced significantly less PAH and soot than the combustion of kerosene. This surprising result was attributed to the flame temperature, and hence the rate of soot burnout, being higher in the benzene case.

The distribution of specific PAH was also studied (Appendix A, Table 3). Both kerosene and benzene showed enrichment of higher molecular weight PAH further from the nozzle. Kerosene produced markedly less PAH containing methyl and phenyl groups. These substituted PAH decreased with increasing distance from the nozzle at a faster rate than did the unsubstituted PAH.

Benzene produced slightly smaller particles of soot than did kerosene. Increased cold gas velocity also produced smaller particles. Both these effects may be caused by a higher flame temperature: the adiabatic flame temperature of benzene is higher than that of kerosene, and higher gas velocities reduce heat loss and raise flame temperature.

These results indicate that poorly maintained combustion sources such as home heating burners may operate under conditions resulting in high soot formation. The use of staged combustion for NO_x emission control may also dramatically increase PAH and soot production, if the first stage is too fuel rich.

A molecular mass beam spectrometer system has been developed for studying molecular distributions within a flame (Appendix B). Aromatic hydrocarbons have been observed under conditions of high soot formation. However, the present sensitivity is too low owing to a high background level of hydrocarbons. This should be improved by the addition of cryogenic pumping in the system to decrease aliphatic hydrocarbons.

Studies were also conducted burning nitrogen and sulfur containing compounds in a combustion system comparable to that used for PAH studies (Appendix C). Fuels containing one percent nitrogen or sulfur were obtained by doping benzene with pyridine, pyrrole, thiophene, or carbon disulfide. Soot production was found to be independent of additives.

Since PAH from different combustion sources differ considerably in type and concentration, a correlation between fuel utilization in an area and composition of air particulate matter would be expected. The airborne PAH of high and low coal burning areas, Indianapolis and Boston, were compared.

PAH emissions from combustion or coal, wood, and kerosene were analyzed by capillary column GC-MS to identify and roughly to quantitate the components (Appendix D). There were several significant differences: (1) there is a greater relative abundance of alkylated PAH in the coal combustion products; (2) higher molecular weight species are relatively more abundant in wood and kerosene combustion products; (3) sulfur containing compounds are present only in the coal soot PAH fraction.

Alkyl homolog plots were constructed for seven groups of isomers (Appendix D, Figure 4). These plots represent the distribution of the alkylated species within a PAH mixture. The curves for the pyrene series show a correlation between the curves for the coal PAH and Indianapolis air particulate PAH, as well as between the kerosene PAH and the Boston sample.

The major differences between coal PAH and Indianapolis PAH are that the concentrations of high molecular weight compounds in soot are higher than those of airborne PAH. This may be due to the sensitivity of these compounds to combustion and collection conditions.

Since the spectra of isomeric PAH are almost identical, GC-MS cannot unequivocally assign structures to many compounds. In charge exchange chemical ionization mass spectrometry, the mass spectra are observed in the presence of argon and methane. The molecule of interest reacts either with an argon ion (Ar^+) or with an ethane carbonium ion ($C_2H_5^+$). The ratio of molecular ions (M^+) and protonated molecular ions ($M + 1^+$) differs for each isomer and can be correlated with the ionization potential (Appendix E). Variations in the ionization potential only affect the rate of ionization by Ar^+ ions, and do not affect the rate of protonation by $C_2H_5^+$. Since ionization potentials can be calculated for a particular isomer from molecular orbital theory, this approach holds promise to identify presently unknown PAH. The correlation also holds for several aromatic nitrogen containing compounds as well as the two sulfur compounds that were available (Appendix F).

Carbon black, a major component of automobile tires, has a wide environmental distribution. GC-MS analysis of four different carbon blacks shows a broad distribution of PAH, somewhat dependent on conditions of formation (Appendix G). The higher temperature of formation of one of the carbon blacks reduced the total PAH by a factor of ten. The distribution of compounds was not affected markedly by conditions of formation, although sulfur analogues of PAH were detected for the first time in carbon blacks produced from sulfur containing petroleum fractions.

Nitrogen containing aromatic compounds (aza-arenes) are produced in combustion of fuels with significant nitrogen contant (Appendix H). Up to this time these compounds have not been widely studied, although they may become important pollutants with the increased use of nitrogen containing fuels. Little is known about the distribution of neutral aza-arenes since the standard analysis procedure only extracts bases. We have used charge exchange chemical ionization mass spectrometry to analyze the neutral aza-arene fraction of compounds produced by the combustion of high nitrogen fuels (Appendix H). The spectra of 1- and 2-cyanonaphthalenes were identified, and confirmed by the use of authentic samples. Other peaks were tentatively identified as isomers of cyanoacenaphthylenes and cyanophenanthrenes. These three classes of compounds accounted for 80% of the aza-arenes in the fraction studied. Nitrogen heterocyclic compounds formed only a minor component (less than 30%). Neutral nitrogen compounds have not been evaluated for biological activity or for environmental effects.

The knowledge gained about the distribution and production of polycyclic

aromatic compounds can promote the effort to control their emissions as well as help evaluate their potential harm.

APPENDIX A

Soot and Hydrocarbon Formation in a Turbulent Diffusion Flame

From: Sixteenth Symposium (International) on Combustion, The Combustion Institute, Pittsburgh, 1977. Reprinted with the permission of the copyright holder.

SOOT AND HYDROCARBON FORMATION IN A TURBULENT DIFFUSION FLAME

G. P. PRADO*, M. L. LEE, R. A. HITES, D. P. HOULT, AND J. B. HOWARD**
Departments of Chemical and Mechanical Engineering, Massachusetts Institute of Technology, Cambridge, Massachusetts.

Formation and emission of soot and polycyclic aromatic hydrocarbons (PCAH) from a turbulent continuous flow combustor have been studied. Measurements included mass concentration of both soot and PCAH, composition of individual PCAH, and size distribution of soot particles, as a function of mixing intensity, fuel equivalence ratio and type of fuel (kerosene or benzene). Both soot and PCAH concentrations reach maxima early in the flame, after which PCAH decays rapidly and soot decays much slower. The maximum PCAH concentration always preceded that of soot in agreement with the concept that certain PCAH may serve as intermediates in soot formation. An approximate calculation based on the assumptions of local equilibrium with respect to soot formation and a Gaussian distribution of air-fuel mixedness gave satisfactory correlations of the data on soot formation at the higher cold gas velocity. At the lower velocity, the amount of soot and PCAH formed was drastically increased and strongly dependent on fuel atomization.

1. Introduction

In gas turbine and most other practical combustors, fuel and air are fed separately and the combustion occurs primarily within a relatively confined region. Turbulent mixing rates in such systems have important effects on emission of pollutants such as nitric oxide, carbon monoxide, soot and polycyclic aromatic hydrocarbons (PCAH). The present investigation was focussed on soot and PCAH formation in a turbulent diffusion flame. The understanding of the formation of these species is important in relation both to flame radiation and to air pollution. Knowledge of the concentration of soot particles is necessary to predict flame emissivities for radiative heat transfer problems. In addition, some PCAH known for their carcinogenic properties are associated with soot particles, and because these small particles are easily injested deep into the respiratory system, they may be one of the types of particulates most hazardous to human health. Also, the NO_x control strategies such as lower-temperature and/or staged combustion presently being considered tend to increase PCAH and soot formation. Use of highly aromatic fuels made from coal would focus increased attention on emissions of particulate organic matter.

In turbulent flames, the nonuniform distribution of fuel in air can be represented as pockets of gas or eddies of different fuel-air ratios, some of which are sufficiently fuel rich to form soot and PCAH while others are fuel lean, compared to the mean. Although the air and fuel eventually may become mixed by molecular diffusion, soot and possibly PCAH emissions will still occur if the rate of mixing is slow enough to allow the amount of such materials formed to exceed that which can be burned out in the residence time available.

In recent studies at M.I.T.[1,2] of the role of turbulent mixing on nitric oxide and carbon monoxide formation, nonuniformities associated with mixing were allowed by either

*On leave from: Centre de Recherches sur la Physico-Chimie des Surfaces Solides, Centre National de la Recherche Scientifique, 24 Avenue du President Kennedy 68200-MULHOUSE, FRANCE.

**To whome correspondence should be sent. Room 66-454, Department of Chemical Engineering, Massachusetts Institute of Technology, Cambridge, Massachusetts 02139.

assuming that burnt gas eddies have a normal distribution of equivalence ratio about the mean value, or by representing the mixing by a large number of fluid "particle" interactions simulated by a random number generator.

The objective of the present work was to study the role of turbulent mixing in the formation of soot and PCAH in the same combustor used previously to characterize nitric oxide and carbon monoxide emissions.

2. Experimental

The burner used in this study is described elsewhere.[2] It is basically a cylindrical burner in which the combustion air is supplied at atmospheric pressure at one end through a 45-degree blade angle swirler. Kerosene or benzene was supplied through an air assist atomizer (De Lavan model 3060-9-11) on the burner axis. The atomizer nozzle air-pressure drop was controlled independently of the fuel flow rate. The atomizer air flow amounted to about 5% of the total air flow.

Gas samples containing soot and PCAH were collected at different flame positions with a stainless steel water-cooled probe (Fig. 1) in which about 1% of the cooling water was injected into the sampled gas at the probe tip in order to quench the reactions and to prevent deposition of soot along the walls. The movable tube permitted control of the amount of water injected into the probe. This design allowed quantitative collection of the soot and condensibles without tedious scraping of the probe after each sample is taken. A similar probe was previously designed and used elsewhere.[4] The sample stream, comprised of water, gases and particulates, passed through a glass fiber filter where the soot and essentially all the PCAH were deposited. The water and gas then passed through a condenser for further cooling, after which the water was collected in a large flask and the gas passed through a wet test meter after flowing through an ice bath condensate trap and vacuum pump. For the preliminary runs, the amount of soot and associated PCAH was determined by weighing the dried filter before and after collection. The filter and soot deposit was then extracted with methylene chloride and the filter was again dried and weighed. The soot was thus classified as carbonaceous residue (referred to as soot in the text) and methylene chloride soluble material. The carbonaceous residue was removed from the filter, dispersed in an ultrasonic bath and deposited on perforated carbon electron microscope grids for particle size distribution analysis. A Philips E.M. 300 microscope, containing an anti-contamination device was used. The size distributions were determined by measuring about 2,000 particles per sample, using a semi-automatic Zeiss particle counter. The reproducibility was about 5% with the same operator, 20% with different operators.

The methylene chloride extract of flame soot was concentrated to a volume of from 0.1 ml to 10 ml, depending on the concentration of organics, and analyzed by gas chromatography. A Perkin-Elmer 3920 gas chromatograph with flame ionization detector and model-1 computing integrator was used for quantitative analysis of individual PCAH. A standard solution consisting of phenanthrene (representative of 3 ring compounds), pyrene (4 rings), perylene (5 rings) and coronene (7 rings) was used for calibration of the integrator, and each chromatographic peak in a sample run was compared to the standard compound with the closest retention time. A 1.83 m (6 ft) × 3.175mm (1/8 in) O.D. stainless steel column packed with 3% OV-17 on 100/120 mesh Gas Chrom Q was used throughout these experiments. After injection of a sample, the

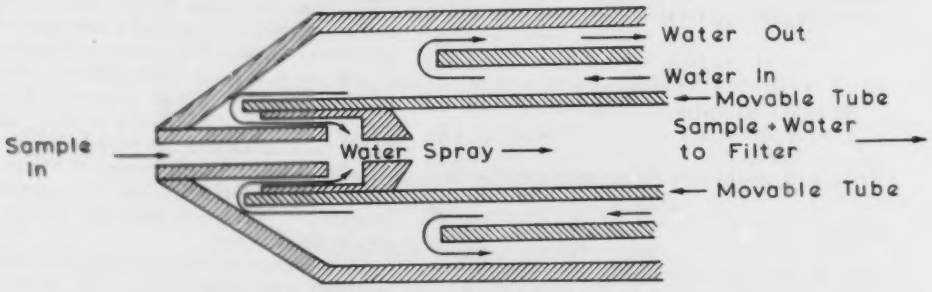

FIG. 1. Water-flushed soot sampling probe.

gas chromatograph was programmed from 70°C to 320°C at the rate of 12°C/min.

Identification of individual compounds was accomplished with a Hewlett-Packard 5982 *A* gas chromatograph/mass spectrometer which is interfaced with an HP 5933 *A* data system. The same gas chromatographic conditions were used as previously described for quantitative measurements. Mass spectral data were automatically acquired during a gas chromatographic run and stored on disc for future interpretation. Structural assignments of individual PCAH were made from mass spectral data and relative gas chromatographic retention as compared with standard compounds.

The separation of phenanthrene and anthracene isomers was accomplished by high resolution gas chromatography using a 19 m × 0.26mm, i.d., glass capillary column coated with SE-52 methylphenyl silicone stationary phase. The column was programmed from 70°C to 170°C at 2°C/min after sample injection.

The reliability of the sampling technique was tested by performing reproducibility tests on the amount of soot collected. The reproducibility was better than ±10% when the sampling time was long enough (10 minutes to one hour depending on conditions) to collect at least 20 mg of material.

Another concern was the possible oxidation of PCAH and soot particles by the injected water. Such oxidation would cause a decrease of the weight of products collected, and possibly a change of the size of the particles if they do not burn internally. The effect on the amount of products collected could not be determined, due to sticking of material within the probe when no water was introduced. However, gas analysis with and without water injection (Table I) indicated no significant reaction between the water and the gas. In general, the addition of about 3 l per hour of water inside the probe gave rise to slightly higher CO and O_2 concentrations and slightly lower CO_2 concentration. This was probably due to better quenching of the CO/CO_2 reaction with water than without. In light of this observation and the short quenching time ($\sim 10^{-4}$s), reaction between water and the solid materials collected should not be important.

TABLE I

Effect of injected water on gas composition (volume%). Kerosene; fuel equivalence ratio = 1.0; distance from nozzle = 10 cm; cold gas velocity = 0.96 m/s; atomizing-air pressure = 184 kPa (12 psig)

	CO	CO_2	O_2
no water	2.8	12.0	1.25
3 l water/hour	3.0	11.3	1.60

3. Results

Three types of experiments were carried out, using aviation kerosene as fuel. The total air flow was always held constant at 56.7 kg/hr. The mean fuel equivalence ratio was varied by changing the fuel flow rate. Then, at a constant mean fuel equivalence ratio of 1 (stoichiometric), the atomizing air pressure was varied in order to change the intensity of fuel-air mixing within the burner. Three atomizing air pressures were studied: 184 kPa (12 psig), 205 kPa (15 psig) and 239 kPa (20 psig). The variation of atomizing air pressure was carried out for two cold gas velocities: 0.96 m/s and 2.67 m/s. The cold gas velocity was varied at constant total flow rate by using two different burner diameters, 12.70 cm and 7.62 cm. Finally, at a fuel equivalence ratio of 1, a cold gas velocity of 0.96 m/s and an air atomizing pressure of 184 kPa, kerosene was replaced by benzene and by benzene doped with 0.5% by weight anthracene. These fuels were chosen in order to compare the behavior of a pure aromatic fuel with that of aviation kerosene which contains about 17% by weight monoaromatic compounds and 1% PCAH.

3.1 *Soot and Total PCAH Mass Loading*

Soot concentrations along the burner axis between 4cm from the nozzle and the exhaust (53 cm from the nozzle) for the case of kerosene fuel are shown in Fig. 2 for a cold gas velocity of 0.96 m/s, and in Fig. 3 for a cold gas velocity of 2.67 m/s. For the lower velocity, the total PCAH concentrations are shown in Fig. 4. It was not possible to obtain reliable data on total PCAH concentration for the runs at higher velocity, due to the obscuring of the chromatographic PCAH profile by appreciable amounts of unburned kerosene all along the axis of the burner.

For a cold gas velocity of 0.96 m/s, it appears that soot formation occurs very early in the flame, well within the recirculation zone. The soot concentration profile exhibits a strong increase between 1/2 and 1 burner diameter

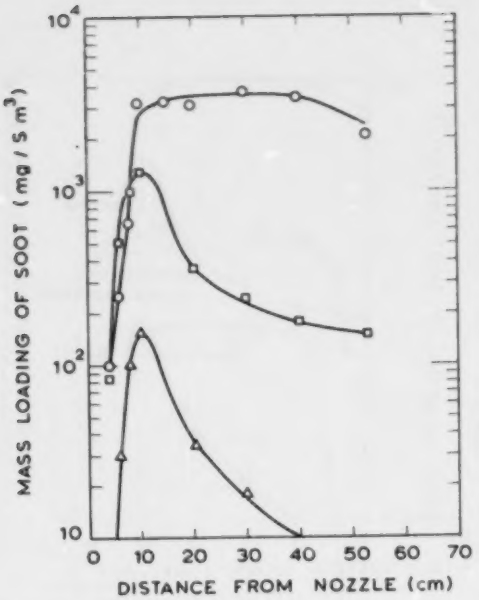

FIG. 2. Influence of atomizing-air pressure on axial profile of soot mass loading. Kerosene/air; fuel equivalence ratio = 1.0; cold gas velocity = 0.96 m/s; atomizing-air pressure = (o) 184 kPa (12 psig), (□) 205 kPa (15 psig), and (△) 239 kPa (20 psig).

from the nozzle, followed by a slow decrease to the exhaust for the 205 and 239 kPa cases.

At 184 kPa the profile does not exhibit a maximum, the strong increase being followed by a smaller one. The profiles of PCAH also exhibit a maximum, just upstream of the soot maximum. However, the decrease in PCAH concentration is more drastic than for the carbonaceous residue, indicating that either PCAH are intermediates of soot formation, or their burnout is more rapid than that of soot. For this cold gas velocity (0.96 m/s), the atomizing air pressure was found to have a strong effect on soot loading all along the axis of the burner, particularly at the exhaust. For example, Fig. 2 indicates that a decrease in atomizing air pressure from 239 to 184 kPa results in a 20 fold increase of the maximum of soot formation and a 10^4 fold increase in soot emission.

From these mass loading profiles, the flame can be divided into two distinct zones, in the first of which (first 10 cm from the nozzle) the soot formed and in the second of which soot combustion occurred. For a cold gas velocity of 2.67 m/s, these two zones were found to have rather different characteristics than in the 0.96 m/s case. The maximum of soot formation was lower, much less dependent on atomizing pressure, and located downstream of the recirculation zone (about 15 cm from the burner). Also, more burnout of soot occurred at lower rather than at higher air atomizing pressure.

The profiles of soot and PCAH when burning pure aromatic fuels (benzene and anthracene-doped benzene) are shown in Figs. 5 and 6 respectively. The profiles obtained with kerosene are also shown for comparison. It appears, within the limit of reproducibility, that anthracene has very little effect on the amount of soot or PCAH formed. The difference at 4, 6 and 8 cm between benzene and anthracene-doped benzene results mainly from the presence of unburned anthracene, as shown by the gas chromatographic analyses described below. The comparison between kerosene and benzene shows also that the combustion of benzene generates PCAH and soot particles i) earlier in the process and ii) in larger amounts (about three times as much)

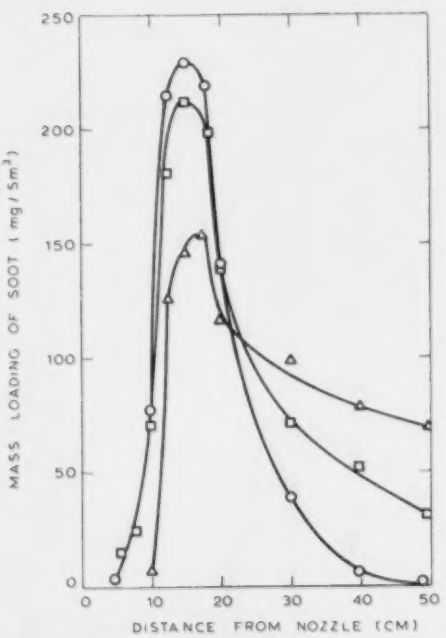

FIG. 3. Influence of atomizing-air pressure on axial profile of soot mass loading. Kerosene/air; fuel equivalence ratio = 1.0; cold gas velocity = 2.67 m/s; atomizing-air pressure = (o) 184 kPa (15 psig), (□) 205 kPa (15 psig) and (△) 239 kPa (20 psig).

at the maximum of formation. On the other hand, the amount of PCAH formed with benzene decreases at a faster rate than with kerosene to reach a lower total amount near the exhaust. This may be due to the fact that the adiabatic flame temperature for benzene is higher than for kerosene, resulting in more severe pyrolysis and post-combustion of the PCAH. For example, the adiabatic flame temperature for benzene and kerosene are respectively: 2330 K and 2281 K at a fuel equivalence ratio of 1, and 1363 K and 1107 K at a fuel equivalence ratio of 3.

Finally, increasing the fuel equivalence ratio resulted in an increase of the amount of soot formed as shown in Table II. It was not possible to measure the total amount of PCAH for these conditions, due to obscurring of the gas chromatogram by unburned kerosene, as pointed out above. However, it was possible to measure the higher mass compounds. For example, the concentration of cyclopenta[*cd*]pyrene ($C_{18}H_{10}$) had a larger dependence than soot on variations of fuel-equivalence ratio.

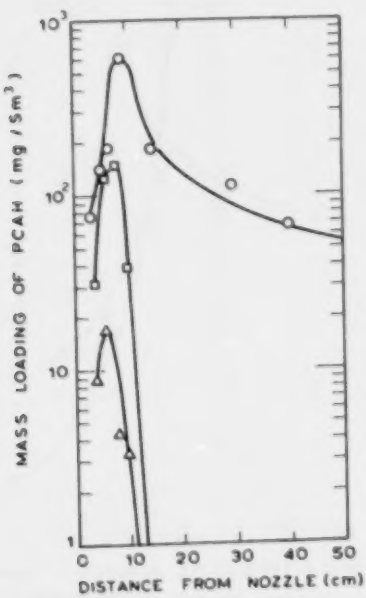

FIG. 4. Influence of atomizing-air pressure on axial profile of PCAH mass loading. Kerosene/air; fuel equivalence ratio = 1.0; cold gas velocity = 0.96 m/s; atomizing-air pressure = (○) 184 kPa (12 psig), (□) 205 kPa (15 psig) and (△) 239 kPa (20 psig).

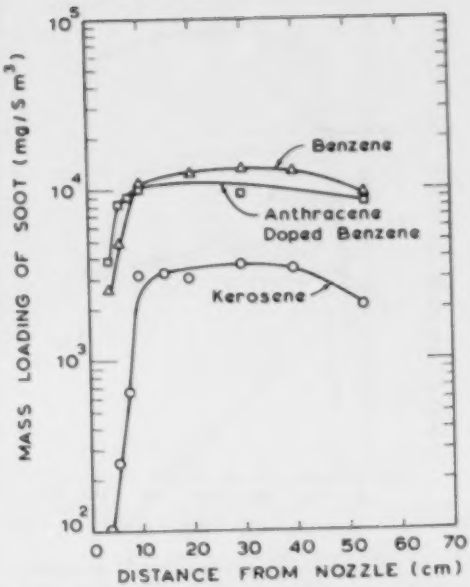

FIG. 5. Influence of the type of fuel on axial profile of soot mass loading. Fuel equivalence ratio = 1.0; air atomizing pressure = 184 kPa (12 psig); cold gas velocity = 0.96 m/s.

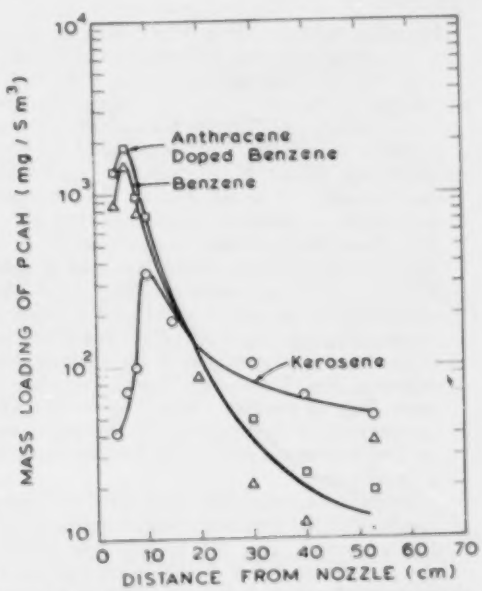

FIG. 6. Influence of the type of fuel on axial profile of PCAH mass loading. Fuel equivalence ratio = 1.0; air atomizing pressure = 184 kPa (12 psig); cold gas velocity = 0.96 m/s.

TABLE II

Computed and experimental soot mass loading. Kerosene; cold gas velocity = 2.67 m/s; air-atomizing pressure = 184 kPa (12 psig); distance from nozzle = 15 cm; Φ = fuel equivalence ratio; σ = standard deviation of Gaussian distribution of fuel/air ratios.

Φ	0.8	0.9	1.0	1.1	1.2
experimental values (mg/sm^3)	96	125	230	255	410
computed values (mg/sm^3) σ = 0.8	60	80	105	190	280
computed values (mg/sm^3) σ/Φ = 0.8	6	30	105	400	800

3.2 *Individual PCAH Analysis*

Although the total mass of PCAH found in the combustion products is useful in understanding general trends in PCAH production for various systems, this information is not particularly useful in determining the health effects of these products. It is well documented[5,6,7] that the majority of PCAH are noncarcinogenic; however, those that are carcinogenic range in activity from very weak to extremely potent. Because of this fact, recent emphasis has been placed on the determination of the exact identities and concentrations of these potential carcinogens in exhausts representative of those that may be of environmental importance.

Gas chromatographic-mass spectrometric analysis of the methylene chloride extracts of the soot samples, and subsequent peak area integration of the chromatographic peaks have provided detailed quantitative and qualitative compositional information on the polycyclic aromatic hydrocarbons formed within the flame. Table III lists the identities and structures of these compounds as determined by gas chromatography-mass spectrometry. Quantitative values for 26 PCAH ranging from two- to seven-ring structures measured at different points along the burner axis at an atomizing air pressure of 184 kPa are reported for kerosene and benzene in Table IV. The lack of data at 4, 6 and 8 cm is due to the obscurring of the chromatographic PCAH profile by appreciable amounts of unburned kerosene at these short distances from the burner nozzle.

These tables form the data base for the total amount of PCAH plotted in Fig. 4 and 6 and described above. Some additional conclusions can be drawn:

a) With kerosene as well as with benzene, there is an enrichment of heavier PCAH as samples are collected at greater distances from the burner nozzle.
b) There is a gross reduction and in some cases an absence of PCAH containing methyl and phenyl groups for kerosene fuel as compared to benzene.
c) In both cases the disappearance of PCAH containing methyl and phenyl groups and those containing a saturated carbon (such as fluorene) with increasing distance from the burner nozzle is faster than the disappearance of more stable PCAH.

3.3 *Particle Size Analysis*

Selected samples were subjected to particle size analysis by electron microscopy at a magnification of 81,000, which was brought to 200,000 by further photographic magnification. Two types of carbonaceous material were observed. Close to the nozzle, in the zone of soot formation, the particles looked like agglomerates of partially coalesced spherical units. This type of material was observed previously in different systems, namely a flow reactor for the thermal decomposition of benzene,[8] a propane-oxygen premixed flame,[9] and a diesel engine.[10] It has been attributed to the coalescence of viscous carbonaceous particles through collisions occurring possibly in the sampling system.[8,11] It has been suggested that such material may indicate the evolution of soot particles through a liquid state to a solid material by dehydrogenation and carbonization reactions.[8] Alternatively, rapid surface growth during particle agglomeration might contribute to the observed shape. The individual spherical units in this material were very poorly defined and it was not possible to measure their size. Farther from the nozzle, the material had the classical appearance of necklace-like units of spherical particles, indicating that the collisions occurred mainly between already solidified particles. The size of these well defined spherical units are reported in Tables V and VI. In these tables, the poorly defined material refers either to the above described coalesced material or to a strongly oxidized material (Table VI, 239 kPa, exhaust) having a different structure than the coalesced

TABLE III

Polycyclic aromatic hydrocarbons in the combustion products of kerosene and benzene. The structure of number 11 is unknown, its mass is 176 ($C_{14}H_8$).

Number	Name	Structure
1	Indene	
2	Naphthalene	
3	Methylnaphthalene	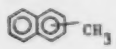
4	Biphenyl	
5	Biphenylene	
6	Acenaphthylene	
7	Acenaphthene	
8	Methylbiphenyl	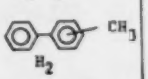
9	Fluorene	
10	Methylacenaphthylene	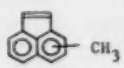
12	Phenanthrene + Anthracene	
13	Methylphenanthrene	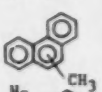
14	4H-cyclopenta[def]phenanthrene	
15	2-phenylnaphthalene	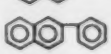
16	Fluoranthene	

Number	Name	Structure
17	Benzacenaphthylene	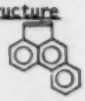
18	Pyrene	
19	Benzofluorene	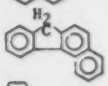
20	Methylfluoranthrene + Methylpyrene	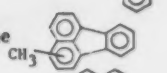 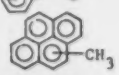
21	Benzo[ghi]fluoranthene	
22	Cyclopenta[cd]pyrene	
23	Methylcyclopenta[cd] pyrene	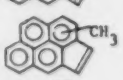
24	Benzofluoranthene	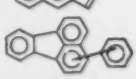
25	Benzo[e]pyrene + Benzo[a]pyrene	
26	Perylene	
27	Indeno[1,2,3-cd]pycene	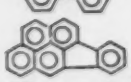
28	Benzo[ghi]perylene + Anthanthrene	
29	Coronene	

TABLE IV

Distribution of PCAH (mg/sm³) for kerosene and benzene fuel along the burner axis. X—Unable to measure because of unburned kerosene peaks; K—kerosene; B—benzene

Compound Number[c]	Distance from burner nozzle (cm)													
	4		6		8		10		20		30		40	
	K	B	K	B	K	B	K	B	K	B	K	B	K	B
1	X	8.9	X	12	0	3.8	0	0	0	0		0	0	0
2	X	117	X	151	X	63	X	42	0.8	11	1.2	2.7	1.9	3.1
3	X	55	X	88	X	28	9.0	12	0	0.4	0	0.5	0	0.3
4	X	135	X	160	X	107	7.5	84	0	1.0	0	1.0	0	0.4
5	X	38	X	57	X	25	22	18	0.3	0.8	0	0.4	0	0.2
6	X	121	X	162	X	131	185	130	18	28	29	3.5	19	3.7
7	X	4.9	X	6.8	X	3.0	10	3.0	0.8	1.9	0.5	0.3	0.6	0.2
8	X	8.1	X	16	X	5.9	0	7.3	0	0	0	0	0	0
9	X	32	X	62	X	30	27	30	0.3	0.6	0.4	0.2	0.2	0.1
10	X	24	X	39	X	15	7.0	5.0	0	0	0	0	0	0
11	X	20	X	43	X	14	22	10	2.2	2.0	2.5	0.6	0.9	0.3
12	X	52	X	108	X	62	53	73	2.1	1.8	2.5	0.4	1.3	0.1
13	X	10	X	19	X	5.8	0	4.6	0	0	0	0	0	0
14	X	20	X	38	X	18	19	16	1.2	1.2	1.3	0.3	0.6	0.1
15	X	9.0	X	19	X	8.3	0	6.7	0	0.5	0	0.3	0	0.2
16	2.4	26	7.5	51	8.7	31	35	50	4.5	4.9	6.1	1.0	3.2	0.5
17	X	17	X	35	X	20	21	20	2.1	2.0	2.5	0.4	1.2	0.2
18[a]	6.9	24	12	49	16	31	55	43	16	10	19	2.5	9.2	1.5
19	X	12	X	25	X	9.8	2.4	9.1	0	0.1	0	0.1	0	0
20	X	11	X	26	X	9.8	6.8	5.0	0.5	0.4	0.5	0.2	0.3	0
21	0.9	11	4.9	24	6.7	13	17	21	3.7	3.6	4.5	0.8	2.2	0.3
22	4.4	21	11	45	16	29	53	11	17	9.9	25	2.7	16	1.1
23	X	5.8	X	15	X	5.2	4.0	3.9	0	0.7	0	0.2	0	0
24	X	3.6	X	14	X	8.0	11	15	1.3	0.9	1.8	0.4	1.1	0.1
25	X	4.3	X	9.4	X	5.7	6.6	13	1.2	0.9	1.5	0.3	0.8	0
26	X	1.8	X	8.7	X	4.8	3.0	6.2	0.9	1.3	1.7	0.1	1.2	0
27	X	4.2	X	8.5	X	9.0	5.4	9.2	0.8	1.0	1.1	0	0.7	0
28	X	4.0	X	6.3	X	9.2	17	14	5.4	2.6	12	0.1	5.8	0
29	X	1.5	X	2.6	X	3.0	6.4	5.8	2.6	2.1	4.3	0.1	3.9	0
Total	75[b]	802	130[b]	1302	179[b]	709	603	665	81	90	117	19	68	12

[a] Calculated 95% confidence limits for measurement of pyrene concentration = ±18%.

[b] These values have been derived by assuming that the relative concentration of pyrene (compound no. 18) to total PCAH is the same at 4, 6 and 8 cm as at 10 cm. In fact, there is an enrichment of heavier PCAH as samples are collected at greater distances from the burner nozzle. As a result, the actual values at 4, 6 and 8 cm are probably higher than the values in the table.

[c] See Table 3 for key.

particles but so strongly agglomerated that it was very difficult to distinguish the individual particles. The arithmetic mean particle diameter is defined as $\Sigma n_i d_i / \Sigma n_i$, n_i being the number of particles contained in a diameter interval centered on d_i.

From these tables, several conclusions can be drawn:

a) The atomizing-air pressure, even when drastically changing the total amount of soot emitted, does not affect the particle size.

b) Burnout of soot tends to increase slightly the average diameter of the population of particles. This is an indication that small particles burn out first and possibly also that particles are oxidized internally and then collapse, as observed by others.[9] Indeed, even if burnout does not reduce the diameter of the particles, it reduces strongly their mass (at least for 205 and 239 kPa). If particles were not burning internally, one would expect an eventual decrease in their average size.

c) Benzene produces slightly smaller parti-

TABLE V

Arithmetic mean particle diameter (Å). Cold gas velocity = 0.96 m/s; mean fuel equivalence ratio = 1.0.

	atomizer air pressure, kPa			
	kerosene			benzene
Distance from nozzle, cm	184	205	239	184
6	191	•	•	189
10	211	220	254	184
53 (exhaust)	249	298	•	223

• poorly defined carbonaceous material

cles than kerosene, even though the total mass is much larger. The same effect, with even a larger impact, was observed when increasing the cold gas velocity (Table VI). This effect in both cases may result from an increase in temperature. The adiabatic flame temperature for benzene is indeed higher than for kerosene, as pointed above, and consequently so is the final temperature. Increasing the cold gas velocity results in a higher temperature through the reduction of heat loss per unit of energy input. It has been previously observed[11] that an increase in temperature results in a decrease in the size of particles through an increase in the number of particles formed per unit volume, other parameters being constant. For a given amount of carbonaceous material, the final size of the particles will be smaller if a larger number of nuclei is generated. However, smaller particles will be produced also if for a given number of nuclei there is less carbonaceous material to provide surface growth. Since the total amount of soot associated with the smaller particles is equal to (effect of cold gas velocity at 239 kPa) or larger than (benzene as compared to kerosene) the amount associated with larger particles, the effect is one of nucleation, probably related to the change in temperature. For the effect of cold gas velocity at 184 kPa and 205 kPa, both the amount of soot and the particle size decrease, and it is not possible to distinguish between nucleation and surface growth effects.

TABLE VI

Arithmetic mean particle diameter. Kerosene. Cold gas velocity = 2.67 m/s; atomizer air pressure = 184 kPa (12 psig); distance from nozzle = 20 cm.

mean fuel equivalence ratio	0.8	0.9	1.0	1.2
diameters (Å)	•	146	145	139

• poorly defined carbonaceous material

4. Discussion

Any model of soot formation in a turbulent fuel spray combustor has to combine both the mixing of fuel and air and the chemistry of soot formation and burnout. Neither of these two processes is well understood and only very approximate modelling of soot formation in this system is now possible.

An approximate mixing model previously used[1,2] assumed that the nonuniform distribution of fuel and air can be represented by a Gaussian distribution of uniformly premixed pockets of gas, or eddies, of different fuel-air ratios, centered on the mean fuel-equivalence ratio. Such a model may be used with reasonable accuracy i) downstream of the recirculation zone and ii) after all the fuel has been evaporated.

The recirculation zone in our burner is assumed to extend 1.5 to 2 burner diameters from the nozzle. Accordingly, the maximum of soot formation (Fig. 2 and 3) occurred inside the recirculation zone at the lower velocity and outside at the higher velocity. Since the fuel is most probably entirely evaporated outside the recirculation zone, the above two-conditions are presumably obeyed for the data obtained at the higher air velocity.

By combining the Gaussian distribution of fuel/air ratios and the amount of soot produced in each eddy, the total soot concentration could in principle be computed. However, the chemistry of soot formation is not well known and few data are available on the amount of soot emitted for a given fuel equivalence ratio. Several reviews of this subject are available.[9,10,11] Studies of premixed flames indicate that soot begins to form at lower C/O

ratios than would be predicted from an equilibrium calculation (roughly, for $C/O \simeq 1$). To assess the departure of soot emission from equilibrium in premixed flames, we employed the equilibrium program developed recently by Svehla and McBride[12] which uses a free energy minimization technique to compute the equilibrium composition of 56 molecular or radical species in the C/H/O/N/Ar system. Soot was assumed to have the thermodynamic properties of graphite. Comparison of equilibrium values of soot formation and experimental values available in the literature indicates that experimental values can be as high as five times the equilibrium value (premixed benzene/oxygen flame[13] or as low as one fifth of the equilibrium value (premixed acetylene/oxygen flame[6]. However, in the absence of data on premixed kerosene-air flames, and neglecting the fact that actual values are probably higher due to the aromatic fraction contained in the fuel, we used equilibrium values to approximate the concentration of soot formed when burning kerosene.

The values so computed, assuming a Gaussian distribution of fuel/air ratios centered on the mean ratio Φ, are reported in Table II together with the experimental values. The standard deviation σ of the distribution was assumed to be either independent of Φ, and equal to 0.8, or dependent on Φ with σ/Φ being 0.8. The value of 0.8 agrees with values reported by others[2] for similar conditions in the early zone of the burner.

It is worth noting that, in this picture, soot will be formed only in the small fraction of eddies having a fuel equivalence ratio larger than about 2.8 and contained in the tail of the distribution. As a result, the computed soot concentrations are very sensitive to the values selected for σ. In spite of the above limitations, it appears from Table II that this approximate calculation predicts the right order or magnitude for both soot concentration and the general effect of Φ for the higher velocity runs.

As indicated before, at low velocity the maximum of soot formation appeared inside the recirculation zone, and its magnitude was extremely sensitive to the fuel atomization conditions. A possible reason for this behavior is that the relative velocity between the larger droplets and the air remains smaller than the extinction velocity in the low velocity runs, in contrast to the high velocity runs where the combustion air velocity is expected to be high enough to extinguish the droplet flame. Individual diffusion flame envelopes around large droplets are known to generate soot in fuel spray combustors.[17] The extinction velocity is proportional to the square root of the droplet diameter[17] and the size of the droplets decreases with increasing atomizing air pressure. These factors offer a plausible explanation for the effect of atomizing air pressure on soot formation at a relative velocity lower than the extinction velocity and for the lack of sensitivity at higher velocity.

With regard to soot burnout, the soot concentration in the exhaust (50 cm from the nozzle) decreases with increasing atomizing air pressure, and hence with increasing intensity of mixing, at the lower gas velocity (Fig. 2) but increases at the higher velocity (Fig. 3). Although these trends in the two figures may at first appear to be mutually inconsistent, further inspection reveals substantial agreement. The mass of soot burned out, as measured by the decrease in soot loading between the point of maximum concentration and the exhaust, decreases consistently with increasing atomizing air pressure in both figures. While this behavior may appear to be opposite to that generally expected for improved mixing of fuel and air, it should be noted as observed previously[2] that an increase in atomizing air pressure will increase the consumption of oxygen in the first zone of the flame thereby lowering the oxygen concentration in the second zone. Accordingly, the observed decrease in mass of soot burned with increased atomizing air pressure can be attributed to decreased oxygen availability for soot burnout in the second zone. The amount of unburned soot emitted in the exhaust can either decrease (Fig. 2) or increase (Fig. 3) with increased atomizing air pressure depending on whether the amount of soot formed in the primary zone is extremely sensitive (Fig. 2) or relatively insensitive (Fig. 3) to changes in the atomizing air pressure.

5. Conclusions

The results of this study can be utilized in the consideration of two general types of practical combustors. The first type corresponds to a system with a high combustion air velocity typical of gas turbine combustors, and the second type corresponds to a system with a low combustion air velocity typical of domestic home heating burners. The amount of soot formed in the second case is usually higher than in the first and is very sensitive to fuel atomization characteristics. One practical consequence is that the common, unmaintained domestic home heating burner may be the source of considerable soot and PCAH, some of which may have considerable effects

on human health. The identification of individual PCAH is therefore important in order to assess the exact health hazard generated by a particular combustion system.

Acknowledgment

We are grateful to C. Clampitt, J. Dillon, R. Flagan and K. Shamsavari for valuable help at different steps of this project. The work was initiated with support of Honeywell, Inc. and continued under Contract No. NSG3076 of the National Aeronautics and Space Administration (Lewis Research Center) and Grant No. R803242 of the Environmental Protection Agency. One of us (Gilles P. Prado) was supported in part by the Centre National de la Recherche Scientifique, Ministère de l'Education Nationale, France.

BIBLIOGRAPHY

1. Pompei, F. and Heywood, J. B.: Combustion and Flame *19*, 407 (1972).
2. Appleton, J. P. and Heywood, J. B.: *Fourteenth Symposium (International) on Combustion*, p. 777, The Combustion Institute, Pittsburgh, 1973.
3. Flagan, R. C. and Appleton, J. P.: Combustion and Flame *23*, 249 (1976).
4. Lahaye, J. and Laragne, J.: Centre de Recherches sur la Physico-Chimie des Surfaces Solides, C.N.R.S., Mulhouse, France, Personal Communication.
5. Schoental, R.: Carcinogenesis by Polycyclic Aromatic Hydrocarbons and by Certain Other Carcinogens, *Chapter in* "Polycyclic Hydrocarbons" (E. Clar, Ed.), p. 133, Academic Press, 1964.
6. Fishbein, L., Flamm, W. G. and Falk, H. L.: Chemical Mutagens, p. 275, Academic Press, 1970.
7. Miller, E. C. and Miller, J. A.: Chemical Mutagens, Vol. 1 (A. Hollaender, Ed.), p. 105, Plenum Press, 1971.
8. Prado, G. P.: *Mechanisme de Formation des Particules de Noir de Carbone lors de la Decomposition Thermique de Benzene*. Ph.D. Thesis, C.U.H.R. and U.L.P. of Strasbourg, France, 1972.
9. Wersborg, B. L.: *Physical Mechanisms of Carbon Formation in Flames*. Sc.D. Thesis, M.I.T., Cambridge, Mass., 1972.
10. Vuk, C. T., Jones, M. A. and Johnson, J. H.: *The Measurement and Analysis of the Physical Character of Diesel Particulate Emissions*. Paper presented at Automotive Engineering Congress and Exposition, Detroit, Michigan, February 1976.
11. Lahaye, J., Prado, G. P. and Donnet, J. B.: Carbon *12*, 27 (1974).
12. Donnet, J. B. and Voet, A.: Carbon Black, Physics, Chemistry, and Elastomer Reinforcement, p. 96, Marcel Dekker Inc., 1976.
13. Palmer, H. B. and Cullis, C. F.: The Formation of Carbon from Gases, *Chapter in* "The Chemistry and Physics of Carbon," Vol. 1 (P. L. Walker, Jr., Ed.), p. 265, Marcel Dekker, 1965.
14. Lahaye, J. and Prado, G. P.: Mechanisms of Carbon Black Formation, *Chapter in* "The Chemistry and Physics of Carbon," Vol. 13, (P. L. Walker, Jr., Ed.), Marcel Dekker, to be published.
15. Svehla, R. A. and McBride, B. J.: *Fortran IV Computer Program Calculation of Thermodynamic and Transport Properties of Complex Chemical Systems*, NASA TN D. 7056, 1973.
16. Homann, K. H., Morgeneyer, W. and Wagner, H.Gg.: *Combustion Institute European Symposium*, p. 396, Academic Press, N.Y., 1973.
17. Sjogren, A.: *Fourteenth Symposium (International) on Combustion*, p. 919, The Combustion Institute, Pittsburgh, 1973.

COMMENTS

P. J. Pagni, University of California, USA. Your mass data are very interesting. However, the size data are at best qualitative because of the extensive sample manipulation. Two techniques which might be useful in this apparatus are: (1) Particle replication which permits micrographs to be obtained without removing the particles from the filter on which they are originally collected[1] and (2) air-aspirated, porous walled probes which nearly eliminate wall effect difficulties.[2]

REFERENCES

1. Kay, D. H. (Ed), "Techniques for Electron Microscopy," 2nd ed., p. 115, F. A. Davis Co., Philadelphia (1967).
2. Mitchell, C. A. and Silverman, L.; "The Boundary Layer Diluter—A New Gas and Particulate Calibration Device," Air Pollution Control Association Paper, presented to the New England Section, April (1963).

Authors' Reply. As indicated in the paper, the soot appears as aggregates of individual, spherical particles. Any collection technique which allows collisions of particles in the sampling train, as is the case in this study, may affect the aggregate characteristics. However, the sizes of the individual, spherical units are not affected by such collisions as long as they are solid before entering the probe, which is the case in this study for samples collected farther than 10 cm from the burner. Because this study focussed only on the size of these individual units, we believe that the data reported are accurate to within 10%. We are not familiar with the particle replication technique, but we are not optimistic that such a technique would permit the detection of particles as small as 20 Å diameter which are directly measured with the electron microscope.

•

Richard G. Gann, National Bureau of Standards, USA. In your paper, you make the important assumption that the combusting system is essentially premixed. It is critical that this be verified since variation in residual fuel droplet size and concentration or gaseous fuel-rich pockets could easily dominate the soot formation characteristics. Would you expand on the theoretical or experimental approaches you need to establish the homogeneity of the system and the confidence limits.

Authors' Reply. It is correct that fuel-rich pockets as well as possible fuel droplet combustion dominate the soot formation characteristics in turbulent diffusion fuel spray systems. Here, for the high velocity runs, we believe that droplets evaporate prior to combustion, but that might not be the case for the low velocity runs, as indicated in the paper. We do not assume that the system is premixed; on the contrary, we represent the mixing of fuel and air by a gaussian distribution of pockets (or eddies) of different fuel-air ratio, in which only very fuel-rich pockets from soot. We are presently measuring the CO/CO_2 ratio in axial as well as traverse directions in the flame in order to determine more precisely the distribution of eddies (see ref. 1, 2 and 3 in the paper). In parallel, computations are being developed to determine the trajectory of fuel droplets and their evaporation characteristics.

•

S. C. Graham, Shell Research Ltd., England. In your presentation, you state that benzene flames with relatively high adiabatic flame temperatures, give smaller soot particles (within the agglomerated chains) than the lower temperature kerosene flames. You then attribute this to the effect of temperature on the particle nucleation rate—i.e. the higher the temperature, the greater the rate,—on the assumption that the final number density of individual particles is strongly dependent on, if not identically equal to, the total number of nuclei that are formed within a unit volume of gas throughout the combustion process. I should like to point out that your interpretation ignors the collisions that must occur between the (very small) soot nuclei, and I suggest that the particle number densities involved are far too high for such collisions to be ignored,[1,2] whether they lead to chain formation or to the formation of bigger particles via coalescence.

An alternative and very different model, in which coalescent collisions between particles (partly soot, partly PCAH) dominate the early stages of particle growth, also leads to the result that the ultimate size of the particles within the agglomerated chains decreases with increasing temperature. In its simplest form[3] this model leads to the equation for free-molecule coagulation

$$\bar{V}^{5/6}(t) = k' \left[\bar{V}_o^{5/6} + k'' \int \phi(t)\, dt\right]^{6/5}$$

where V is the particle volume, k' and k'' are constants and ϕ is the particulate volume fraction. For simplicity consider the situation where ϕ is constant. This gives

$$\bar{V} = k''' \phi^{6/5} \Delta t^{6/5}$$

where Δt is the interval between the onset of nucleation and the time at which particle collisions cease to result in the coalescence of individual particles. However it is inevitable that coalescent collisions will give way to chain-forming or possibly to non-sticky collisions either.

i) when the gas is quenched to room temperature so that the condensed phase (partly soot, partly hydrocarbon) is wholly solid, or
ii) when the chemical processes of dehydrogenation/cracking/pyrolysis of the condensed phase have proceeded sufficiently for the condensed phase to have turned completely into soot.

Whenever ii above is the limiting factor, an increase in temperature will result in a shorter Δt giving smaller particles within the agglomerated chains.

REFERENCES

1. Graham, S. C. and Homer, J. B.: Faraday Symposium; Chem. Soc., 7, 86 (1973).
2. Graham, S. C., Homer, J. B. and Rosenfeld, J. L. J.: Proc. Roy. Soc. (London). A344, 259 (1975).
3. Graham, S. C., Homer, J. B. and Rosenfeld, J. L. J.: Second Symposium (European) on Combustion, p. 374 (1975).

Authors' Reply. The qualitative interpretation that the increase of particle number density may be attributed to increased flame temperature does not ignore particle collisions, but the validity of the interpretation clearly depends upon the relative rates of nucleation and coagulation with the latter rate in turn depending on the rate of particle growth by reaction with gaseous species.

Grahm's coagulation equations are interesting but their application to soot formation would appear to require a suitable treatment of nucleation and surface growth, both of which processes significantly overlap the coagulation process.[1,2]

REFERENCES

1. HOWARD, J. B., WERSBORG, B. L., AND WILLIAMS, G. C.: "Coagulation of Carbon Particles in Premixed Flame," Faraday Symposium of the Chemical Society (London), No. 7, pp. 109–119, 1973.
2. WERSBORG, B. L., HOWARD, J. B., AND WILLIAMS, G. C.: "Physical Mechanisms in Carbon Formation in Flames," *Fourteenth Symposium (International) on Combustion*, p. 229, The Combustion Institute, Pittsburgh, 1973.

APPENDIX B

Formation of Soot and Polycyclic Aromatic Hydrocarbons in Combustion Systems

From: Proceeding of the Stationary Source Combustion Symp., Vol I: Fundamental Research, EPA Report 600/2-76-152a, June 1976.

FORMATION OF SOOT AND POLYCYCLIC AROMATIC HYDROCARBONS IN COMBUSTION SYSTEMS

Development of a Molecular Beam Mass Spectrometer

By

James D. Bittner
Department of Chemical Engineering
Massachusetts Institute of Technology
Cambridge, Massachusetts 02139

ABSTRACT

The overall objective of this research program has been to study the production of soot and polycyclic aromatic hydrocarbons (PCAH) in combustion systems. The program has two phases. In one phase the production of soot and PCAH in a turbulent diffusion flame was studied. The results have been reported elsewhere. In the phase to be discussed in this paper, a low pressure flat laminar premixed flame is being used to study the kinetic relationships between soot, PCAH and other hydrocarbon species that may be important as soot nuclei or surface growth species. The molecular beam-mass spectrometer system developed to study the gas phase species will be described. Preliminary mass spectral data on an acetylene-oxygen flame will be reported.

INTRODUCTION

The formation of soot in combustion systems has been studied for many years with the objective of attaining a working knowledge of the process to aid in predicting flame emissivities for radiative heat transfer problems. Recently, concern has been expressed that soot and some of the organic compounds associated with incomplete combustion are pollution problems that may have to be controlled. It is known that some polycyclic aromatic hydrocarbons (PCAH) produced in flames and adsorbed on soot particles are carcinogenic. Soot and other organic particulate matter may not be the most abundant particulates emitted, but because the small particles (<0.2 μm) are easily injected deep into the respiratory system, they may be one of the types of particulates most hazardous to human health. The effects of two expected changes in the operation of combustion systems threaten to increase the emissions of particulate organic matter. First, the staged combustion strategy for controlling NO_x requires primary combustion in a fuel rich atmosphere that leads to increased soot and PCAH formation. Second, the planned increased use of coal and coal derived liquids will also lead to increased soot and PCAH formation since aromatic fuels are known to be troublesome in this respect (1,2). The necessity for learning how to burn low H/C fuels (aromatics) without considerable soot and PCAH formation is especially important for small systems such as gas turbines and internal combustion engines where residence times available for burnout are limited (3).

The mechanism of soot formation in combustion systems is not well understood. Some of the mechanisms proposed over the years and the confusion surrounding the role of PCAH in the process are illustrated in Figure 1. Since soot particles contain many more carbon atoms and a much lower H/C ratio than the fuel molecules, soot formation must involve processes of aggregation (top to bottom) and dehydrogenation (left to right). The extreme routes, the C_2 route and the saturated polymer route, are unlikely to occur under typical combustion conditions. The C_2 route may be important at temperatures around 3000°K. At lower temperatures, around 700°K, and long reaction times the saturated polymer route may occur. But, in the range 1200-2200°K most mechanisms can be represented by the central portion of Figure 1. From this figure it is seen that PCAH species have been postulated to serve as nuclei for soot growth by surface decomposition of any number of hydrocarbon species (including themselves). They have been postulated to have sufficiently low vapor pressures to physically condense to liquid droplets which then form soot. They have also been postulated to be stable by-products of the soot formation process.

In light of the concern over particulate organic matter as a pollutant and the confusion surrounding soot formation mechanisms and the role of PCAH,

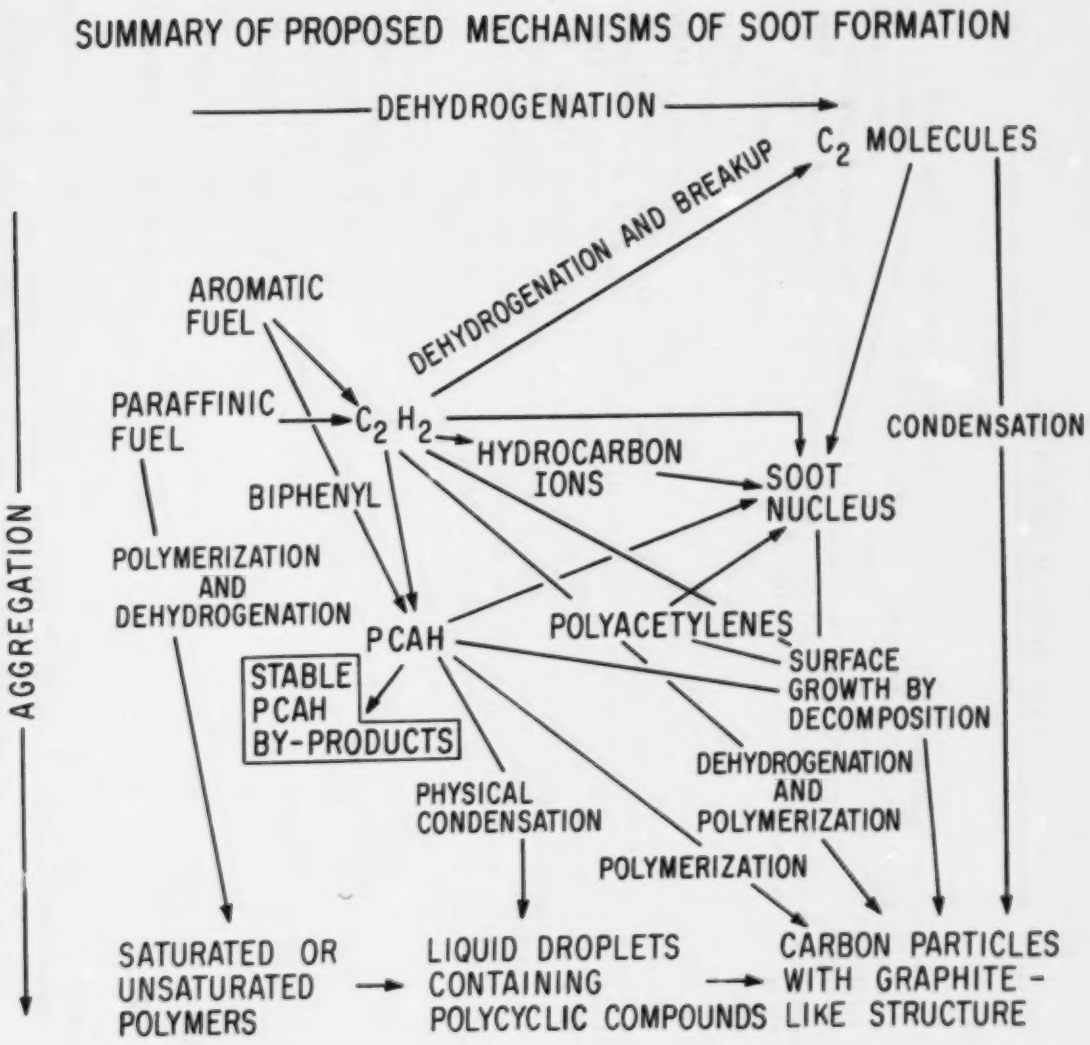

FIGURE 1. SUMMARY OF PROPOSED MECHANISMS OF SOOT FORMATION

the specific objective of this research is to study the chemistry of soot and PCAH formation. Emphasis is on the identification and measurement of relative concentration profiles of the gas phase hydrocarbon species and the measurement of soot particle concentrations, size distributions and total mass of soot at different stages of combustion in a flat premixed flame.

EXPERIMENTAL APPARATUS

DESCRIPTION

The molecular beam mass spectrometer system that has been developed during this project to study premixed low-pressure flat flames is schematically represented in Figure 2. The flame is stabilized on a flat water-cooled drilled copper plate burner that is 7.1 cm in diameter. The burner chamber is pumped by a 60 cfm Stokes mechanical pump. The flame is sampled along the centerline of the burner by moving the burner relative to the rest of the apparatus. The sample is withdrawn supersonically through a quartz nozzle. The nozzle is a hybrid type, as discussed by Biordi et al.(4). The tip has about a 40° outside angle that expands to a 90° angle about 1.5 cm from the tip. The central core of the expanding flame gases passes through the orifice in the top of the cone-shaped (60° total outside angle) aluminum skimmer. Formation of the molecular beam is completed by collimation with a circular orifice placed between the second and third (mass spectrometer) stages. The beam is modulated by an American Time Products tuning fork chopper placed near the entrance to the ionizer of the Extranuclear quadrupole mass spectrometer. Orifice diameters, separation distances and typical operating pressures are shown in the following table. The partition between the second and third stages is a hollow annulus designed to be filled

	Orifice diameter, mm	Distance from nozzle, cm	Pressure downstream, flame at 20 torr, torr
nozzle	0.7	-	1.1×10^{-4} (stage 1)
skimmer	0.9	1.8	1.2×10^{-6} (stage 2)
collimator	3.0	$\sim$ 36	1.4×10^{-7} (stage 3)
ionizer	3.0	$\sim$ 40	

with liquid nitrogen to provide cryogenic pumping near the ionizer to reduce the amounts of water and other condensible species, especially hydrocarbons, in the background. This recent improvement has been fabricated but not yet tested and the pressures reported in stages two and three are without the benefit of cryogenic pumping. The system is equipped with an effusive source that can be moved into place to calibrate for mass spectrometer sensitivities and study mass discrimination effects in the beam.

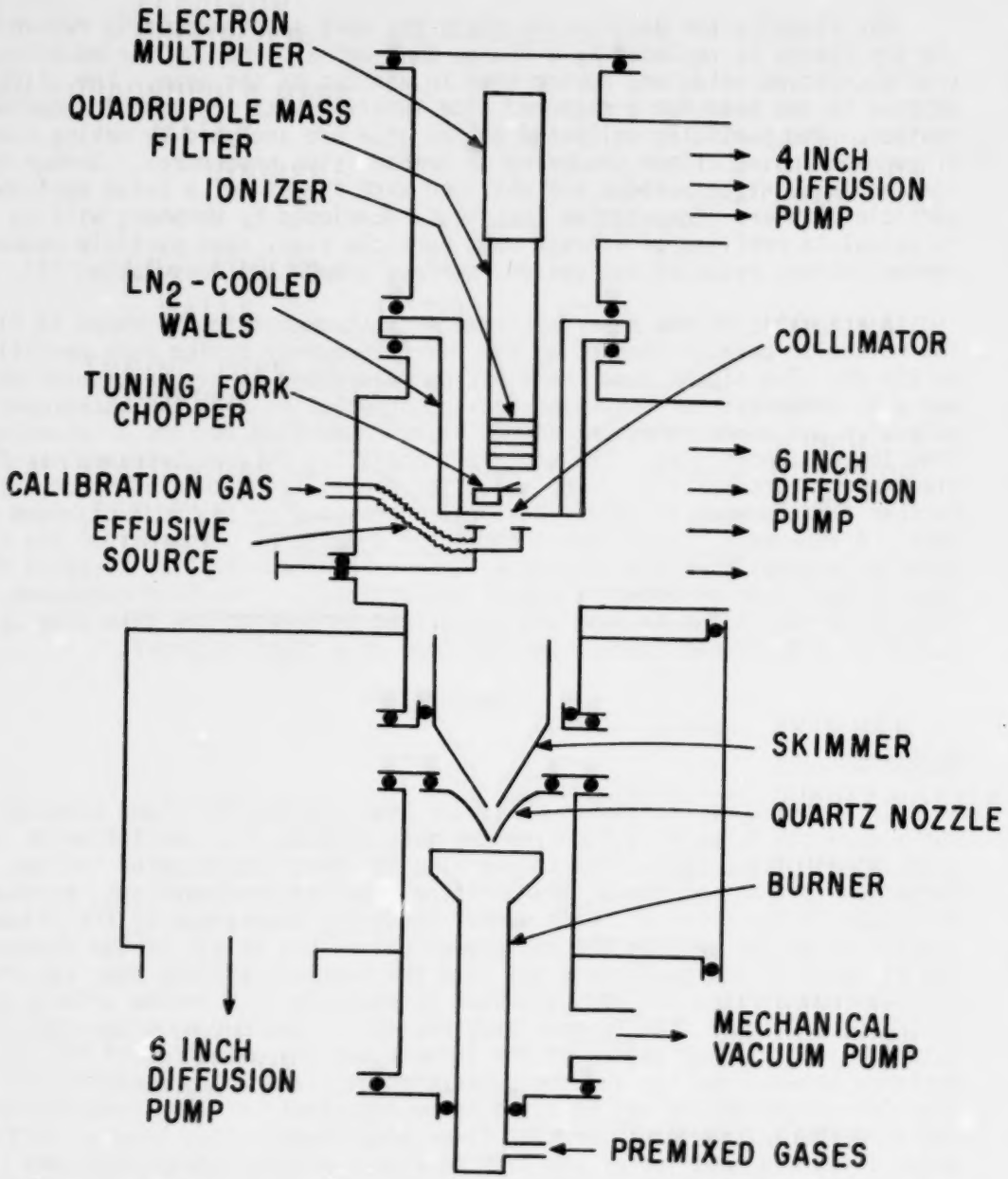

FIGURE 2. MOLECULAR BEAM MASS SPECTROMETER SYSTEM

For studying the particulate phase the mass spectrometer is removed and the top flange is replaced by a flange that has a mechanism for mounting electron microscope grids and moving them in and out of the beam. The grids are exposed to the beam for a measured time interval with the use of a mechanical shutter. The particles collected on the grid are analyzed by making electron micrographs using either shadowing or transmission procedures. Number densities and size distributions are obtained with the aid of a Zeiss semi-automatic particle counter. Computation techniques developed by Wersborg will be used to calculate profiles of average soot particle size, soot particle number concentration, rates of nucleation, surface growth and coagulation (5).

A schematic of the mass spectrometer instrumentation is shown in Figure 3. The molecular beam is chopped by the fixed-frequency tuning fork operating at 220 Hz. The signal from the electron multiplier at any particular mass has a DC component corresponding to ions originating from the background gas molecules and an AC component at 220 Hz corresponding to ions originating from the beam molecules. The signal is amplified with an Extranuclear fast electrometer preamplifier. The amplified signal is DC coupled to an Extranuclear electrometer to obtain a signal corresponding to the background component. A reference signal from the chopper and the AC component of the signal from the preamplifier are introduced into a Princeton Applied Research HR-8 lock-in amplifier to obtain a signal proportional to the beam component. Signals corresponding to beam and background components are then displayed either on a dual-beam storage oscilloscope or a chart recorder.

CALIBRATION

Considerations

Calibration of supersonic molecular beam systems for flame sampling is not a straight forward task due to the many effects that can influence the composition of the beam prior to reaching the mass spectrometer ionizer. Shock formation in front of the skimmer orifice, species condensations, pressure diffusion in the free jet, Mach number focussing downstream of the skimmer, scattering of the beam by the background gas in any or all of the chambers, and effusion of the background gas into the beam are effects that can distort the beam composition and are discussed extensively in a review article by Knuth (6). Skimmer interference problems can be avoided by proper design of external and internal angles of the skimmer and the selection of the proper distance between the tip and the supporting wall. Species condensations in free jet expansion are not believed to be important at flame temperatures and sub-atmospheric pressures for most flame constituents (6), however little is known about the behavior of the high molecular weight hydrocarbons and care must be taken to look for condensation effects in the interpretation of the data. Pressure diffusion, Mach number focussing and background scattering and effusion are more difficult effects to avoid altogether and all can be functions of source conditions. A study of their importance in this system and techniques for calibration of these effects is now underway. The limited data indicate that background scattering and effusion are negligible under the flame conditions presented here. Pressure diffusion and Mach number focussing are lumped together as "mass discrimination" and can be studied in this

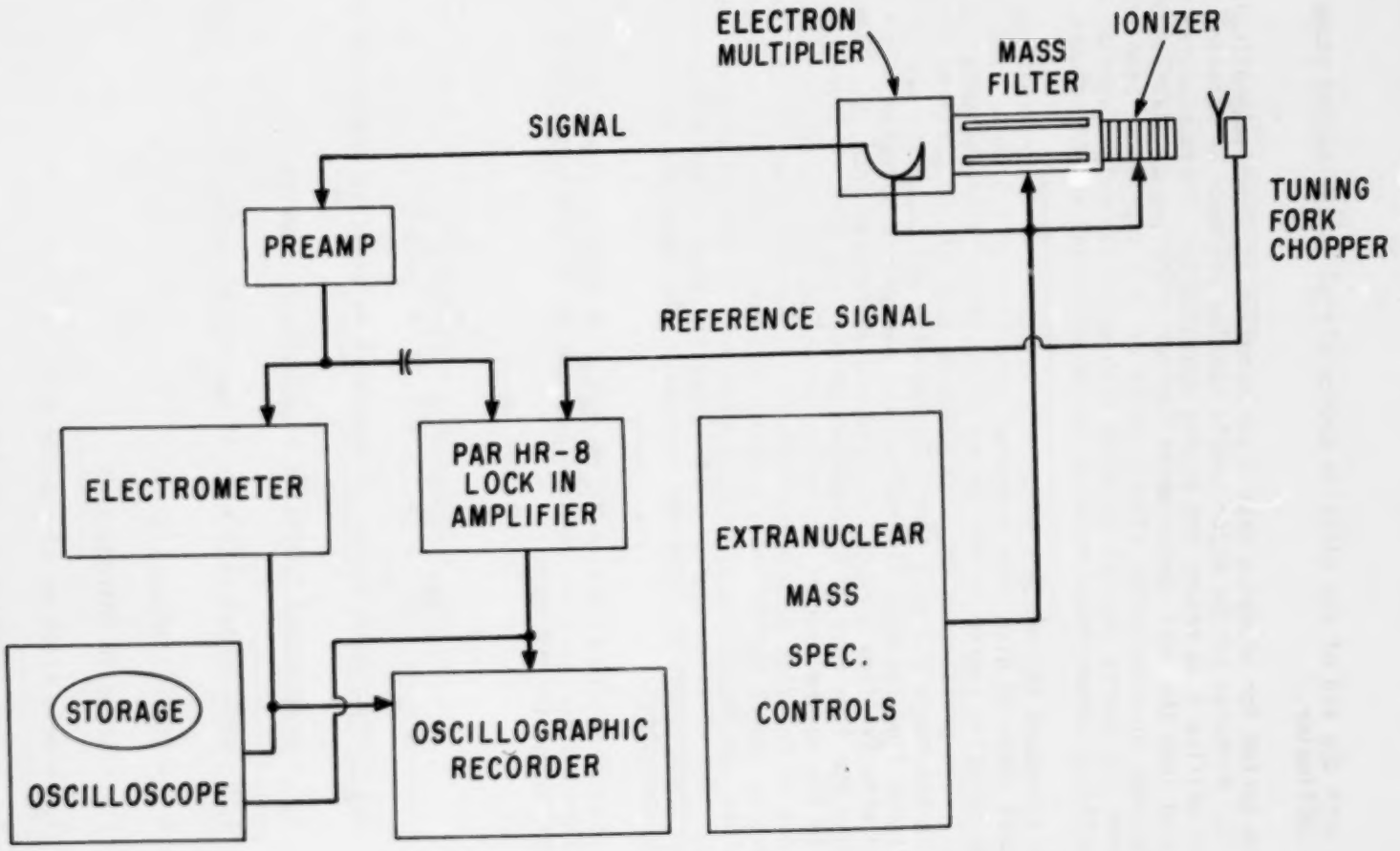

FIGURE 3. SCHEMATIC OF MASS SPECTROMETER INSTRUMENTATION

system with the aid of the effusive source placed in the second stage upstream of the collimator.

The system for studying mass discrimination is shown schematically in Figure 4. Mixtures of the major stable species are made by metering through critical orifice flow meters and mixing dynamically. These mixtures may be introduced into the mass spectrometer ionizer either as an effusive beam in which no mass discrimination effects occur or as a supersonic beam (through the burner and quartz nozzle) in which high molecular weight species are usually preferentially concentrated relative to low molecular weight species.

To introduce the mixture effusively without mass discrimination, a stainless steel sintered disc with a nominal pore size of 0.5 μm is used to leak into the effusive source in the second stage about 1% of the total gas flow by the disc. The pressure on the high pressure side of the sintered disc is maintained in the range 0.1 to 1 torr. Tubing size and pressures are designed to give viscous flow (no mass discrimination) everywhere upstream of the sintered disc and effusive flow through the disc and downstream from it. Under these conditions the flow rate of a component through the disc is inversely proportional to the square root of its molecular weight but its density anywhere downstream of the disc is proportional to its partial pressure upstream. Since the electron impact ionizer is a density detector, ratios of ion signals are proportional to the ratios of partial pressures in the gas mixture upstream of the disc. The effusive source inlet system has been tested with commercially prepared standard gas mixtures and reproduces the suppliers analysis to within 2% on any component.

By comparing signal ratios in the effusive beam to signal ratios in the sonic beam the mass discrimination between two species in a mixture can be characterized by an enrichment factor, α_{AB}:

$$\alpha_{AB} = \left(\frac{I_A}{I_B}\right)_S \Big/ \left(\frac{I_A}{I_B}\right)_E = \left(\frac{X_A}{X_B}\right)_S \Big/ \left(\frac{X_A}{X_B}\right)_E$$

where α_{AB} = enrichment factor of species A relative to species B, dimensionless

I_A = beam signal intensity of species A, amperes

I_B = beam signal intensity of species B, amperes

S = sonic introduction

E = effusive introduction

X_A = mole fraction of species A

X_B = mole fraction of species B

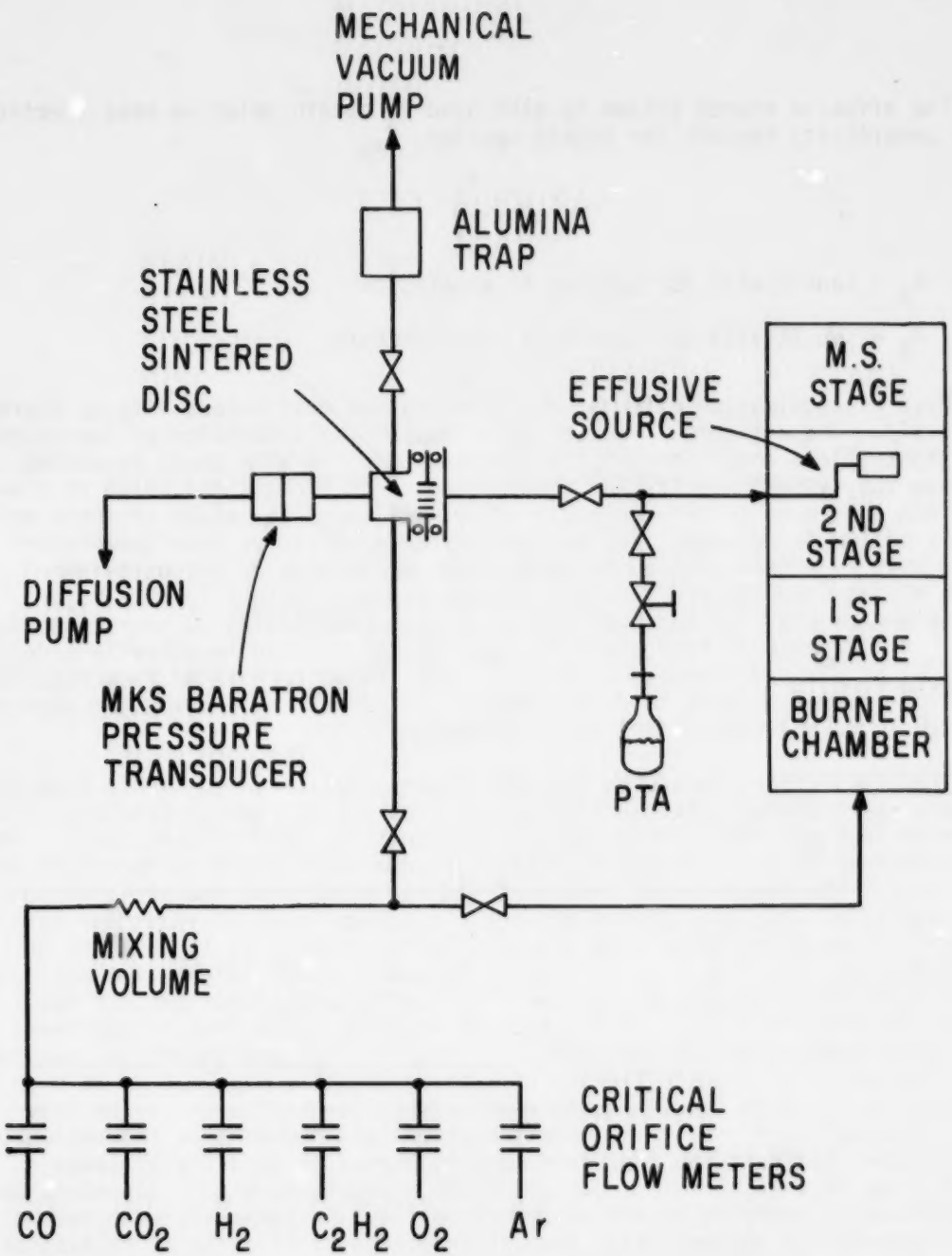

FIGURE 4. SCHEMATIC OF GAS INTRODUCTION SYSTEM FOR STUDYING MASS DISCRIMINATION

The effusive source system is also used to obtain relative mass spectrometer sensitivity factors for stable species, S_{AB}:

$$S_{AB} = \frac{k_A}{k_B}$$

where k_A = sensitivity for species A, amperes/torr

k_B = sensitivity for species B, amperes/torr

Mass discrimination effects have been studied most extensivity by Sharma et al. (7). The enrichment factor may or may not be a function of the source conditions (flame conditions at the sampling point in this case) depending upon how the system geometry and source conditions dictate the point of transition from continuum to free molecular flow. Although the study of these effects in this system is not complete, preliminary experiments ar room temperature with a mixture approximating the burned gas composition of the acetylene-oxygen flames studied here indicate that enrichment factors for the major species except that for hydrogen are relatively insensitive to source conditions. An increase in source density by a factor of five resulted in a decrease in $\alpha_{H_2,CO}$ of 23% and changes in all other enrichment factors of less than 12%. Further experimental work to assess the effect of gas composition and source density on the enrichment factors is planned.

The calibration procedures for mass discrimination in the sonic beam and for mass spectrometer sensitivities are carried out at room temperature. The effect of temperature on these two calibration steps must be considered. The mass spectrometer relative sensitivities in some cases might be functions of temperature. In conventional (residual gas analyzer) mass spectrometer ionizers variation with temperature of absolute ionizer sensitivities for total ionization have been found to be due only to the effects of temperature on gas density and the speed of the neutral molecule (which effects ion collection efficiency), implying that actual total ionization cross-sections are not temperature sensitive (8). In the type of molecular beam ionizer used here the neutral beam molecules are directed along the axis and toward the quadrupoles, therefore the ion collection efficiency might be expected to be high and less sensitive to translational temperatures perpendicular to the beam axis. Although total ionization cross-sections are temperature independent, fragmentation patterns and therefore mass spectrometer sensitivity (when a specific ion is used to follow concentration changes) is highly dependent upon the vibrational energies of the molecule-ion (9). As temperature increases more fragmentation occurs. With current knowledge of vibrational relaxation processes in supersonic expansions vibrational energies are impossible to predict and one must if possible avoid the use of high electron energies where fragmentation occurs. The appearance potentials of fragment ions, like heats of reaction, seem to vary but little with temperature (10). So, if fragmentation does not occur in room temperature calibrations it is not likely to occur in the case of the flame. However, in spite of these arguments, care must be taken in the interpretation of the data and simple experiments must be done to check temperature effects on mass spectrometer sensitivies due to

fragmentation effects whereever possible.

The effects of temperature on the mass discrimination enrichment factors must be assessed using the models designed to handle the prediction of enrichment factors for pressure diffusion and mach number focussing (5,6). Analysis of these models suggests that these mass discrimination effects depend upon temperature in only the way in which it effects the source density. Therefore enrichment factors from room temperature calibrations carried out at a reduced pressure to reproduce the source density conditions should apply to the higher pressure and temperature conditions in the flame.

Major Stable Species

In accordance with the considerations discussed above, the calibration for most major stable species involves the measurement of enrichment factors and relative mass spectrometer sensitivities. With this calibration information, ratios of mole fractions in the flame are calculated from ratios of signal intensities. In the flames studied here 5 mole % argon has been added to the unburned gases as an aid in following density changes in the flame front. Since calibration of this system for water is very uncertain the following relationships are used to calculate mole fractions from ratios of mole fractions in the tail of the flame where diffusion effects are negligible:

$$X_{O_2} + X_{Ar} + X_{CO} + X_{CO_2} + X_{H_2} + X_{H_2O} + X_{C_2H_2} = 1$$

an oxygen balance

$$\frac{n_I}{n_F}(X_{O_2})_I = X_{O_2} + \frac{X_{CO}}{2} + X_{CO_2} + \frac{X_{H_2O}}{2}$$

and argon balance

$$\frac{n_I}{n_F}(X_{Ar})_I = X_{Ar}$$

and from experimental measurements

$$\frac{X_{H_2}}{X_{Ar}}, \frac{X_{C_2H_2}}{X_{Ar}}, \frac{X_{O_2}}{X_{Ar}}, \frac{X_{CO}}{X_{Ar}}, \frac{X_{CO_2}}{X_{Ar}}$$

where n_I/n_F is the ratio of initial number of moles to final number of moles and $(X_A)_I$ refers to the mole fraction of species A in the unburned gas. Carbon and hydrogen balances can then be used to check the consistency of the data and calibrations. From the calculated ratio $\frac{X_{H_2O}}{X_{Ar}}$ in the tail of the flame and

experimental $\frac{I_{H_2O}}{I_{Ar}}$ ratio it is possible to obtain a calibration factor for water:

$$\frac{X_{H_2O}}{X_{Ar}} = C_{H_2O,Ar} \frac{I_{H_2O}}{I_{Ar}}$$

where I_i = signal intensity of species i, amperes

X_i = mole fraction of species i

$C_{H_2O,Ar}$ = calibration factor for water relative to argon.

Now with this additional piece of experimental information the oxygen and argon balances are not needed in the reaction zone where steep gradients require the use of diffusional terms. The assumption is made that $C_{H2O,Ar}$ is constant throughout the flame (i.e. the enrichment factor is not a function of gas density or composition and mass spectrometer relative sensitivity factors are not functions of flame position.)

Higher Molecular Weight Hydrocarbons

Due to the difficulty of introducing compounds that are liquids of low vapor pressure and solids at room temperature into the system to obtain mass spectrometer sensitivities and mass discrimination enrichment factors, all higher molecular weight hydrocarbon species measurements are made on a relative basis. To account for any changes in mass spectrometer relative sensitivities that might occur, the fragmentation pattern at 20 eV electron energy of perfluorotributylamine is recorded before and after each experiment.

EXPERIMENTAL PROCEDURE

To check out the experimental technique and procedures several fuel-rich acetylene-oxygen flames have been investigated. All flames had a cold gas velocity of 50 cm/sec and burned at a pressure of 20 torr. Five mole percent argon was added to the unburned gas. Four fuel equivalence ratios were investigated, ϕ = 1.5, ϕ = 2.0, ϕ = 2.4 (sooting limit) and ϕ = 3.0. Complete profiles were made for ϕ = 1.5, 2.0 and 2.4. Two points near the end of the oxidation zone were sampled in the ϕ = 3.0 flame.

The mass spectrometer resolution controls were set to give unit resolution from 18 to 502 a.m.u. The electron energy was set at a nominal 20eV which corresponded to an actual electron energy of 17.1eV according to argon ionization potential measurements. At these conditions, room temperature

fragmentation of O_2, CO_2, CO and H_2O does not occur. For acetylene peak 25 is less than 1% of peak 26. Mass spectrometer sensitivity and beam enrichment factor calibrations were made before and after each flame run. Two sweeps across the mass range 0 - 230 a.m.u. were made at each flame position at a speed of $\sim$ 1 a.m.u./sec.

RESULTS AND DISCUSSION

Profiles of signal intensities relative to argon for the ϕ = 2.4 flame are shown in Figures 5 and 6. The mole fractions of the major stable species in the burned gas, as calculated from the procedure described above, are included in Figure 5.

The experimental points with the most scatter are the hydrogen and water profiles. The characteristics of quadrupole mass spectrometers make it difficult to have a high sensitivity for hydrogen and high molecular weight hydrocarbon species simultaneously. To improve upon this measurement different tuning conditions can be used for the low molecular weight gases and the high molecular weight hydrocarbons. The noise in the water signal is due to a large background peak at 18 a.m.u. The additional cryogenic pumping in the ionizer region should improve this measurement.

The general features of the profiles are in agreement with the measurements on a similar flame by Homann and colleagues (11,12). About 5.5 mole % of the acetylene is present in the burned gases. The other hydrocarbons in the burned gases are mostly polyacetylenes. They increase through the early part of the oxidation zone and maximize at about 1 cm. Detectable amounts of polyacetylenes up to C_8H_2 are still present in the burned gas. Polyacetylene formation is preceded in the oxidation zone by vinylacetylene (C_4H_4) and a C_6H_6 compound that could be benzene or a straight chain hydrocarbon. These compounds have concentration maxima that are at least an order of magnitude lower than the polyactylene of the same carbon number.

The interaction between the major stable species and the hydrocarbon species throughout the flame is complex and interesting. Oxygen is completely consumed by about 1.4 cm. At this point CO and H_2 have nearly reached their final values. CO_2 and H_2O molefractions peak near 1 cm and decrease slightly into the burned gas. Acetylene continues to decrease until about 2.5 cm above the burner. These basic features can be explained qualitatively by the following scheme of competing reactions early in the oxidation zone:

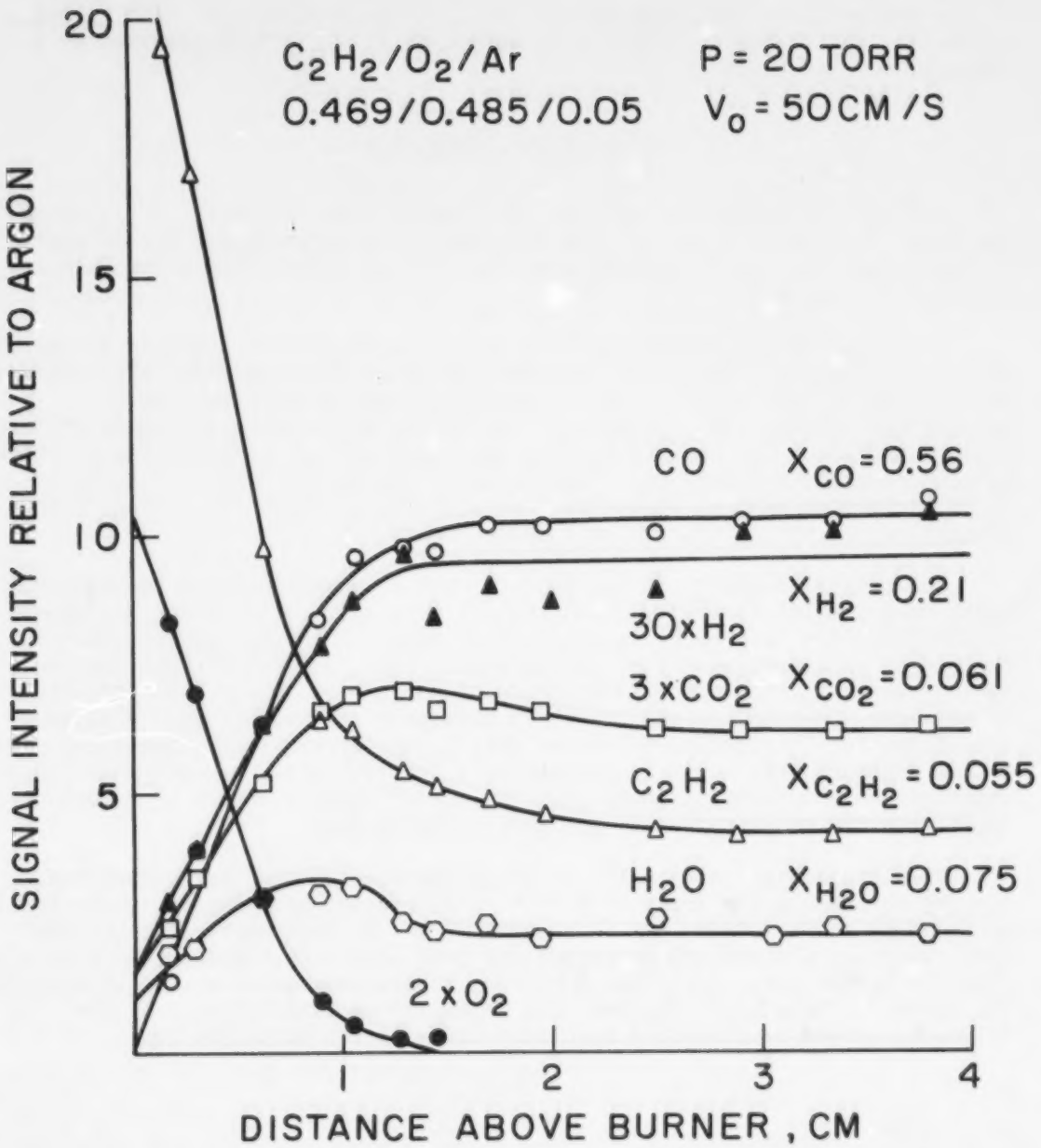

FIGURE 5. PROFILES OF SIGNAL INTENSITIES RELATIVE TO ARGON FOR MAJOR STABLE SPECIES IN AN ACETYLENE-OXYGEN FLAME NEAR THE SOOTING LIMIT. ϕ = 2.4, P = TORR, V_0 = 50 CM/S, 5M% ARGON

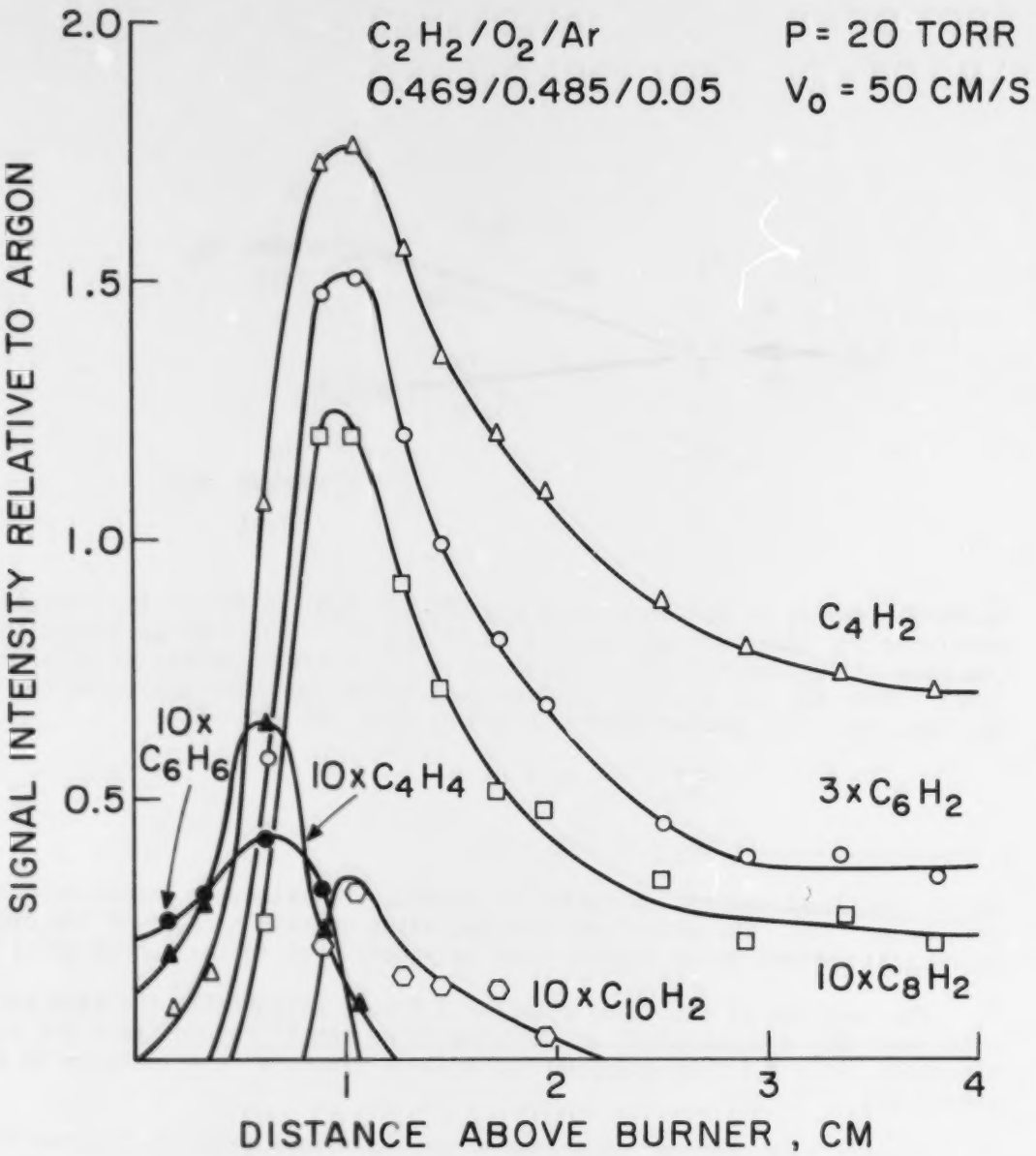

FIGURE 6. PROFILES OF SIGNAL INTENSITIES RELATIVE TO ARGON FOR MINOR SPECIES IN AN ACETYLENE-OXYGEN FLAME NEAR THE SOOTING LIMIT. ϕ = 2.4, P = 20 TORR, V_0 = 50 CM/S, 5M% ARGON

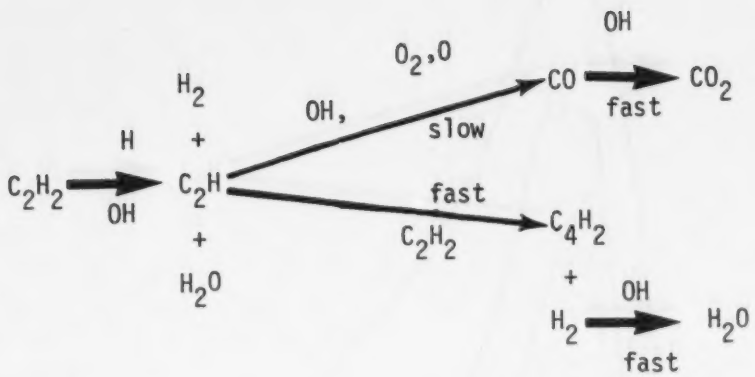

Reaction leading to polyacetylenes and CO_2 and H_2O are faster than reactions involving the same radicals leading to CO and H_2. This ties up oxygen in the form of CO_2 and H_2O and produces super equilibrium amounts of polyacetylenes. Near the end of the oxidation zone where the temperature reaches its maximum, reactions producing OH, CO and H_2 from CO_2 and H_2O:

$$H_2O + H \rightarrow OH + H_2$$

$$CO_2 + H \rightarrow CO + OH$$

become important and the oxidation of polyacetylenes becomes faster than their production (13). The oxidation rate decreases quickly because of the drop in OH radical concentration leaving some polyacetylenes in the burned gas (14).

The features of the flame with ϕ = 2.0 were essentially the same but with lower CO, H_2, acetylene and polyacetylene concentrations as might be expected. At ϕ = 1.5 no acetylene or polyacetylenes were detectable in the burned gas.

Signals were observed at masses other than those shown in Figures 5 and 6. Table I lists those masses at which positive identifications were not made or contributions from several species were not sorted out. Masses 15, 16 and 17 peak in the middle of the oxidation zone. The most probable contributor to peaks 15 and 16 is methane in this fuel rich flame. Masses 29 and 30 are maximum at the lowest sampling point, 0.17 cm and the contribution of H_2CO to peak 29 has not been determined at these mass spectrometer conditions. Mass 34 appears only at the lowest sampling point. Mass 39 maximizes at 0.62 cm from the burner. Mass 42, probably corresponding to propylene, maximizes at 0.35 cm. Appearance potential measurements along with measurements at lower electron energies to prevent contributions from fragmentation of hydrocarbons must be made to make positive identifications.

TABLE I. MASSES AT WHICH SIGNALS WERE OBSERVED BUT POSITIVE IDENTIFICATIONS WERE NOT MADE. $\phi = 2.4$, P = 20 TORR, V_0 = 50 CM/S

MASS	POSSIBLE CONTRIBUTING SPECIES
14	CH_2
15	CH_3, CH_4
16	CH_4 (MOST PROBABLE), O
17	OH
25	C_2H , C_2H_2
29	HCO , H_2CO, $C^{13}O$
30	H_2CO, C_2H_6 (UNLIKELY)
34	H_2O_2
38	C_3H_2
39	C_3H_3 , $C_3H_3^+$
42	C_3H_6

Mass spectra were observed at two points near the end of the oxidation zone of a sooting flame of fuel equivalence ratio $\phi = 3.0$. In addition to the species observed in the $\phi = 2.4$ flame several higher molecular weight aromatic hydrocarbons were observed. Their masses, molecular formula and possible structures are listed in Table II. The sensitivity for higher molecular weight hydrocarbons (100 a.m.u. and above) should be increased by an order of magnitude when the cryogenic pumping in the ionizer region is added since the present sensitivity is limited by noise in the beam spectrum caused by high levels of hydrocarbons in the background.

SUMMARY

A molecular beam mass spectrometer system has been developed for studying sooting flames. Preliminary measurements suggest that molecular beam mass discrimination effects may be relatively insensitive to source conditions and that absolute concentration measurements of major stable species profiles will be possible.

Profiles of relative signal intensities of several non-sooting and barely sooting acetylene-oxygen flames have been made. The results are in agreement with those of previous investigators. Polyacetylenic hydrocarbons up to mass 146 were detected and are the major hydrocarbons present other than the unburned fuel. Maxima in the carbon dioxide and water profiles are supportive of the suggestion that reactions that store oxygen in these species are rapid compared to reactions that lead to CO formation from the fuel in the early part of the flame. At the higher temperatures present at the end of the oxidation zone this oxygen is released in the form of OH that attacks polyacetylene and unburned fuel.

Under strongly sooting conditions ($\phi = 3.0$) aromatic hydrocarbons have been detected. The addition of cyrogenic pumping in the ionizer region is expected to increase the sensitivity for these species by an order of magnitude.

ACKNOWLEDGEMENTS

This work has been done under EPA Grant No. R 803242.

TABLE II. ADDITIONAL SPECIES NEAR THE END OF THE REACTION ZONE IN A C_2H_2/O_2 FLAME, ϕ = 3.0, P = 20 TORR, V_0 = 50 CM/S

MASS	MOLECULAR FORMULA	POSSIBLE SPECIES	STRUCTURE
92	C_7H_8	TOLUENE	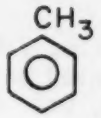
102	C_8H_6	PHENYLACETYLENE	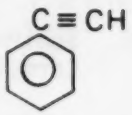
104	C_8H_8	STYRENE	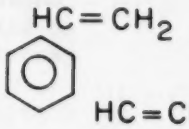
118	C_9H_{10}	METHYL STYRENE	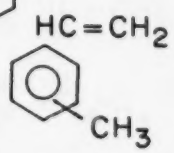
128	$C_{10}H_8$	NAPHTHALENE	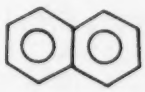
130	$C_{10}H_{10}$	PHENYL BUTADIENE	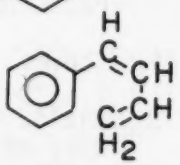
		DIHYDRONAPHTHALENE	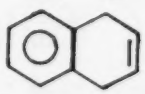
142	$C_{11}H_{10}$	METHYL NAPHTHALENE	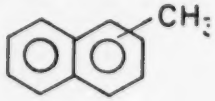
146	$C_{12}H_2$	HEXACETYLENE	$HC\equiv C(-C\equiv C-)_4C\equiv CH$

REFERENCES

1. Butze, H.F., and R.C. Ehlers NASA Tech. Mem. NASA JMX-71789. Paper presented at Western States Section of the Combustion Institute, Palo Alto, CA. Oct. 20, 1975.

2. Schirmer, R.M. in "Emissions from Continuous Combustion Systems", W. Cornelius and W.G. Ahnew, ed., p. 189, Plenum Press, N.Y. (1972).

3. Longwell, J.P., "Synthetic Fuels and Combustion" Plenary lecture presented to Sixteenth Symposium (International) on Combustion, Cambridge, Massachusetts, August, 1976.

4. Biordi, J.C., C.P. Lazzara, and J.F. Papp, Combust. Flame 23, 73 (1974).

5. Wersborg, B.L., J.B. Howard, and G.C. Williams, Fourteenth International Symposium on Combustion, p. 929, The Combustion Institute (1973).

6. Knuth, E.L., "Direct Sampling Studies of Combustion Processes" in "Engine Emissions, Pollutant Formation and Measurement", G.S. Springer and D.J. Patterson, ed., p. 319, Plenum Press, N.Y. (1973).

7. Sharma, P.K., E.L. Knuth and W.S. Young, J. Chem. Phys. 64, 4345 (1976).

8. Field, F.H. and J.L. Franklin, "Electron Impact Phenomena and the Properties of Gaseous Ions," pp. 202-203, Academic Press, N.Y. (1970).

9. Ibid. pp. 203-204.

10. Ibid., p. 81.

11. Homann, K.H. and H.Gg. Wagner, Berichte der Bunsengesellschaft 69, 20 (1965).

12. Bonne, U., K.H. Homann, and H. Gg. Wagner, Tenth Symposium (International) on Combustion, p. 503, The Combustion Institute (1965).

13. Homann, K.H. Combust. and Flame 11, 265 (1967).

14. Bonne, U., H. Gg. Wagner, Berichte der Bunsengesellschaft 69, 35 (1965).

APPENDIX C

Soot Concentration Measurements in Fuels Doped with Nitrogen and Sulfur Containing Compounds (Unpublished)

SOOT CONCENTRATION MEASUREMENTS IN FUELS DOPED WITH NITROGEN AND SULFUR CONTAINING COMPOUNDS

by

William J. Kausch,Jr.
Department of Chemical Engineering
Massachusetts Institute of Technology
Cambridge, Massachusetts 02139

September, 1977

INTRODUCTION

The purpose of this experimental program was to study the formation of soot and polycyclic aromatic hydrocarbons (PCAH) in fuels doped with nitrogen and sulfur containing compounds. The main fuel studied was benzene, but for purposes of comparison a few experiments were also conducted with hexane and methane, representing (H/C) ratios of 1, 2.3, and 4, respectively. The oxidant used was oxygen rather than air to allow comparison with other flame studies conducted with oxygen, and to assure that the origin of any nitrogen contained in polycyclics formed in the inner cone of the flame would have to be the fuel rather than atmospheric nitrogen.

The use of pure oxygen rather than air led to a benzene flame speed greater than could be stabilized at convenient gas flows on a one-inch diameter burner, without resorting to a fuel equivalence ratio (ϕ) greater than 1. As a flame this rich was undesirable, methane was added to the fuel in order to lower the flame speed to an acceptable level. A smaller diameter burner was not substituted since the water-cooled sampling probe might create too much disturbance in a smaller flame.

The benzene and hexane studies were conducted with a CH_4/C_6H_x (x = 6 or 14) ratio of 1.5 and a ϕ = 4.5. For all studies the cold gas velocity (v) was kept constant at 31.8 cm/sec. Soot collected by the probe was trapped in glass wool packed filters and the PCAH extracted and analyzed by gas chromatography.

APPARATUS AND EXPERIMENTAL DESIGN

The arrangement of the apparatus is shown in Figure 1. The burner used was a modified Meker burner (see Fig. 2). The four air inlets were replaced with oxygen feeds, and the fuel inlet was attached to 0.25 inch stainless steel tube through which the benzene/methane mixture was fed. The fuel mixture was preheated electrically with heating tape to vaporize the benzene. The oxygen feeds were also preheated to approximately the same temperature (300-320°C) to prevent benzene condensation inside the burner.

Temperatures were measured via thermocouples in the lines; CH_4 and O_2 flows were monitored by critical orifices, and the benzene flow was measured before vaporization by passing the liquid through a capillary tube with the upstream and downstream pressures carefully measured. The liquid flows used corresponded to Reynolds numbers of between 800-1000 through the capillary tube. Thus the flow was always laminar and proportional to the pressure drop through the tube.

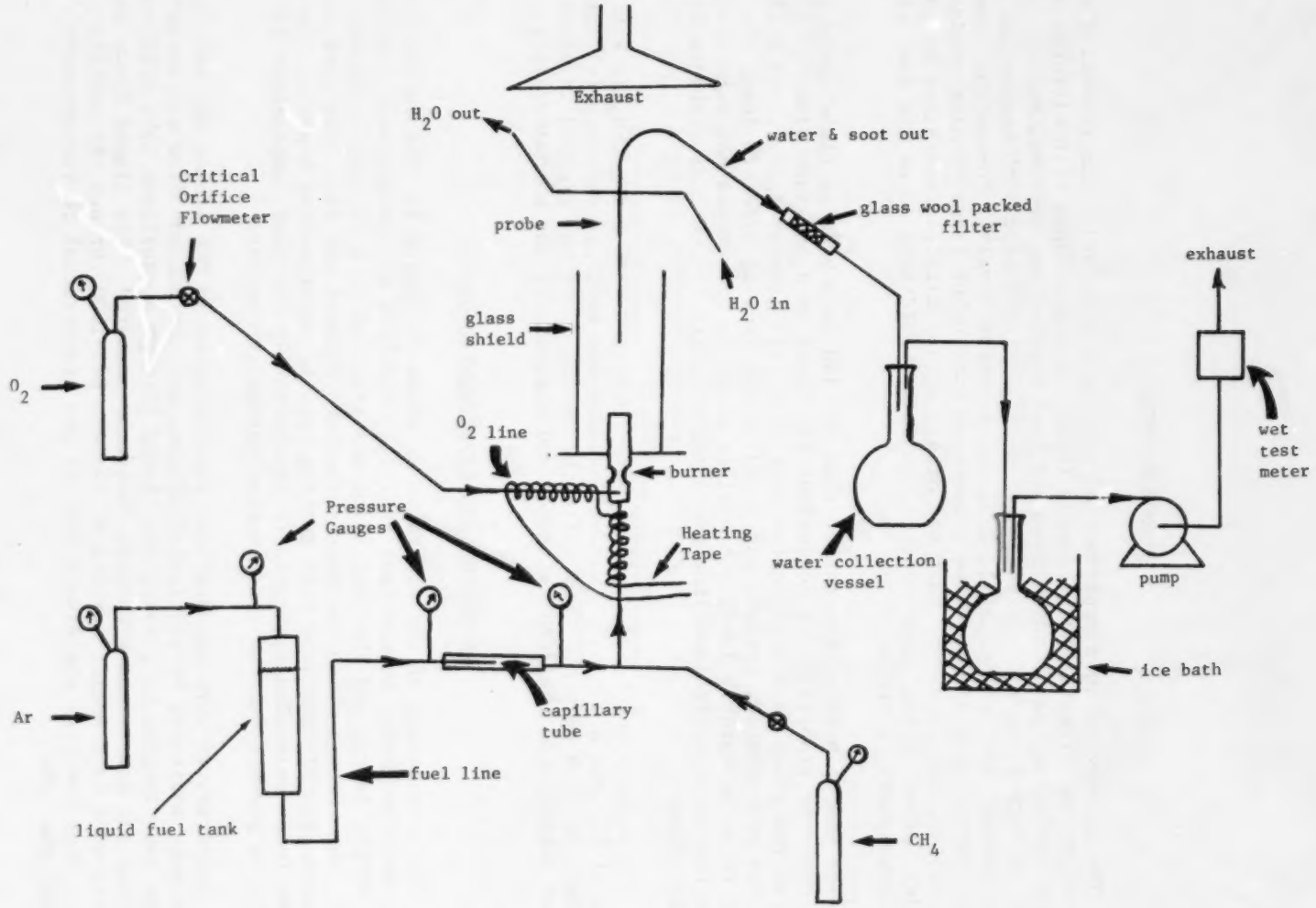

FIGURE 1. Overall Experimental Arrangements

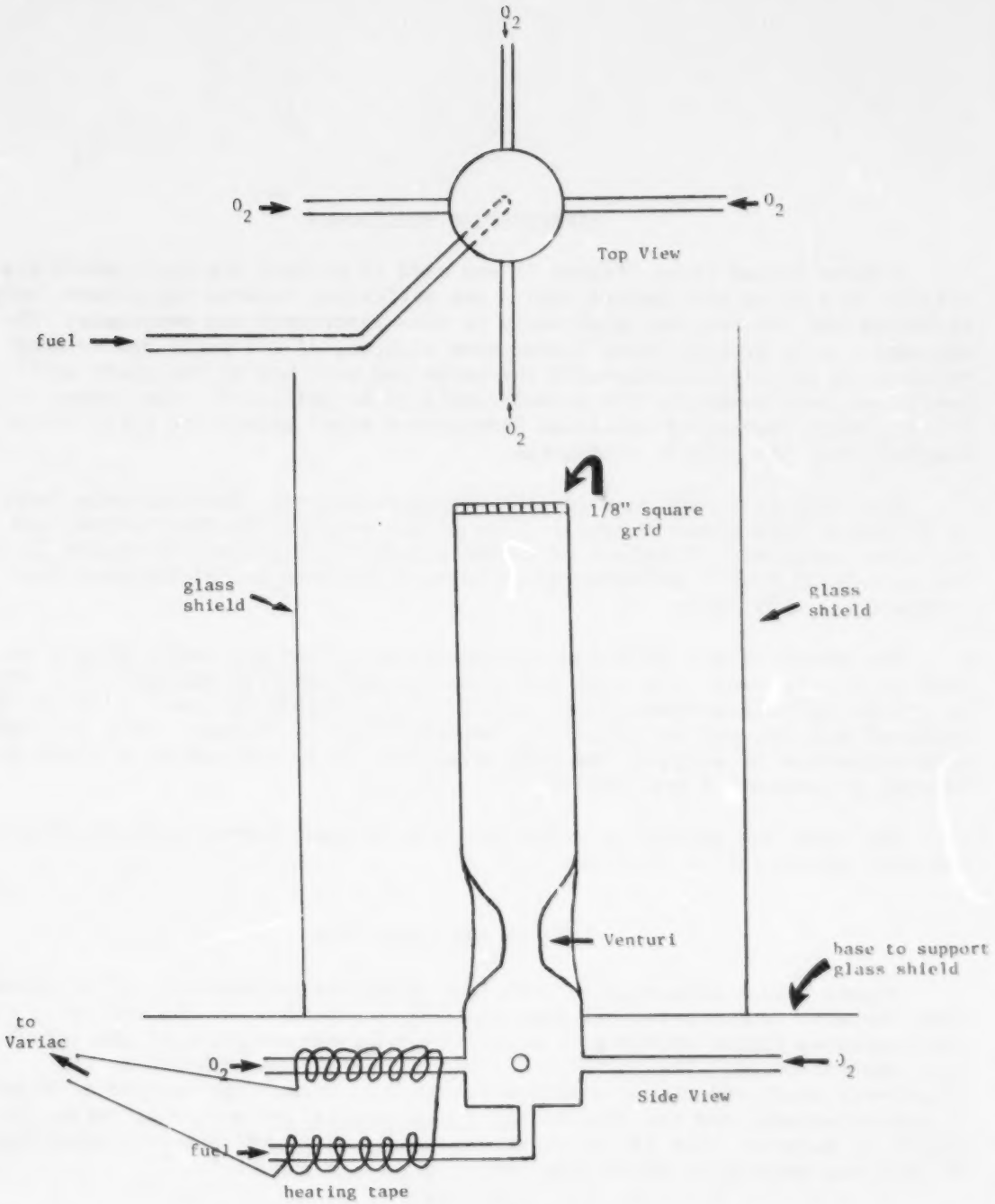

FIGURE 2. Burner Details

EXPERIMENTAL PROCEDURE

A water cooled probe (Figure 3) was used to collect the soot, which was trapped in a glass wool packed tube. One difference between the present sampling technique and the one used previously in this laboratory was necessary. The extremely sooty benzene flame caused some clogging of the probe due to soot build-up at the tip; consequently the probe was kept out of the flame until all conditions were ready for the actual sample to be collected. The bypass filter, which previously collected "extraneous soot" before and after the actual sampling run, was totally eliminated.

Four additives were used for the doping procedure. Two compounds (pyrrole or pyridine) were added to obtain 1% by weight nitrogen in the benzene, and two other compounds (thiophene or carbon disulfide) were used to obtain 1% sulfur. One percent of N or S was selected as being representative of the practical interest for many fuels.

The amount of gas collected through the probe was monitored using a wet test meter. As usual, the soot was extracted with acetone and methylene chloride to obtain the yellow-orange colored PCAH. The analysis of these solutions is achieved with GC, and as necessary, combined GC/MS techniques. Soot concentrations were calculated by weighing the soot collected (after extraction of PCAH) and knowing the amount of gas sampled.

The flame was sampled at different heights above burner (HAB) to obtain the soot concentration profiles.

RESULTS AND DISCUSSION

Figure 4 is a composite for all four additives to benzene. It is assumed that the soot concentration is approximately independent of the additive; thus the composite figure should give a fairly good representation of the actual soot concentration. The validity of this approximation is based on the relatively small amounts of additive required to obtain the desired 1% N and S concentrations, and the similarity of the chemical structure of these compounds to benzene. The 1% concentrations were calculated based on molecular weights and densities, as follows (using CS_2 as an example):

MW CS_2 = 76.14

Atomic wt. S in CS_2 = 64.14

MW benzene = 78.11

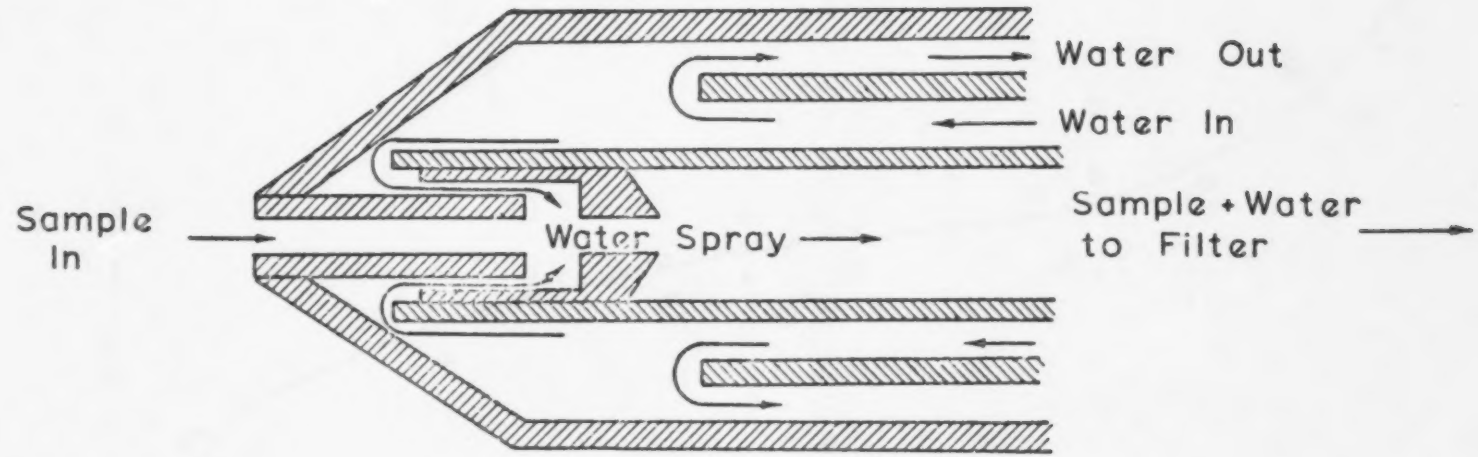

FIGURE 3. Water-Cooled Sampling Probe

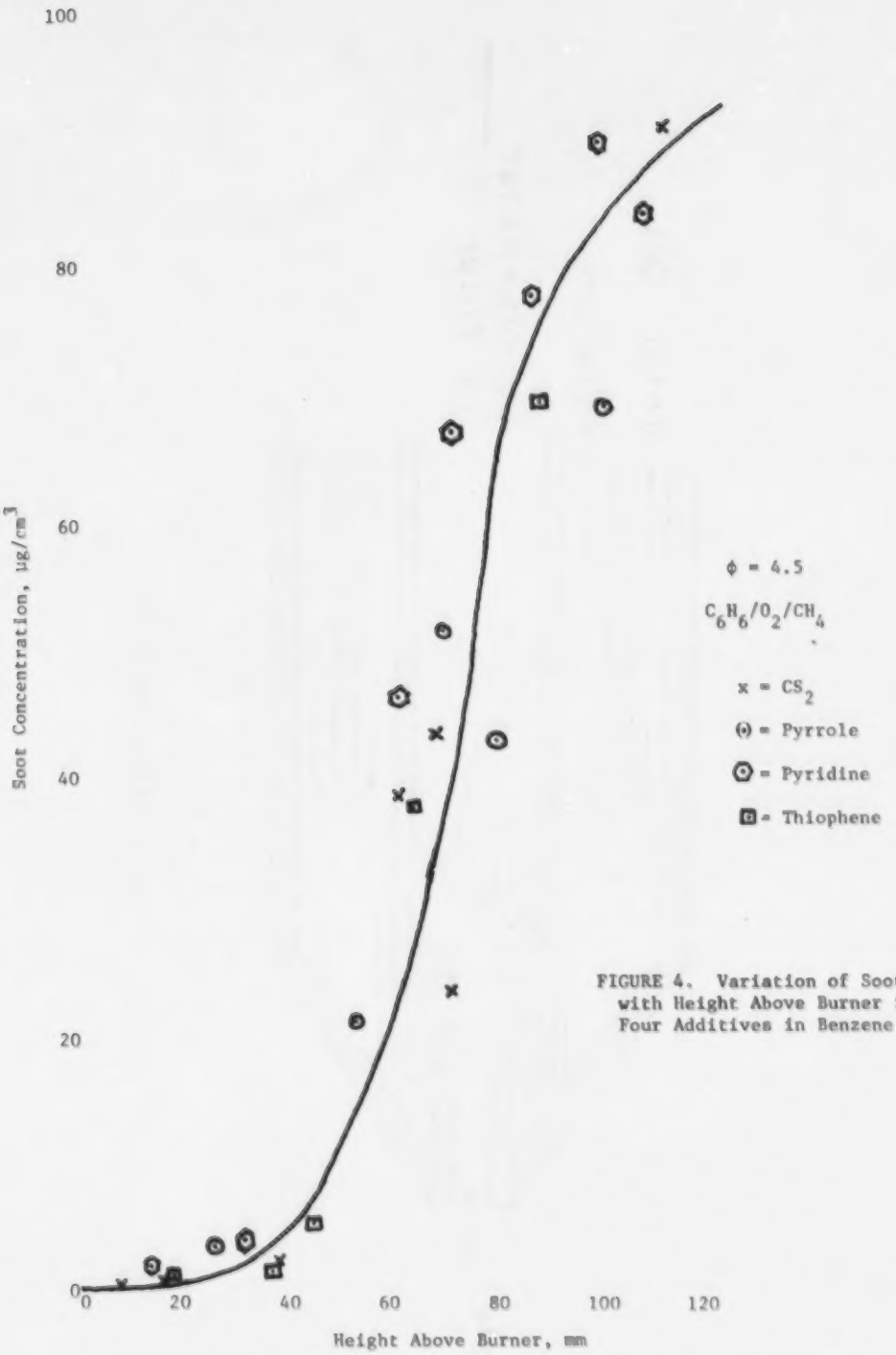

FIGURE 4. Variation of Soot Concentration with Height Above Burner for Each of Four Additives in Benzene

Letting x = wt. fraction (benzene/CS_2),

$$\frac{64.14}{76.14 + x(78.11)} = 0.01$$

Solving, x = 81.14. This implies that we need 1 g of CS_2 per 81.14 g of benzene. Using densities @ 20°C,

density C_6H_6 = 0.8786 g/ml

density CS_2 = 1.2632 g/ml

one obtains 1.00 ml of CS_2 per 116.67 ml of C_6H_6.

This is admittedly the lowest ratio of the four additives, but for the other three compounds the (C/H) ratio is approximately one, as is that of benzene. Furthermore the structures are all or mostly aromatic, benzene being of course totally aromatic (see Table 1). In all cases the carbon atoms are in aromatic or at least double-bonded positions. Thus we confidently make the aforementioned approximation, and also consider only the C_6H_6 and CH_4 in the balanced chemical reaction to determine the 4.5 fuel equivalence ratio.

The benzene/oxygen/methane flame had a very bright and distinct inner cone of approximately 70 mm height, thus points shown in Fig. 4 below 70 mm HAB can be assumed to be similar to a premixed flame, while those above 70 mm HAB are from the diffusion-like tail of the flame. Concentrations are reported in $\mu g/cm^3$ at 20°C and 1 atm. on a water free basis.

The curve in Fig. 4 has been drawn to favor the lower concentration points (at a given HAB) especially at low HAB. The reason for this is that the small shell-like diffusion flame which formed around the edges of the burner was observed to have much more soot than inside the flame (probably due to low temperatures which prevented soot burnout), and due to the sampling probe being moved quickly in and out of the flame at the beginning and ending of the sample collection, the probe was exposed to this soot for a fraction of a second. This effect is negligible in the upper portions of the flame (> 70 mm) where there was so much soot that 40-50 mg were usually collected; however, in the lower portions of the flame (< 40 mm), this effect might have some small significance since usually less than 10 mg of soot was collected. The curve is thus drawn very low at HAB's less than 40 mm, despite some high points in this region.

Unfortunately, Fig. 4 does not represent the whole story, as some highly suspect points have been removed. These points are shown in Figs. 5-8, which represent each of the additives separately. The curves drawn through the data ignore the suspected bad points. These curves tend to differ slightly from the composite graph (Fig. 4), probably due only to an insufficient number of points.

Table 1. Information on Benzene and Additives

Compound	Structure	MW	Density	Volume ratio ml additive / ml benzene 1% N or S	C/H ratio	% Aromatic Atoms (C,S, or N)
Benzene		78.11	.8786	-	1.0/1.0	100%
Pyridine	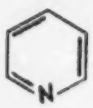	79.1	.9812	1.00/18.88	1/1	100%
Pyrrole		67.04	.9691	1.00/18.81	4/5	80% (not N)
Thiophene		84.14	1.0882	1.00/49.52	1/1	80% (not S)
Carbon Disulfide	S=C=S	76.14	1.2632	1.00/116.64	1/0	100%

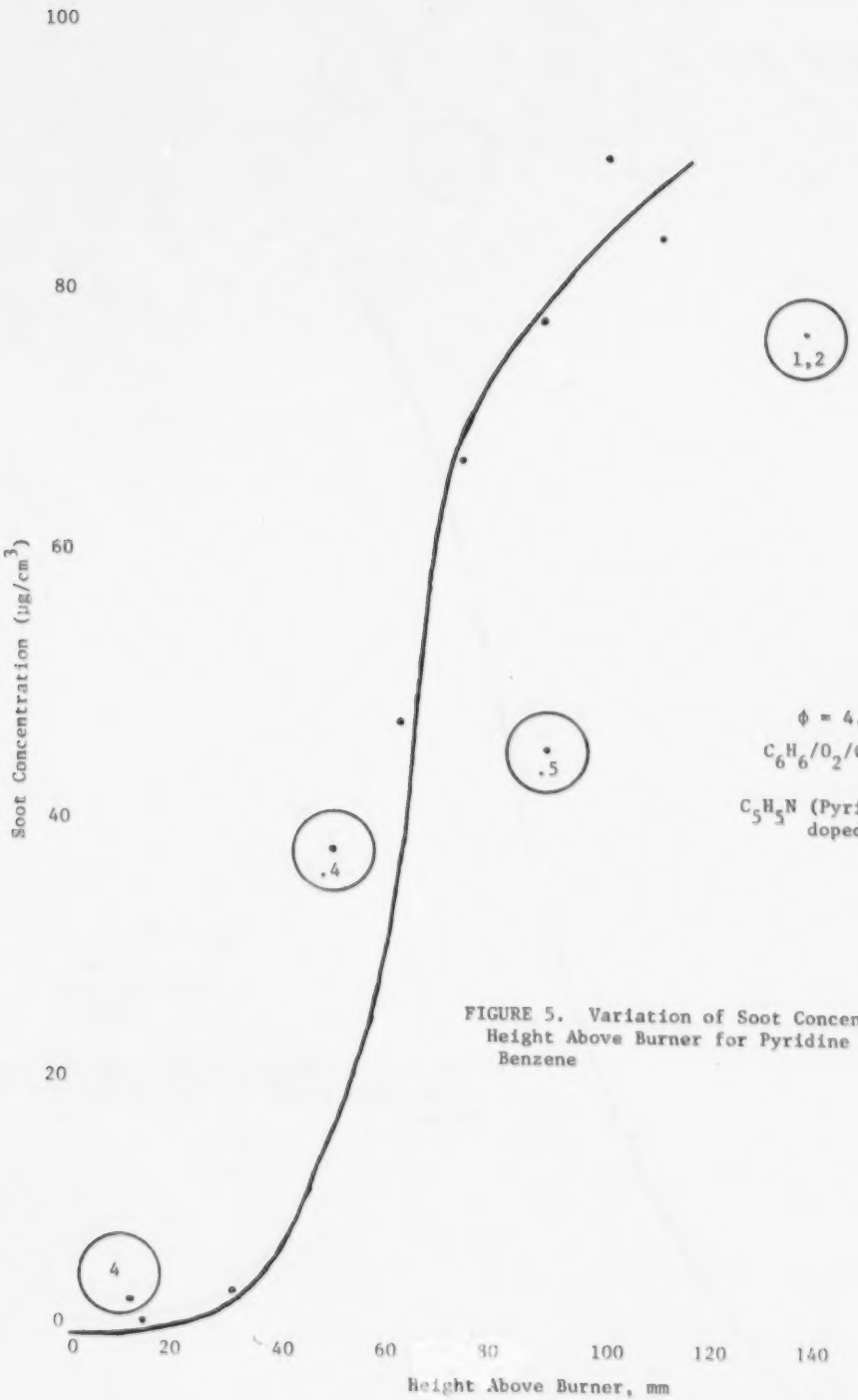

FIGURE 5. Variation of Soot Concentration with Height Above Burner for Pyridine Additive in Benzene

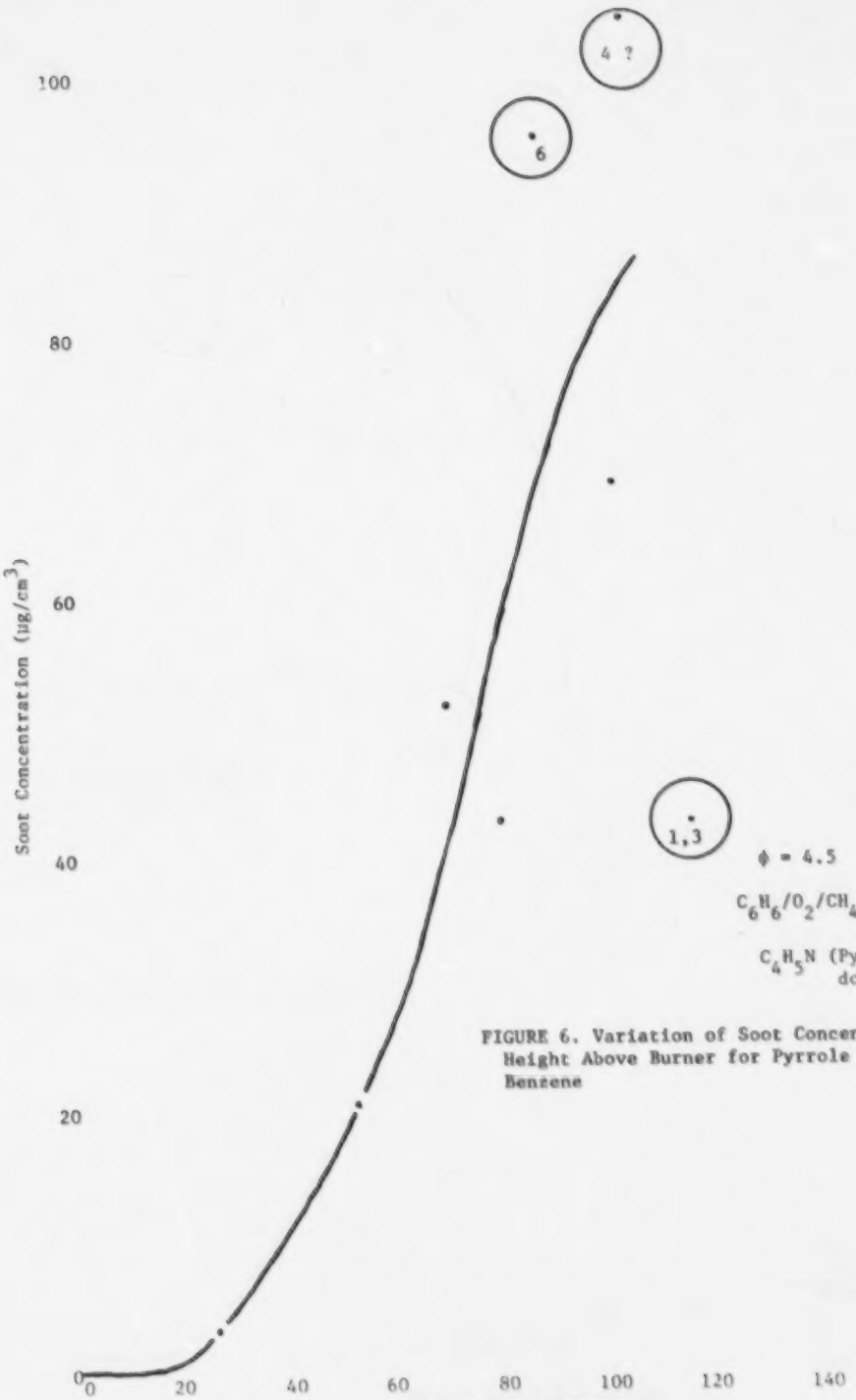

FIGURE 6. Variation of Soot Concentration with Height Above Burner for Pyrrole Additive in Benzene

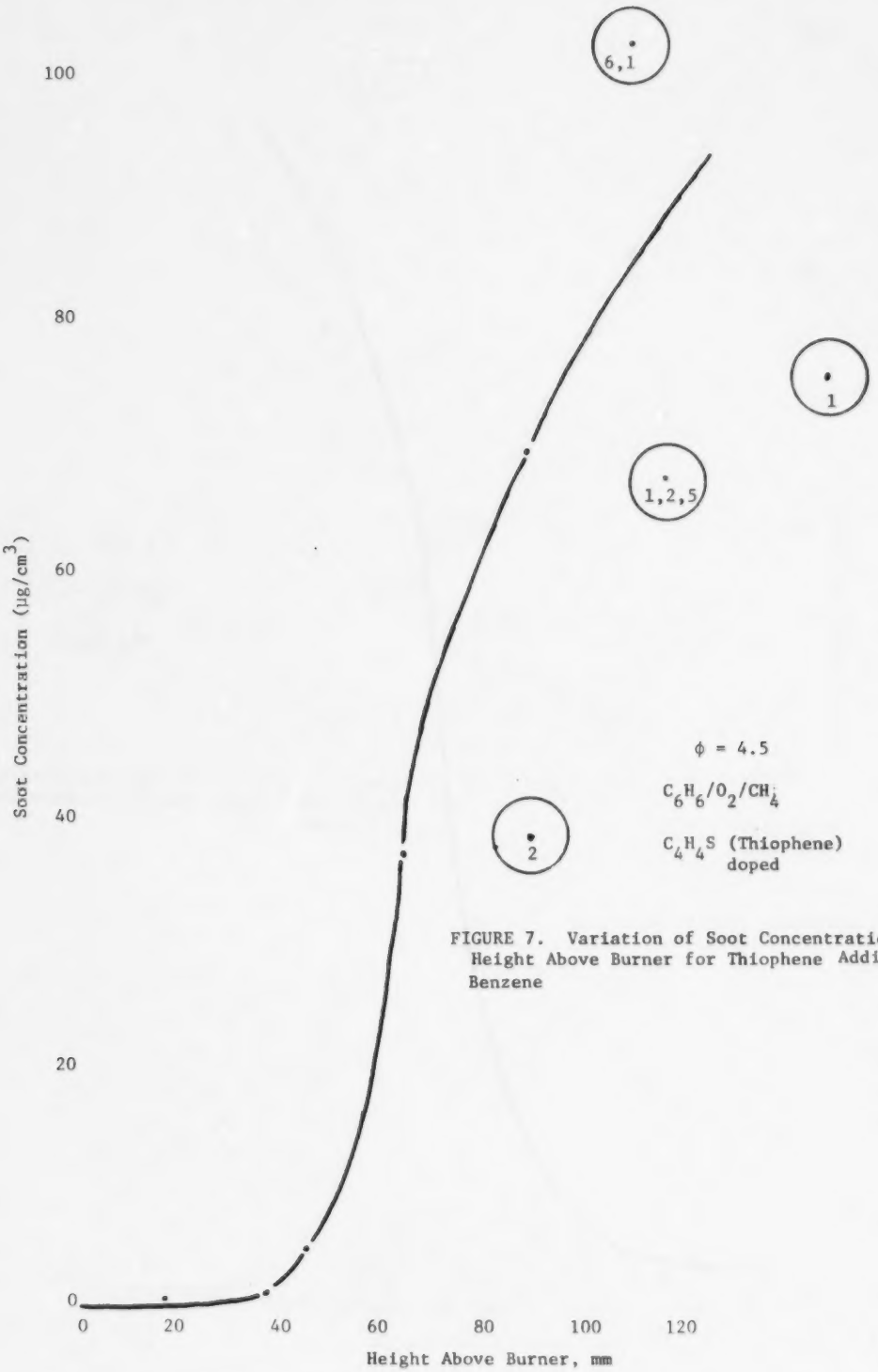

FIGURE 7. Variation of Soot Concentration with Height Above Burner for Thiophene Additive in Benzene

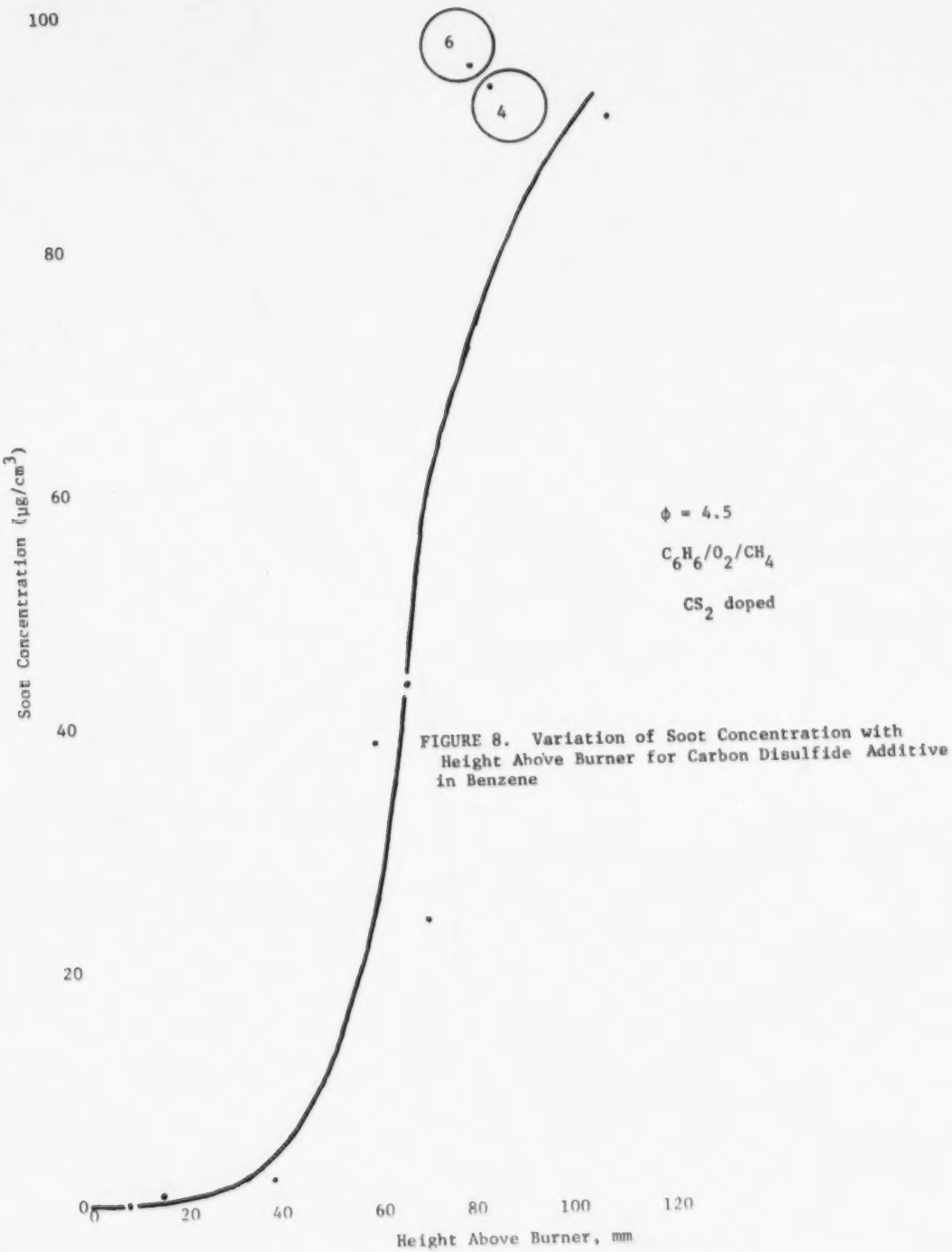

FIGURE 8. Variation of Soot Concentration with Height Above Burner for Carbon Disulfide Additive in Benzene

A circle around a point indicates that it does not appear on the composite. The reasons why the points are believed to be in error are listed below with numbers, referring to the numbers in the figures.
(1) Sample was taken at a height greater than 110 mm, where, due to quivering of the diffusion flame, it was difficult to tell when the probe was in the flame and when it was not.
(2) A very large amount of soot was collected and some leaked through the filter during the PCAH extraction.
(3) The probe appeared to clog slightly.
(4) The probe was exposed to the outer diffusion flame shell (discussed above) for much longer than usual, typically due to the probe slipping during a run.
(5) Much lower than usual gas suction rate through the filter.
(6) Much higher than usual gas suction rate through the filter.
(7) Filter containing soot chipped after completion of sampling. Pieces were weighed, but a small piece of glass must have been lost.

Two other fuels (methane and hexane) were also tested on this burner at the same ϕ and v. Graphs of data from these two cases are shown in Fig. 9 and 10. The methane/oxygen flame was not doped with any additive, but the hexane/oxygen/methane flame contained both thiophene and pyrrole (both five member rings) in proportions such that the final liquid mixture had 1% N and 1% S. The (CH_4/C_6H_{14}) ratio was also set at 1.5, the same as for the benzene studies. Despite the same ϕ and v, neither the hexane nor the methane flame exhibited an inner cone; however the shape of the soot concentration curves are approximatly the same as before. The range of soot concentration curves are approximately the same as before. The range of soot concentrations with hexane is 1/25th of that for benzene (from 0-100 $\mu g/cm^3$ to 0-4 $\mu g/cm^3$) and for methane it is 1/50th (from 0-100 $\mu g/cm^3$ to 0-2 $\mu g/cm^3$).

It was earlier stated that the presence of the additive was negligible calculating the fuel equivalence ratio. This approximation may become suspect when one extends it to two additives, as was done with hexane. However, calculations show that the approximation is still very good.

A few samples were also made at a $\phi = 4.0$, using once again a benzene and methane mixture as fuel. In order to attain this lower ϕ with the same v on our one-inch diameter burner, the ratio (CH_4/C_6H_6) unfortunately had to be increased from 1.5 to 2.0. The resultant flame had an inner cone height of only 54 mm, rather than 70 as with the (CH_4/C_6H_6) ratio = 1.5 and $\phi = 4.5$.

The presence of more methane and less benzene, as well as a lower ϕ would lead one to expect lower soot concentrations at a given HAB, yet a comparison of Figs. 4 and 11 show that this is not the case. This phenomena can perhaps best be explained by the difference in inner cone heights. If one were to plot the concentration versus the height, above this inner cone, the resultant shift to the right of the $\phi = 4.0$ curve would bring it under the $\phi = 4.5$ curve, as expected.

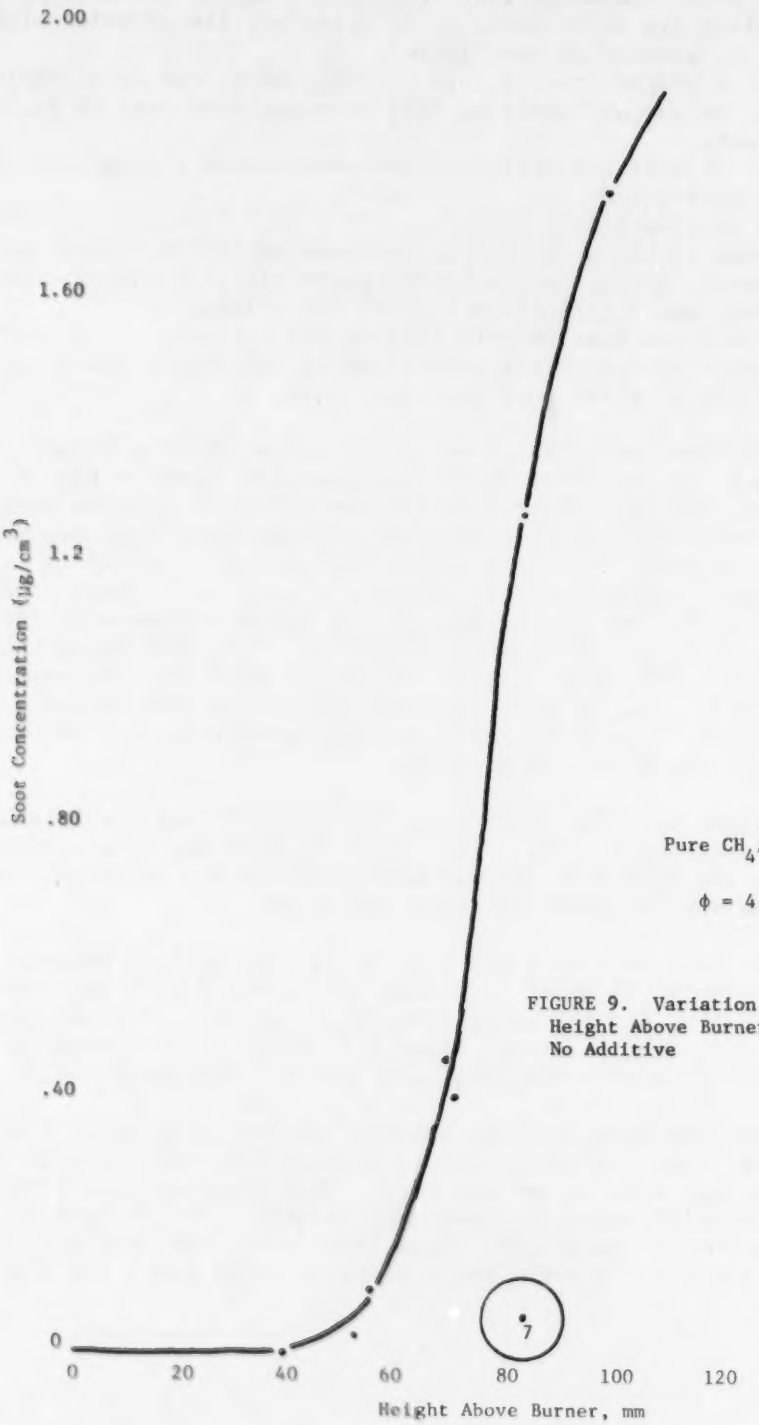

FIGURE 9. Variation of Soot Concentration with Height Above Burner for Pure Methane Fuel with No Additive

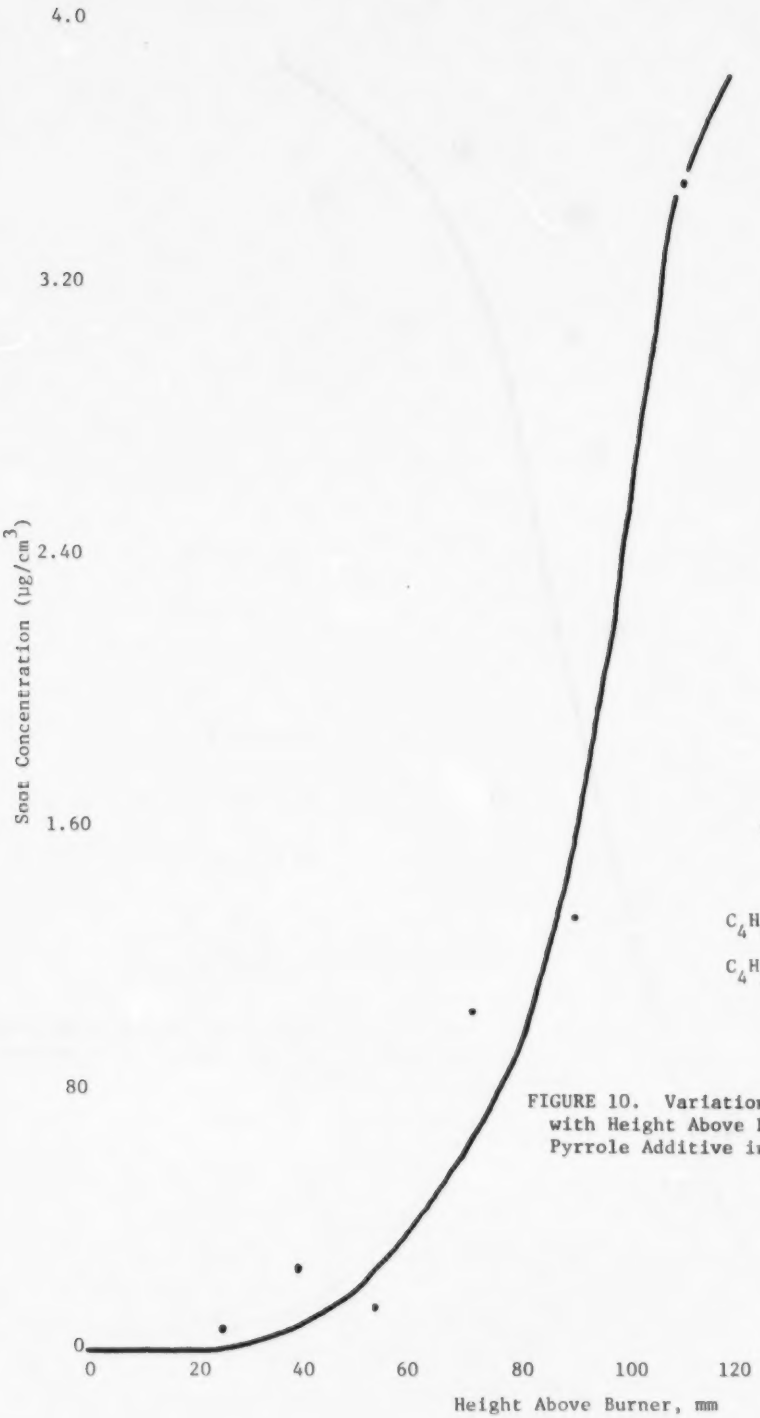

FIGURE 10. Variation of Soot Concentration with Height Above Burner for Thiophene and Pyrrole Additive in Hexane

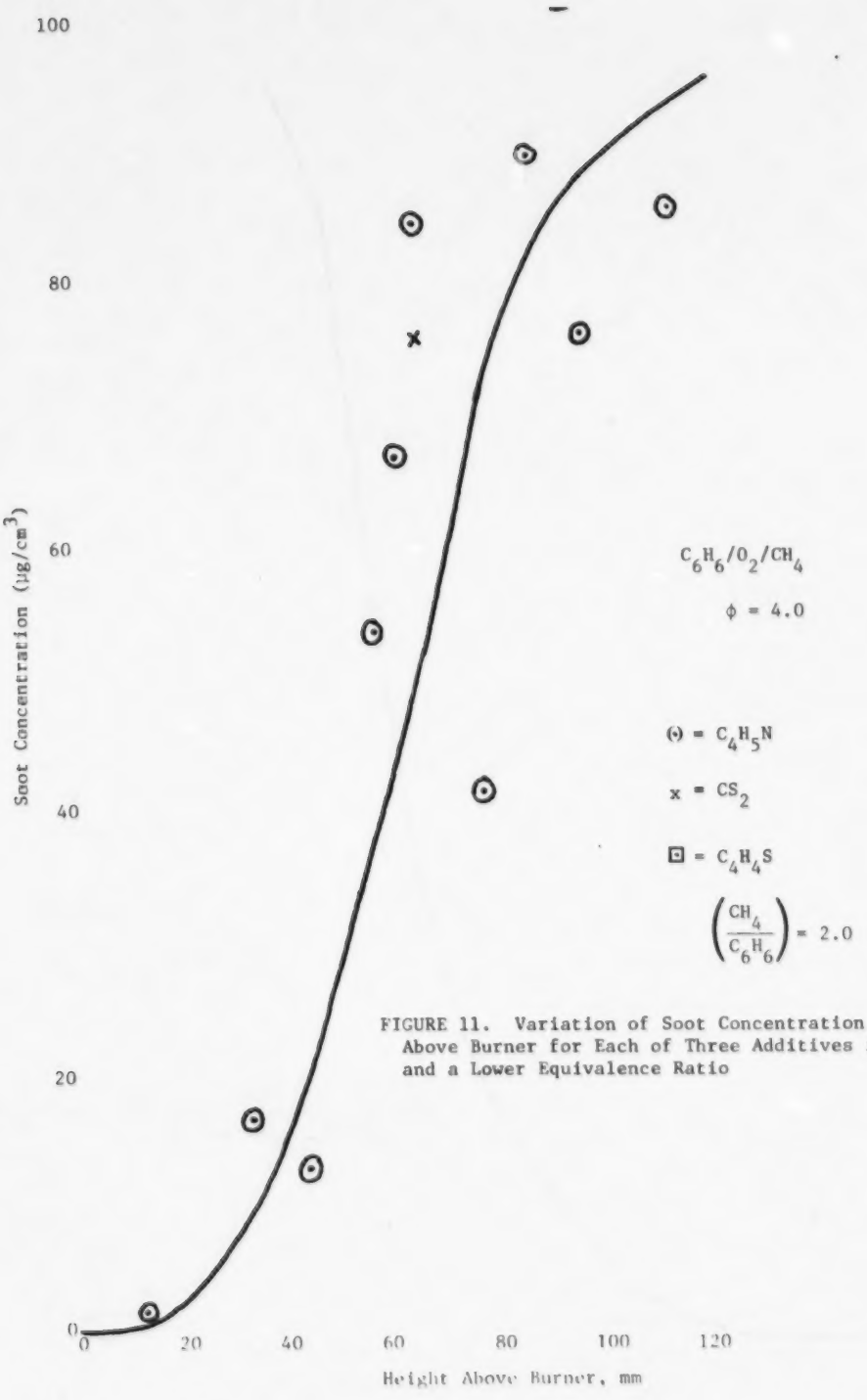

FIGURE 11. Variation of Soot Concentration with Height Above Burner for Each of Three Additives in Benzene and a Lower Equivalence Ratio

SUMMARY AND CONCLUSIONS

The benzene/methane mixture used to obtain the majority of data in this report was approximately 25 times more sooty than the hexane/methane mixture and 50 times more sooty than the pure methane/oxygen flame. The general shape of the soot concentration profiles are about the same for all fuels, as they should be since all of the cold gas velocities were the same.

The data for each individual additive is somewhat sketchy, but the composite seems to yield a fairly firm picture of the soot concentration profile. This is probably due to many sources of error inherent in the techniques used, necessitating a large number of data points. The single most important source of error is the deposition of soot at the inlet to the probe, sometimes making the opening smaller or even clogging it.

The data taken at a $\phi = 4.0$ do not exhibit much, if any, evidence of reproducibility. Apparently many more runs would have been necessary at these conditions to obtain a firm idea concerning the actual location of the concentration profile. Consequently these results are only included here for the sake of completeness, not because they convey too much meaning.

APPENDIX - DATA TABLE

Notes for Table:

(a) A blank indicates an entry is unchanged from the last listed value, except in the Error Code Column, where a blank indicates that the concentration reported is reasonably accurate.

(b) Fuel column indicates fuel in addition to CH_4, which was present in all runs.

(c) All $\phi = 4.0$ runs have $(CH_4/C_6H_6) = 2.0$, whereas all $\phi = 4.5$ runs have $(CH_4/C_6H_6) = 1.5$

Run No.	Additive 1 % N or S	HAB (mm)	ϕ	Fuel	Soot (mg)	Gas (ℓ)	Conc. ($\mu g/cm^3$)	Error Code
1	CS_2	20.7	4.5	C_6H_6	11.0	NA	NA	NA
2		8.2			2.6	13.5	.19	
3		15.7			11.2	15.5	.72	
4		71.05			24.8	1.05	23.76	
5		61.3			59.1	1.53	38.56	
6	C_4H_5N	80.85			25.3	0.592	42.73	
7		53.25			32.8	1.59	20.7	
8		26.65			4.2	1.23	3.42	
9		101.6			65.95	0.943	68.87	
10		116.35			40.1	0.943	42.57	1,3
11		111.25	4.0		25.76	0.298	86.27	
12		85.0			200.7	2.22	90.19	
13		95.45			55.9	0.732	76.48	
14		63.65			89.3	1.06	84.53	
15		59.95			73.3	1.09	67.28	
16		33.1			14.6	.898	16.28	
17		12.5			2.1	1.14	1.88	

(continued)

APPENDIX - DATA TABLE (continued)

Run No.	Additive 1 % N or S	HAB (mm)	ϕ	Fuel	Soot (mg)	Gas (ℓ)	Conc. ($\mu g/cm^3$)	Error Code
18	C_5H_5N	11.95	4.5		3.37	1.153	2.92	4
19		31.5			4.23	1.18	3.58	
20		71.4			56.67	0.846	66.96	
21		109.3			133.5	1.585	84.27	
22		89.9			33.2	0.737	42.05	5
23		136.9			102.8	1.339	76.77	1,2
24	C_4H_4S	148.7			88.3	1.172	75.42	1
25		116.1			50.1	0.758	67.2	1,2,5
26		88.8			60.9	1.58	38.51	2
27		63.9			32.8	0.876	37.5	
28		37.9			1.8	1.15	1.55	
29		17.7			0.35	0.547	0.639	
30		45.2			4.4	0.903	4.85	
31		89.6			26.6	0.383	69.47	
32		110.0			51.2	0.492	103.95	6,1
33		91.95	4.0		58.4	0.547	101.7	
34	CS_2	88.2	4.5	C_6H_6	38.5	0.410	93.83	4?
35		112			89.6	0.986	90.89	
36		38.1			0.73	0.355	2.05	
37		68.0			20.2	0.465	43.4	
38		84.2			62.6	0.657	95.3	6

(continued)

APPENDIX - DATA TABLE (continued)

Run No.	Additive 1 % N or S	HAB (mm)	ϕ	Fuel	Soot (mg)	Gas (ℓ)	Conc. ($\mu g/cm^3$)	Error Code
39		63.9	4.0		41.2	0.542	76.07	
40	C_4H_5N	70.0	4.5		28.1	0.542	51.77	
41		86.6			46.6	0.488	95.6	6
42		102.1			51.7	0.484	106.71	4?
43		76.25	4.0		22.6	0.456	41.45	
44		55.5			25.9	0.491	52.85	
45		43.6			7.1	0.573	12.4	
46	C_5H_5N	49.2	4.5		22.7	0.607	37.38	4
47		60.95			23.2	0.496	46.65	
48		14.15			0.93	0.685	1.36	
49		86.5			55.57	0.712	78.0	
50		98.95			44.3	0.493	89.88	
51	None	98.95		CH_4	2.38	1.367	1.78	
52		83.25			0.19	2.94	0.065	7
53		83.25			1.39	1.097	1.266	
54		70.3			0.62	1.59	.3897	
55		54.85			0.13	1.426	0.091	
56		52.6			0.51	13.715	0.037	
57		67.9			5.89	13.192	0.446	
58		39.4			0.07	21.147	0.0033	

(continued)

APPENDIX - DATA TABLE (continued)

Run No.	Additive 1 % N or S	HAB (mm)	ϕ	Fuel	Soot (mg)	Gas (ℓ)	Conc. ($\mu g/cm^3$)	Error Code
59	C_4H_4S	25.5		C_6H_{14}	1.01	12.35	0.082	
60	and	44.05			1.02	3.81	0.267	
	C_4H_5N							
61	↓	53.35			1.68	11.59	0.145	
62		71.25			6.06	5.902	1.027	
63		90.25			6.53	5.048	1.294	
64		110.3			10.45	2.91	3.592	

APPENDIX D

Source Identification
of Urban Airborn Polycyclic
Aromatic Hydrocarbons by Gas
Chromatographic Mass Spectrometry
and High Resolution Mass Spectrometry

From: Biomedical Mass Spectrometry,
4, 182 (1977). Reprinted
with the permission of Heyden
& Son Ltd.

Source Identification of Urban Airborne Polycyclic Aromatic Hydrocarbons by Gas Chromatographic Mass Spectrometry and High Resolution Mass Spectrometry†

M. L. Lee, G. P. Prado, J. B. Howard and Ronald A. Hites‡
Department of Chemical Engineering, Massachusetts Institute of Technology, Cambridge, Massachusetts 02139, U.S.A.

Polycyclic aromatic hydrocarbons formed during the combustion of three common fuels (coal, wood and kerosene) were separated and identified by capillary-column gas chromatographic mass spectrometry and were compared to airborne polycyclic aromatic hydrocarbons from Indianapolis, a high coal consuming area, and Boston, a low coal consuming area. High resolution mass spectral data were utilized in the construction of alkyl homolog plots for the comparison of alkyl distribution within each sample.

INTRODUCTION

The suspected relationship between atmospheric pollution and lung cancer is not yet substantiated with good epidemiological and analytical surveillance data to provide good quantitative correlations. It seems clear, however, that a relationship does exist. For example, the incidence of lung cancer is twice as high among city dwellers as among rural residents, and it is most common in cities where general industrial pollution is the heaviest.[1] Polycyclic aromatic hydrocarbons (PAH), well known constituents of air particulate matter, have been credited with being the major class of compounds responsible for this observed carcinogenic activity. Many specific PAH have been shown to be carcinogenic in animals; and, although inferences for man from experimental studies involving animals must be drawn with particular caution, there are good reasons to believe that airborne PAH participate in the induction of human lung cancer.[1]

The distribution of PAH in a particular atmospheric environment, and hence, the carcinogenic potential of that environment, is largely dependent on the sum of its sources. PAH are generally produced from combustion processes utilizing fossil fuels, and their formation is dependent on various combustion parameters such as fuel type, temperature and fuel-to-air ratio. Distributions of PAH in emissions from different combustion sources differ considerably in type and concentration of species. Thus, the sum of contributing sources generally produces an air particulate PAH fraction which is unique to the area sampled.[2,3]

It has been determined that approximately 90% of the PAH emissions in the United States is due to coal combustion processes, including coal-fired furnaces and coal-refuse bank burning, and to coke production.[4] Most of these processes are concentrated in the midwestern states. Coal consumption is highest in Ohio and Pennsylvania with each state consuming more than 60 million tons in 1970.[4] Michigan, Indiana, and Illinois each used between 26 and 50 million tons.[4] Contrast these figures with a total of 4.6 million tons consumed by all of New England during the same period of time.[4] It seems reasonable to expect, therefore, that the PAH isolated from the combustion products of coal would be quite well represented in midwestern air particulate matter. On the other hand, New England airborne PAH should be similar to the products obtained from the combustion of fuel oil and gasoline since these are the major sources of PAH emissions in New England.

The objectives of this study were twofold. First, the PAH fractions obtained from the combustion of three common fuels (coal, wood and kerosene) were analyzed to determine their detailed compositions. Capillary-column gas chromatography combined with mass spectrometry was utilized for separation and identification of the mixture constituents. Of particular interest was the identification of the combustion products of coal, which is the major source of atmospheric PAH. Since the usage of coal is likely to increase because of the present energy crisis, information on the PAH distribution in coal combustion products is valuable for future studies concerning the health effects of new modes of energy production. Second, the distributions of PAH obtained from the three different fuels were compared with those of air particulate matter from a high coal consumption area (Indiana) and a low coal consumption area (Massachusetts) by high resolution mass spectrometry to see if correlations could be made between fuel utilization and air particulate matter.

EXPERIMENTAL

The apparatus used for burning coal and wood samples was constructed by placing a stainless steel wire mesh screen (no asbestos) on a tripod and placing a 16 cm × 10 cm i.d. metal cylinder endwise on the screen. About ten pieces (approximately 20 g each) of a Pittsburgh seam bituminous coal or wood chips from a construction

† Abbreviation: PAH = polycyclic aromatic hydrocarbons.
‡ To whom correspondence should be addressed.

grade fir were placed in the chimney (cylinder) and ignited from underneath with a Bunsen burner. The burner was removed, and soot samples were collected by repeatedly lowering a 250 ml Erlenmeyer flask, which was cooled by a continuous flow of water through the flask, into the flame for about 30 min, at which time the fuel was completely consumed. The soot collected on the glass surface was scraped with a spatula into a small beaker. Each soot sample (250–400 mg) was then placed in a Soxhlet apparatus and extracted with 250 ml of methylene chloride for 18 h. The extract was evaporated to dryness with a rotary evaporator, dissolved in 50 ml of cyclohexane and transferrred to a separatory funnel. The cyclohexane layer was then washed five times with 50 ml of nitromethane. All nitromethane portions were combined and evaporated to dryness. The residue was then transferred to a 1 cm i.d. glass column packed with 2 g of silicic acid and eluted with 300 ml of hexane. The eluate was evaporated to dryness and dissolved in 0.5–5 ml of methylene chloride prior to gas chromatographic analysis. This procedure was shown previously to be effective in separating and purifying the PAH from the bulk of other organic compounds in the extract.[5] It should be noted that nitrogen-containing polycyclics are removed by this procedure but sulfur-containing polycyclics are not.

Kerosene was burned in a specially constructed turbulent diffusion flame burner using an air-assist atomizer.[6] The air-atomizing pressure was 170 KPa (10 lb in^{-2} g), the cold gas velocity was 0.96 m s^{-1} and the fuel-air equivalence ratio was 1 (stoichiometry). This burner and these conditions simulate a poorly maintained home-heating furnace. Soot samples were collected from this burner using a novel water-cooled probe[7] at the exhaust of the combustion chamber (50 cm from the burner nozzle). The collected soot was extracted with methylene chloride and the extract concentrated for gas chromatographic analysis with a rotary evaporator. All glassware was acid cleaned prior to use, and all solvents were Nanograde (Mallinckrodt) quality. Blank runs demonstrated the absence of contamination. The total yield of PAH in each sample was 2–3% of the soot extracted.

The PAH samples isolated from air particulate matter from Indiana and Massachusetts were utilized in previous studies and descriptions of each sample work-up procedure can be found elsewhere.[8,9]

Gas chromatographic mass spectrometry of each sample was performed with a Hewlett-Packard 5982A g.c.m.s. system interfaced to a HP 5933A data system. A 19 m × 0.26 mm i.d. glass capillary column coated with SE-52 methyl–phenyl–silicone stationary phase was used to separate mixtures prior to mass spectral analysis. The oven temperature was programmed from 70 °C to 250 °C at 2 °C min^{-1} during each chromatographic run. The mass range (from 50 to 350 a.m.u.) was continuously scanned every 2.5 s. The mass spectrometer was operated at 70 eV ionizing energy.

High resolution mass spectral information was obtained on each sample by introducing an aliquot of the methylene chloride extract into a high resolution mass spectrometer through a direct introduction probe system and slowly vaporizing the sample at a continually increasing temperature while making several exposures on a photographic plate. The developed plate was read on a computerized comparator, and the exact masses were converted to elemental composition. The corresponding intensities were then arranged as tables of carbon number vs. number of double bonds and rings. One such table was generated for each exposure and then a composite table was formed by adding the corresponding entries of each table. This technique has been described previously.[10,11] The results from this high resolution m.s. technique have been validated by a comparison with quantitative g.c. data obtained on the Indianapolis air particulate extract. The two methods give results which are highly correlated ($r = 0.93$, $N = 6$) and thus can be considered self-consistent.

The high resolution m.s. system consists of a DuPont Instruments 21-110B mass spectrometer and a D. W. Mann comparator interfaced to an IBM 1802 computer. The ionizing energy was 70 eV and the resolving power was about 20 000. This high resolution m.s. system and its operation are described elsewhere.[12]

RESULTS AND DISCUSSION

Considerable emphasis has been placed on the necessity for improved resolution of components in complex PAH mixtures because of the ongoing interest in exact identification of potential carcinogens.[13,14] Capillary-column g.c. has proven to be the most efficient separation tool presently available for the analysis of PAH, and its use has provided the means for extremely detailed studies of PAH mixtures.[8,14,15] Figures 1, 2 and 3 show high resolution gas chromatograms of the PAH fractions obtained from the three fuels studied here. Table 1 lists the compounds identified by g.c.m.s. and g.c. retention data. Several qualitative and semiquantitative observations result from the comparison of these chromatograms: (1) there is a greater relative concentration of alkylated PAH in the coal combustion products as compared with either wood or kerosene; (2) there is a greater relative concentration of high molecular weight species in the wood and kerosene combustion products as compared with coal; (3) the coal soot PAH fraction contains significant amounts of sulfur-containing compounds, which are absent in the other combustion products.

The construction of alkyl homolog plots from high resolution mass spectral data is an effective way of representing the distribution of alkylated species within a PAH mixture.[10,11] Figure 4 shows the alkyl homolog distribution for seven major groups of isomers found in the coal soot PAH fraction. In agreement with the gas chromatogram, there tend to be considerable amounts of alkylated species. The high sensitivity of this technique shows the presence of alkyl groups containing up to six carbons for the phenanthrene type series ($Z = -18$) and five carbons for the pyrene type series ($Z = -22$). The comparison of the $Z = -22$ series for coal, wood and kerosene combustion products with air particulate matter from Indianapolis and Boston is shown in Fig. 5. There is a remarkable similarity between the curves for coal-soot PAH and Indianapolis air particulates as well as between the kerosene-soot PAH and Boston air particulates.

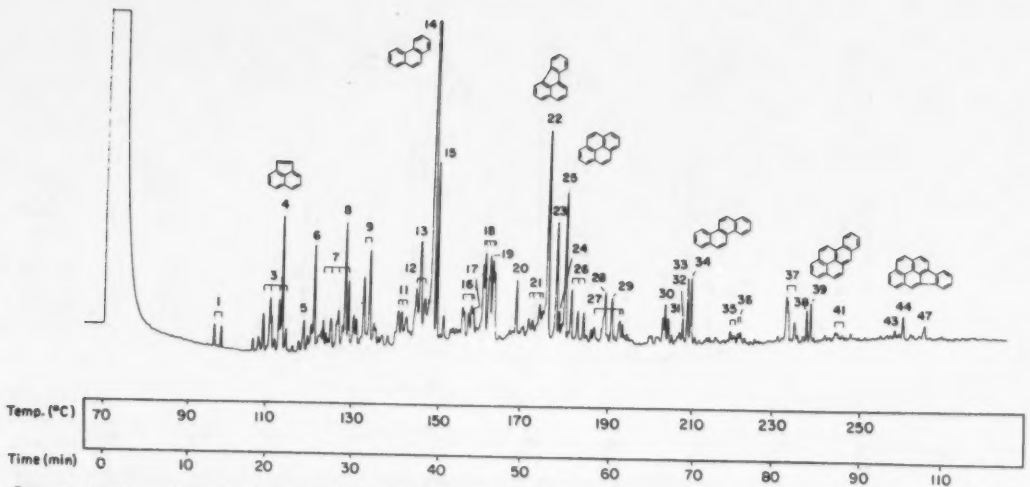

Figure 1. Capillary-column gas chromatogram of the PAH fraction of coal combustion products. Conditions: see text. Key: see Table 1.

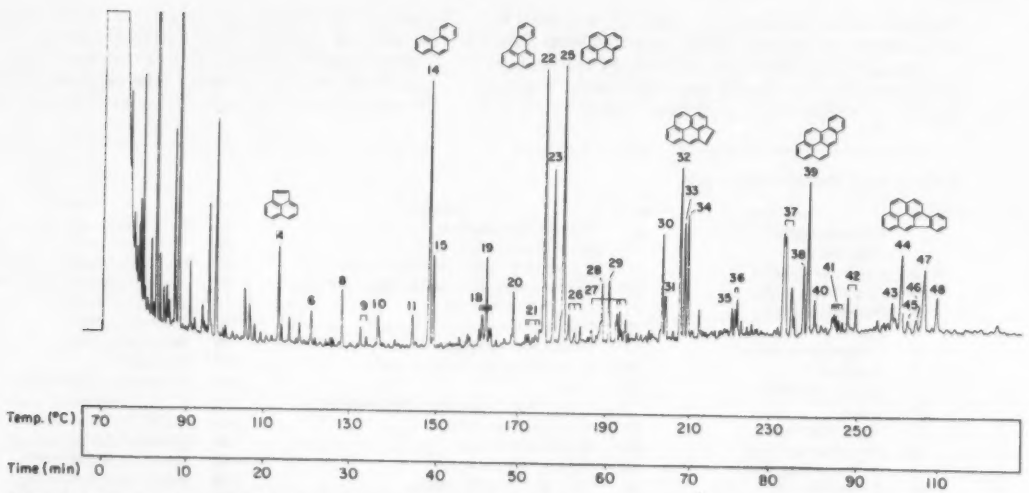

Figure 2. Capillary-column gas chromatogram of the PAH fraction of wood combustion products. Conditions: see text. Key: see Table 1. Early chromatographic peaks with less retention than acenaphthylene have been identified as substituted methoxyphenols and several other nonpolycyclic compounds.

Figure 6 represents composite alkyl homolog plots which were constructed by adding intensities of all parent compounds, all C_1 alkylated compounds, all C_2 alkylated compounds, etc., for all series represented in Fig. 4 and plotting the resulting sums. Again, the similarities observed in Fig. 5 are evident in this composite. The similarity in the results obtained from the turbulent diffusion flame burner and Boston air particulates is consistent with the fact that fuel oil (which is chemically similar to kerosene) is Boston's principal heating and energy producing fuel, while coal burning is practically nonexistent.

The sulfur-containing polycyclic aromatic species in the coal combustion products (see Table 1) are identical to those found in the air particulates from Indianapolis.[8] This observation, in addition to the alkyl homolog distributions, lends support to the belief that the major contributors to Indianapolis airborne PAH are coal combustion processes. The relatively low concentration of high molecular weight compounds in the coal soot

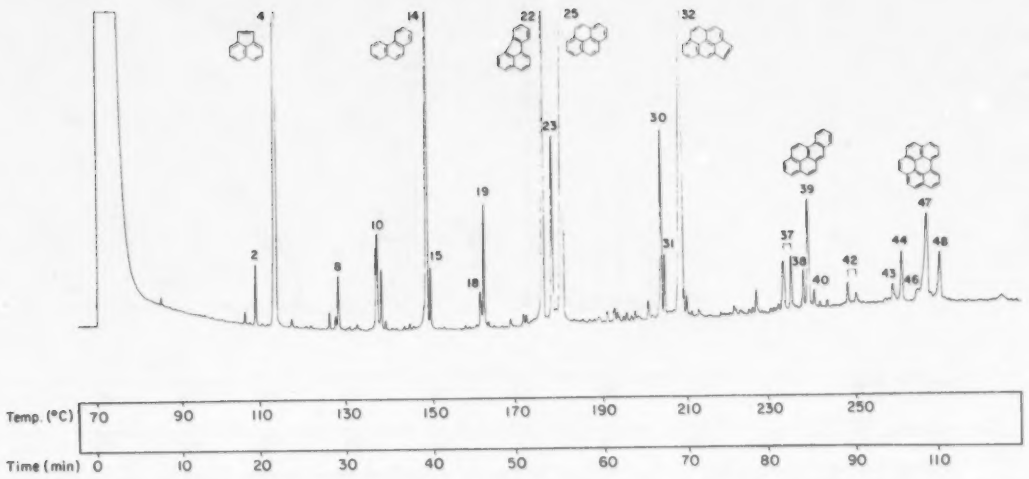

Figure 3. Capillary-column gas chromatogram of the PAH fraction of kerosene combustion products. Conditions: see text. Key: Table 1.

PAH fraction is not consistent, however, with what has been observed in the Indianapolis air particulates. There are three possible explanations for this difference. First, it was found that by altering the combustion conditions (especially temperature) in the production of carbon blacks[15] the relative proportion of higher molecular weight to lower molecular weight PAH species could be either considerably increased or decreased. The same trends are certainly present in the combustion of coal. Second, the practice[16] of sampling air particulate matter

Table 1. PAH identified by g.c.m.s.

Peak No.	Compound	Peak No.	Compound	Peak No.	Compound
1	Methylnaphthalene	17	Propyldibenzofuran[b]	33	Benz[*a*]anthracene
2	Biphenyl	18	Methylphenanthrene[c]	34	Chrysene
3	Ethylnaphthalene[a]	19	4*H*-cyclopenta[*def*]phenanthrene	35	Methylchrysene[a]
4	Acenaphthylene	20	Methyl-4*H*-cyclopenta[*def*]phenanthrene	36	Methylcyclopenta[*cd*]pyrene[f]
5	Methylbiphenyl	21	Ethylphenanthrene[a]	37	Benzofluoranthene
6	Dibenzofuran	22	Fluoranthene	38	Benzo[*e*]pyrene
7	Propylnaphthalene[b]	23	Benz[*e*]acenaphthylene	39	Benzo[*a*]pyrene
8	Fluorene	24	Benzo[*def*]dibenzothiophene	40	Perylene
9	Methyldibenzofuran	25	Pyrene	41	Methylbenzopyrene[g]
10	$C_{14}H_8$[h]	26	Ethyl-4*H*-cyclopenta[*def*]phenanthrene[a]	42	$C_{21}H_{12}$ (unknown)
11	Methylfluorene	27	Methylfluoranthene[d]	43	$C_{21}H_{12}$ (unknown)
12	Ethyldibenzofuran[a]	28	Benzo[*a*]fluorene	44	Indeno[1,2,3-*cd*]pyrene
13	Dibenzothiophene	29	Benzo[*b*]fluorene	45	Dibenz[*a,h*]anthracene
14	Phenanthrene	30	Benzo[*ghi*]fluoranthene	46	Dibenz[*a,c*]anthracene
15	Anthracene	31	$C_{18}H_{10}$ (unknown)	47	Benzo[*ghi*]perylene
16	Ethylfluorene[a]	32	Cyclopenta[*cd*]pyrene	48	Anthanthrene

[a] Could be dimethyl.
[b] Could be trimethyl or ethylmethyl.
[c] Could be methylanthracene.
[d] Could be methylpyrene.
[e] Could be methylbenz[*a*]anthracene.
[f] Could be methylbenzo[*ghi*]fluoranthene.
[g] Could be methylbenzofluoranthene.
[h] Probably cyclopent[*bc* or *fg*]acenaphthylene, see Ref. 17.

on glass fiber filters followed by drying at slightly elevated temperatures for accurate weight measurements tends to volatilize many of the lower molecular weight compounds and enrich the sample in higher molecular weight species. The third explanation is drawn from experiments with the turbulent diffusion flame burner in which there was an enrichment of higher molecular weight PAH as samples were collected at greater distances from the burner nozzle. Since the coal- and wood-soot samples were collected from within the flame instead of at greater distances, it is possible that these samples were not as enriched with high molecular weight species as the exhaust from a typical coal combustor.

The complementary use of high resolution gas chromatographic mass spectrometry for detailed compound identification and of high resolution mass spec-

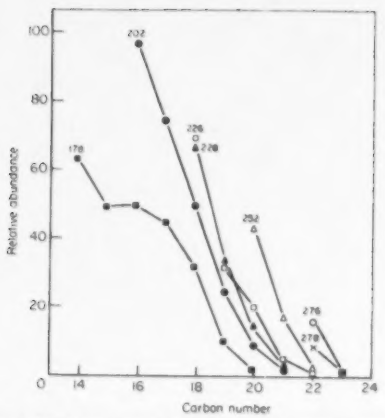

Figure 4. Alkyl homolog distribution plots for several PAH series in coal combustion products. The lines are labeled by the molecular weight of the unsubstituted species. Example isomers are: 178 ($Z = -18$)phenanthrene, 202 ($Z = -22$)pyrene, 226 ($Z = -26$)cyclopenta[*cd*]pyrene, 228 ($Z = -24$)chrysene, 252 ($Z = -28$)benzo[*a*]pyrene, 276 ($Z = -32$)indeno[1,2,3-*cd*]pyrene and 278 ($Z = -30$)dibenzanthracene. The value of Z is derived from the general formula C_nH_{2n+Z}.

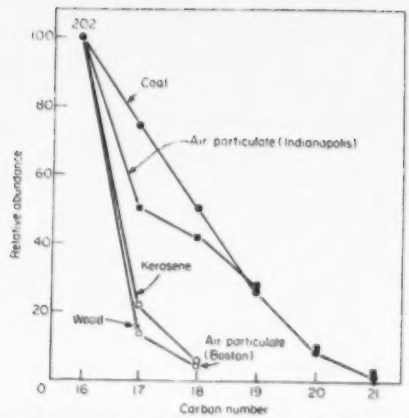

Figure 5. Alkyl homolog distribution plots for the pyrene-type series ($Z = -22$) in the combustion products of coal, wood and kerosene, and in air particulate matter from Indianapolis and Boston. The abundance of the parent compound in each series was normalized to 100.

trometry for alkyl distribution monitoring can greatly aid in the characterization of airborne PAH and in the identification of pollution sources. This information is important for the engineer to design those cleaner combustion processes which will be necessary in the light of the expected increase in the consumption of coal.

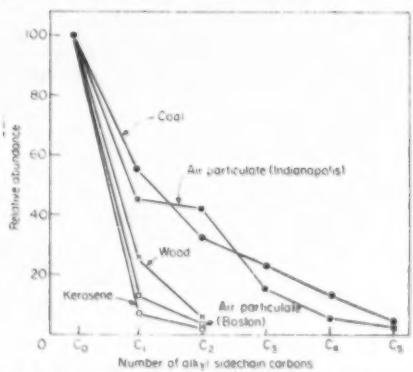

Figure 6. Composite alkyl homolog distribution plots (see text) for PAH in the combustion products of coal, wood and kerosene, and in air particulate matter from Indianapolis and Boston. The abundance of the parent composite in each series was normalized to 100.

Acknowledgements

The authors thank C. Clampitt and J. Dillon for technical assistance during this project. This work was supported by Grant No. R803242 from the Environmental Protection Agency.

REFERENCES

1. *Particulate Polycyclic Organic Matter*. National Academy of Sciences, Washington, D.C. (1972).
2. K. D. Bartle, M. L. Lee and M. Novotny. *Int. J. Environ. Anal. Chem.* **3**, 349 (1974).
3. J. L. Shultz, A. G. Sharkey and R. A. Friedel, *Biomed. Mass Spectrom.* **1**, 137 (1974).
4. H. S. Stoker, S. L. Seager and R. L. Capener, *Energy*, p. 163. Scott Foresman, Glenview, Illinois (1975).
5. M. L. Lee. Ph.D. Thesis, Indiana University (1975).
6. J. P. Appleton and J. B. Heywood, *Fourteenth International Symposium on Combustion*, p. 777. The Combustion Institute, Pittsburgh, Pennsylvania (1973).
7. G. P. Prado, M. L. Lee, R. A. Hites, D. P. Hoult and J. B. Howard, *Sixteenth International Symposium on Combustion*. The Combustion Institute. In press.
8. M. L. Lee, M. Novotny and K. D. Bartle, *Anal. Chem.* **48**, 1566 (1976).
9. A. Hase and R. A. Hites, in *Identification and Analysis of Organic Pollutants in Water*, edited by L. H. Keith, p. 205. Ann Arbor Science, Ann Arbor, Michigan (1976).
10. R. A. Hites and W. G. Biemann, *Adv. Chem.* **147**, 188 (1975).
11. A. Hase and R. A. Hites, *Geochim. Cosmochim. Acta* **40**, 1141 (1976).
12. K. Biemann, *Application of Computer Techniques in Chemical Research*. pp. 5–19. Institute of Petroleum, London (1972).
13. D. Hoffmann, W. E. Bondinell and E. L. Wynder, *Science* **183**, 215 (1974).
14. M. L. Lee, M. Novotny and K. D. Bartle, *Anal. Chem.* **48**, 405 (1976).
15. M. L. Lee and R. A. Hites, *Anal. Chem.* **48**, 1890 (1976).
16. *Particulate Polycyclic Organic Matter*, Appendix A. National Academy of Sciences, Washington, D. C. (1972).
17. B. D. Crittenden and R. Long, *Combust. Flame* **20**, 359 (1973).

Received 29 July 1976

APPENDIX E

Mixed Charge Exchange-Chemical Ionization Mass Spectrometry of Polycyclic Aromatic Hydrocarbons

From: Reprinted with permission from J. Amer. Chem. Soc., 99, 2008 (1977). Copyright by the American Chemical Society.

Mixed Charge Exchange–Chemical Ionization Mass Spectrometry of Polycyclic Aromatic Hydrocarbons

Sir:

The exact structural identification of polycyclic aromatic hydrocarbons (PAH) and their alkylated derivatives is a difficult problem, particularly when they are encountered as complex mixtures. The analytical power of mass spectrometry, which has had wide application in this field,[1-4] has been limited because electron impact mass spectra of isomeric PAH are almost identical. The purpose of this note is to report that charge exchange–chemical ionization mass spectrometry, using an argon–methane reagent gas,[5] easily differentiates PAH isomers.

The mass spectra of a series of PAH were measured with a Hewlett-Packard 5982A gas chromatographic–mass spectrometer system by injecting approximately 200 ng of each compound (dissolved in methylene chloride) on a 180 × 0.32 cm o.d. stainless steel column packed with 3% Dexsil 300 on 80/100 mesh Chromosorb W. The reagent gas mixture (10% methane in argon) served as the carrier gas for the gas chromatographic column which was held isothermally at a temperature appropriate to each sample being analyzed. The mass spectrometer was continuously scanned from 50 to 350 amu at 81.2 amu/s. The ion source pressure was 0.8 Torr and its temperature was 170 °C. Data were collected and processed by a HP 5933A data system. Precautions were taken to assure the absence of water vapor in the ion source, since water is an excellent proton donor and can greatly increase the abundance of the protonated molecular ion. In these experiments, there were no observable traces of water vapor (*m/e* 18 or 19).

The resulting mass spectra showed considerable differences in the relative abundances of the molecular (M^+) and protonated molecular ($M + 1^+$) ions when different PAH isomers were analyzed. Table I lists the compounds analyzed in this study, the resulting ratio of the abundance of the protonated molecular to molecular ion ((M + 1)/M), and the first ionization potential of each compound. It is obvious from this table that the (M + 1)/M ratio has a high positive correlation with ionization potential ($r = 0.877$, $P \ll 0.01$). This trend is consistent with the expectation that as the ionization potential increases, charge transfer processes will be less effective for electron extraction while at the same time protonation becomes more favorable.

Table I. Abundance Ratios for Selected PAH Obtained by CH_4–Ar Chemical Ionization Mass Spectrometry

Compound	Formula	First ionization potential (eV)[a]	Abundance ratio, (M + 1)/M[b]
Pentacene	$C_{22}H_{14}$	6.42	0.32
Tetracene	$C_{18}H_{12}$	6.88	0.45
Anthanthrene	$C_{22}H_{12}$	7.02	0.38
Perylene	$C_{20}H_{12}$	7.03	0.32
Benzo[*a*]pyrene	$C_{20}H_{12}$	7.17	0.73
Anthracene	$C_{14}H_{10}$	7.42	0.82
Benz[*a*]anthracene	$C_{18}H_{12}$	7.47	0.83
Dibenz[*a,h*]anthracene	$C_{22}H_{14}$	7.55	0.95
Pyrene	$C_{16}H_{10}$	7.56	0.73
Coronene	$C_{24}H_{12}$	7.58	0.66
Benzo[*e*]pyrene	$C_{20}H_{12}$	7.58	0.82
Acenaphthene	$C_{12}H_{10}$	7.70	1.00
Chrysene	$C_{18}H_{12}$	7.74	1.26
Fluoranthene	$C_{16}H_{10}$	7.76	1.57
Fluorene	$C_{13}H_{10}$	7.86	1.66
Acenaphthylene	$C_{12}H_8$	8.02	1.34
Phenanthrene	$C_{14}H_{10}$	8.02	1.59
Triphenylene	$C_{18}H_{12}$	8.11	1.73
Naphthalene	$C_{10}H_8$	8.14	1.68
Benzene	C_6H_6	9.29	5.79

[a] Values were averaged from experimental data found in ref 6–8; their variability was usually less than ±0.1 eV. [b] The reproducibility of these measurements was ±4% over a 3-month period. The ratios have been corrected for the natural abundance of ^{13}C.

This technique should be quite useful for the elucidation of specific isomeric structures of PAH. By using a mixed charge exchange–chemical ionization reagent gas, such as described here, different mass spectra can be obtained for most PAH isomers while conventional mass spectral techniques provide little differentiation. This fact is demonstrated by the series of tetracyclic compounds shown in Figure 1. The (M + 1)/M ratio of each compound is plotted as a function of its first ionization potential. It is interesting to note that this abundance ratio increases from 0.45 to 1.73 as the isomer becomes more nonlinear, making differentiation quite easy. If a standard PAH compound were not available, it seems probable that the mass spectrum of that compound could be predicted from its ionization potential. The ability to calculate ionization potentials from molecular orbital theory[7,8] offers considerable promise for the future identification of presently unknown PAH.

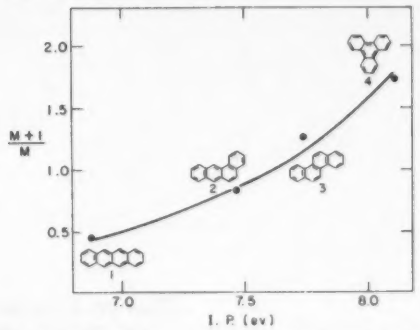

Figure 1. Plot of the abundance ratio ((M + 1)/M) obtained by CH_4–Ar chemical ionization mass spectrometry as a function of ionization potential (IP) for a series of four tetracyclic polycyclic aromatic hydrocarbons: 1, tetracene; 2, benz[*a*]anthracene; 3, chrysene; 4, triphenylene.

Acknowledgments. The authors thank D. P. Beggs (Hewlett-Packard, Avondale, Pa.) and G. P. Arsenault (Chemistry Department, MIT, Cambridge, Mass.) for helpful suggestions concerning this work. This work was supported by grant R803242 from the U.S. Environmental Protection Agency.

References and Notes

(1) R. C. Lao, R. S. Thomas, H. Oja, and L. Dubois, *Anal. Chem.*, **45**, 908 (1973).
(2) R. A. Hites and W. G. Biemann, *Adv. Chem. Ser.*, **No. 147**, 188 (1975).
(3) M. L. Lee, K. D. Bartle, and M. Novotny, *Anal. Chem.*, **48**, 405 (1976).
(4) M. L. Lee and R. A. Hites, *Anal. Chem.*, **48**, 1890 (1976).
(5) The ability of CH_4–Ar mixtures to provide combined CE–CI spectra has been previously described by D. P. Beggs (Hewlett-Packard Applications Note No. 176-19). The methane acts as a low energy proton donor which produces an intense protonated molecular ion while the argon participates in charge exchange reactions to produce a fragmentation pattern normally found in electron impact mass spectra.
(6) H. Kuroda, *Nature (London)*, **201**, 1214 (1964).
(7) M. J. S. Dewar, F. R. S. Haselbach, and S. D. Worley, *Proc. R. Soc. London, Ser. A*, **315**, 431 (1970).
(8) M. S. Sung, *C. R. Acad. Sci., Ser. C*, **278**, 37 (1974).

M. L. Lee, Ronald A. Hites*
Department of Chemical Engineering
Massachusetts Institute of Technology
Cambridge, Massachusetts 02139
Received August 17, 1976

APPENDIX F

Charge Exchange - Chemical Ionization of Polycyclic Aromatic Compounds

Carcinogenesis, Vol. 3: Polynuclear Aromatic Hydrocarbons, edited by P. W. Jones and R. I. Freudenthal. Raven Press, New York © 1978.

Charge Exchange–Chemical Ionization Mass Spectrometry of Polycyclic Aromatic Compounds

Ronald A. Hites and George R. Dubay

Massachusetts Institute of Technology, Department of Chemical Engineering, Cambridge, Massachusetts 02139

Certain polycyclic aromatic compounds (PAC) have been of interest since the early 1800s because of their carcinogenic behavior. Since only specific PAC isomers are carcinogenic, it is important to have an analytical tool which can differentiate among these isomeric compounds. Although GC-MS has had a wide application for the analysis of PAC, one problem remains: isomeric PAC give identical electron impact mass spectra; thus, the unambiguous identification of these compounds is sometimes impossible.

We have found that charge exchange-chemical ionization mass spectrometry can be used to distinguish many isomeric PAC (1). We have established that spectra of PAC have characteristic ratios of the protonated molecular ion to the molecular ion when 5% to 10% methane in argon is employed as the reagent gas. The two most prominent ions in the reagent plasma are $C_2H_5^+$ and Ar^+. The molecule of interest either reacts with the strongly acidic ion, $C_2H_5^+$, to give the protonated molecular ion, or it reacts with Ar^+ ions to give the molecular ion. The relative rates of these two competing reactions determine the intensity ratio of the two ions. Variation in ionization potentials will not significantly affect the rate of protonation by $C_2H_5^+$ ions, but it will affect the rate of ionization by Ar^+ ions. Thus, we have found that ionization potentials are correlated with the ratio of the protonated molecular ion to the molecular ion (M + 1/M).

A wide variety of PAC have been studied, and the characteristic ratios for M + 1/M were determined. A partial listing of the PAC investigated is given in Table 1. (All values have been corrected for the natural abundance of ^{13}C.) Within any of the subgroups listed, it can be seen that the ionization potential (IP) of isomeric PAC correlates with the M + 1/M value. Apparently, an increase in the IP causes the rate of ionization by Ar^+ to decrease while the rate of protonation by $C_2H_5^+$ is unaffected. Thus, there is an increase in the relative rate of protonation as evidenced by an increase in the ratio of M + 1/M.

Table 1 shows that this technique is applicable to the differentiation of

TABLE 1. *Some of the polycyclic aromatic compounds investigated*

Compound	Formula	IP(ev)	M + 1/M[a]	M + 1/M[b]
Tetracene	$C_{18}H_{12}$	6.88[d]	0.45	—
Benzo[a]pyrene	$C_{20}H_{12}$	7.17[d]	0.73	—
Anthracene	$C_{14}H_{10}$	7.42[d]	0.82	—
Benz[a]anthracene	$C_{18}H_{12}$	7.47[d]	0.83	0.70 ± 0.08[c]
Pyrene	$C_{16}H_{10}$	7.56[d]	0.73	0.64 ± 0.02
Benzo[e]pyrene	$C_{20}H_{12}$	7.58[d]	0.82	—
Chrysene	$C_{18}H_{12}$	7.74[d]	1.26	—
Fluoranthene	$C_{16}H_{10}$	7.76[d]	1.57	—
Phenanthrene	$C_{14}H_{10}$	8.02[d]	1.59	—
Triphenylene	$C_{18}H_{12}$	8.11[d]	1.73	1.24 ± 0.03
4-Methylbiphenyl	$C_{13}H_{12}$	8.15[e]	—	1.79 ± 0.10
3-Methylbiphenyl	$C_{13}H_{12}$	8.30[e]	—	2.16 ± 0.10
2-Methylbiphenyl	$C_{13}H_{12}$	8.60[e]	—	2.45 ± 0.23
9-Methylanthracene	$C_{15}H_{12}$	7.36[f]	—	0.62 ± 0.07
2-Methylanthracene	$C_{15}H_{12}$	7.42[f]	—	0.64 ± 0.03
2-Methylphenanthrene	$C_{15}H_{12}$	7.90[g]	—	0.89 ± 0.01
Benz[b]indole	$C_{12}H_9N$	8.11[h]	—	1.03 ± 0.04
Benz[g]indole	$C_{12}H_9N$	8.25[h]	—	1.13 ± 0.07
Benzo[b]quinoline	$C_{13}H_9N$	7.88[i]	—	1.68 ± 0.09
Benzo[f]quinoline	$C_{13}H_9N$	8.14[i]	—	2.20 ± 0.06
Dibenzothiophene	$C_{12}H_8S$	—	—	0.24 ± 0.09
Benzo[1,2]dibenzothrophene	$C_{16}H_{10}S$	—	—	1.25 ± 0.08

[a] Reagent gas was 10% methane in argon (P-10) from Matheson Gas Products.
[b] Reagent gas was 5% methane in argon (P-5) from Matheson Gas Products.
[c] 90% confidence limits on a minimum of 3 measurements.
[d] Values are found in ref. 1.
[e] Determined by photoelectronic spectroscopy, J. P. Maier and D. W. Turner, *Faraday Disc. Chem. Soc.*, 54:149, 1972.
[f] Determined using charge transfer spectra, O. B. Nagy, *Tetrahedron*, 31:2453, 1975.
[g] Determined by appearance potentials, P. Nounou, *J. Chem. Phys.*, 63:994, 1966.
[h] Calculated values, N. S. Hush, A. S. Cheung, and P. R. Hilton, *J. Electron Spec. Rel. Phen.*, 7:385, 1975.
[i] Calculated values, M. J. S. Dewar, A. J. Hargot, N. Trinajstic, and S. D. Worley, *Tetrahedron*, 26:4505, 1970.

simple PAC and to some of their methyl derivatives. It is also useful for some aromatic heterocycles as illustrated by the nitrogen-containing compounds. A difference in the ratios is observed which is dependent on the basicity of the nitrogen in the ring. Lack of available standards has limited the investigation of sulfur-containing aromatic heterocycles; the two we have studied are shown.

In conclusion, it should be noted that this work is in its initial stages. Substantial work is needed to establish the capabilities and limitations of the technique. This charge exchange-chemical ionization technique is not expected to replace electron impact GC-MS; but it should be a useful supplemental tool for differentiating isomeric PAC. In addition, by using ionization potentials calculated from MO theory, it is hoped that this technique can become predictive and be extended to molecules for which no standards are available.

ACKNOWLEDGMENTS

This work has been supported by grants from the U.S. Environmental Protection Agency (R803242) and the Energy Research and Development Administration (EE-77-S-02-4267).

REFERENCE

1. Lee, M. L., and Hites, R. A. (1977): Mixed charge exchange—chemical ionization mass spectrometry of polycyclic aromatic hydrocarbons. *J. Am. Chem. Soc.*, 99: 2008.

APPENDIX G

Characterization of Sulfur-Containing Polycyclic Aromatic Compounds in Carbon Blacks

Reprinted from ANALYTICAL CHEMISTRY, Vol. 48, Page 1890, November 1976
Copyright 1976 by the American Chemical Society and reprinted by permission of the copyright owner

Characterization of Sulfur-Containing Polycyclic Aromatic Compounds in Carbon Blacks

M. L. Lee and Ronald A. Hites*

Department of Chemical Engineering, Massachusetts Institute of Technology, Cambridge, Mass. 02139

Computerized gas chromatographic mass spectrometry and high resolution mass spectrometry have been used to identify sulfur-containing polycyclics and polycyclic aromatic hydrocarbons in carbon blacks obtained from sulfur-containing petroleum feedstocks. Twenty-eight compounds have been identified, seven of which are sulfur-containing polycyclics.

Carbon black is a material of considerable commercial importance: More than 1.5 billion pounds per year of domestic carbon black are used in the manufacture of tires alone (*1*). It is also a material of potentially great environmental concern because of (a) wide environmental distribution of carbon black, primarily in automobile tire dust, and (b) the potent carcinogenicity of a number of compounds adsorbed on carbon black such as certain polycyclic aromatic hydrocarbons (PAH). These considerations have led to several studies of the organic compounds associated with carbon black. For example, two recent studies (*2, 3*) reported the identification of cyclopenta[*cd*]pyrene as a major constituent of carbon black extracts; in addition, 11 other PAH (*2*) and several oxygenated polycyclics (*3*) were also reported.

This paper reports on the analysis of organic extracts of several carbon blacks which were manufactured under varying conditions. Of particular interest is the first reported identification of sulfur-containing polycyclics in carbon black. In addition, the detection of high-boiling PAH has been extended to include compounds of molecular weights up to 376 ($C_{30}H_{16}$). Capillary column gas chromatography combined with mass spectrometry (GC/MS) has allowed the positive identification of 21 compounds and the tentative identification of 10 others (see Figure 1). High-resolution mass spectrometry (HRMS) of these same samples has verified the elemental composition of individual compounds, especially for the sulfur polycyclics.

EXPERIMENTAL

Samples of four different furnace blacks (see Table I) were obtained from a commercial source (Cabot Corporation, Boston, Mass). The aromatic feedstocks used in the production of three of these furnace blacks were derived from refinery and naphtha-based ethylene type tars. They were over 90% aromatic hydrocarbons, and had a considerable amount of organic sulfur (1.2–3.1%). Appropriate amounts (see Table I) of each furnace black were extracted with methylene chloride for 18 h in a Soxhlet apparatus. Soxhlet thimbles were extracted with Nanograde methylene chloride (Mallinckrodt) for several hours prior to each sample extraction to remove any organic contaminants in the thimble or apparatus. The methylene chloride extracts were then evaporated to minimal volumes (1–10 ml) by rotary evaporation under

Figure 1. Compounds identified in carbon blacks by GC/MS and HRMS

[a] Structure is presumed correct but has not been verified by comparison with authentic compounds. [b] Exact position of benzo group is not known. [c] The increase in molecular weight of PAH species also increases the number of possible isomers; the lack of authentic compounds in this molecular weight range prevents the elucidation of the exact structures for these particular GC peaks. The structures given are examples only; many other isomers are possible. [d] Detected only by high resolution mass spectrometry. The structures given are examples only; many other isomers are possible

1
naphthalene

2
acenaphthylene

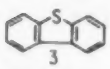

3
dibenzothiophene

4
phenanthrene

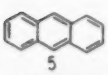

5
anthracene

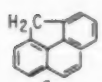

6
4H-cyclopenta[def]-phenanthrene

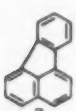

7
fluoranthene

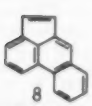

8
benz[e]acenaph-thylene[a]

9
benzo[def]dibenzo-thiophene[a]

10
pyrene

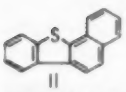

11
benzo[a]dibenzo-thiophene

12
benzo[ghi]fluoran-thene

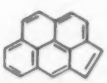

13
cyclopenta[cd]py-rene

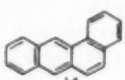

14
benz[a]anthracene

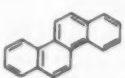

15
chrysene

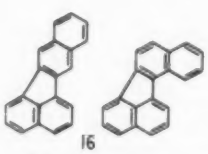

16
benzo[j]fluoran-thene and benzo[k]fluoranthene

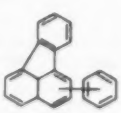

17
benzofluoranthene[b]

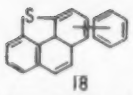

18
benzo[def]naphtho-benzothiophene[a,b]

19
benzo[e]pyrene

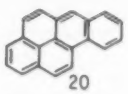

20
benzo[a]pyrene

21
perylene

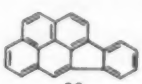

22
Indeno[1,2,3-cd]pyrene

23
benzo[ghi]perylene

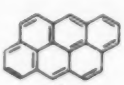

24
anthanthrene

25
coronene

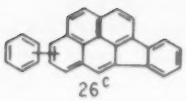

26[c]

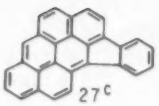

27[c]

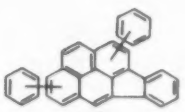

28[c]

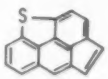

29[d]

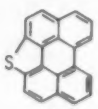

30[d]

31[d]

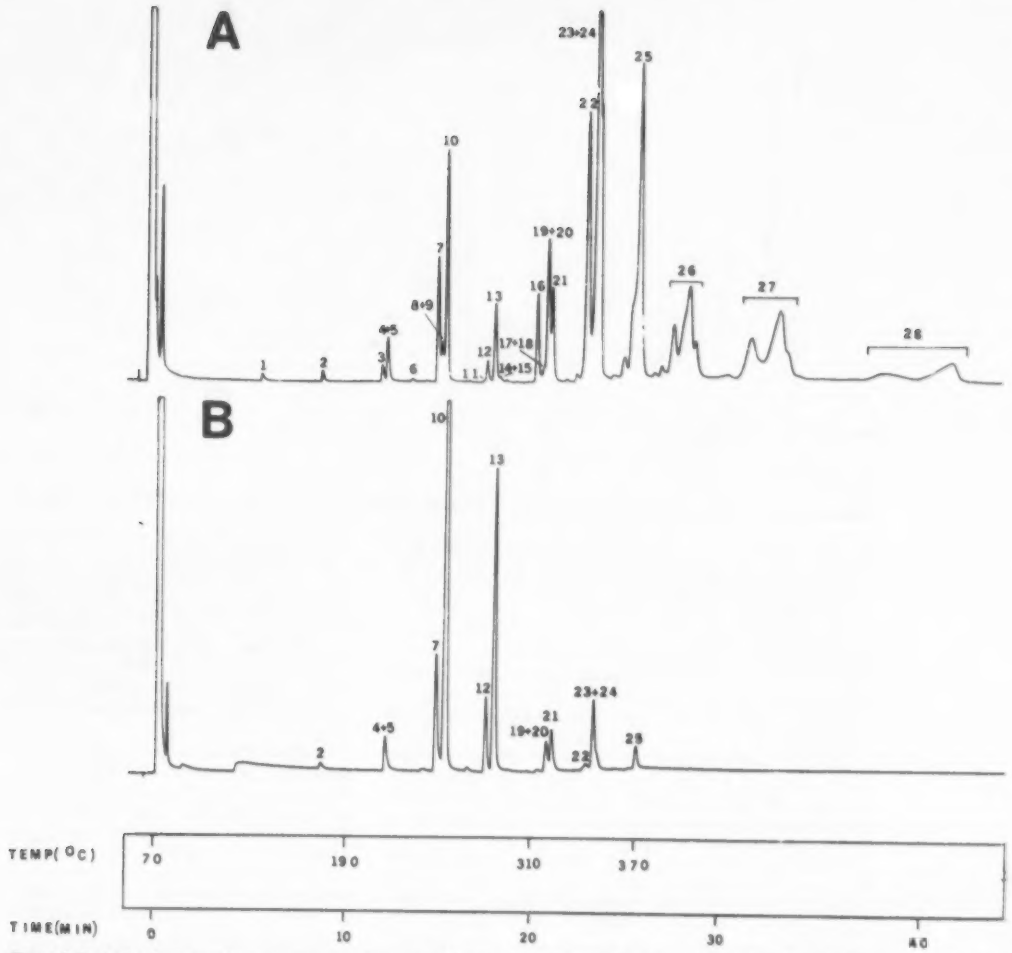

Figure 2. Packed-column gas chromatograms of the extract of (*A*) furnace black 1 and (*B*) furnace black 3 (see Table I). GC conditions: See text. Key: See Figure 1

Table I. Carbon Black Characteristics

No.	Feedstock	Furnace temp, K	Particle size, nm	Weight of carbon black extracted, g	Yield of PAH, %
1	Ethylene tar	1400–1600	260	8	0.2
2	Refinery tar	1400–1600	75	2	0.1
3	Natural gas	1400–1600	75	2	0.1
4	Ethylene and refinery tars	1800–2000	30	34	0.01

vacuum prior to gas chromatographic analysis. The total yield of PAH from the four carbon blacks is given in Table I.

Gas chromatographic mass spectrometry of each sample was performed on a Hewlett-Packard 5982A GC/MS system interfaced to a HP 5933A data system. A 19 m × 0.26 mm i.d. glass capillary column coated with SE-52 methylphenylsilicone stationary phase was used to separate mixtures prior to mass spectral analysis. The oven temperature was programmed from 70 to 250 °C at 2 °C/min during each chromatographic run. High-temperature gas chromatograms were run on a HP 5720A gas chromatograph with a 180 cm × 0.32 cm o.d. stainless steel column packed with 3% Dexsil 300 on 80/100 mesh Chromosorb W which was programmed from 70 to 370 °C at 12 °C/min with a carrier gas flow rate of 25 ml/min.

High resolution mass spectral information was obtained on each sample by introducing an aliquot of the methylene chloride extract into a high-resolution mass spectrometer through a direct introduction probe system and slowly vaporizing the sample at a continually increasing temperature while several exposures on a photographic plate were made. After development, the plate was read on a computerized comparator, and the exact masses were converted to elemental compositions. The HRMS system consists of a DuPont Instruments 21-110B mass spectrometer and a D.W. Mann comparator interfaced to an IBM 1802 computer. This system and its operation have been previously described elsewhere (*4*). Both mass spectrometers were operated at 70-eV ionizing energy.

RESULTS AND DISCUSSION

Figure 2 compares packed-column gas chromatograms of extracts from furnace blacks 1 and 3 (see Table I). Peak numbers refer to compounds listed in Figure 1 which were identified by gas chromatographic mass spectrometry and retention data. In all cases where an exact identity is reported,

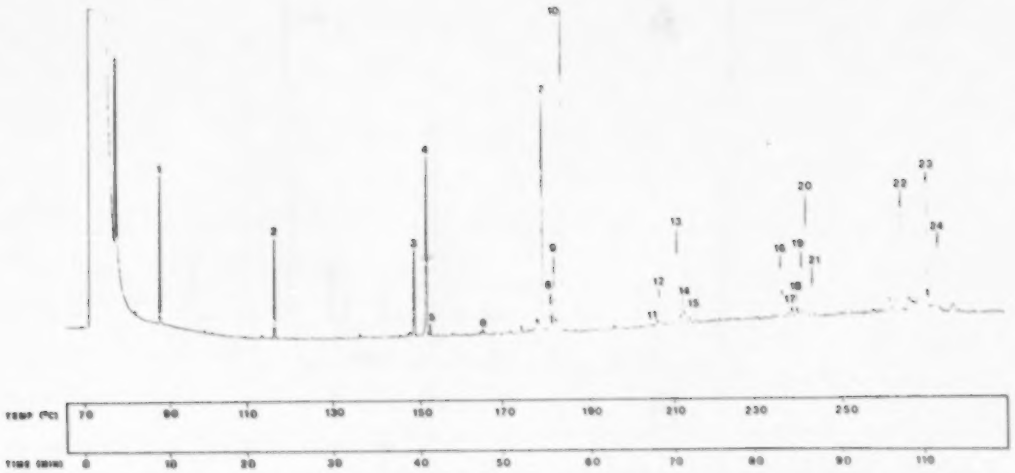

Figure 3. Glass capillary-column gas chromatogram of the extract of furnace black 1 (see Table I). GC conditions: See text. Key: See Figure 1

the mass spectrum and GC retention time were identical with those of authentic materials. The gas chromatograms of extracts from carbon blacks 2 and 4 are very similar to that of carbon black 3 (Figure 2*B*) and are, therefore, not shown.

These GC/MS data, taken together with the PAH yields given in Table I, indicate that the amounts and structures of PAH associated with carbon blacks are quite dependent on the conditions of carbon black formation. Wallcave et al. (2) found that of eight carbon blacks examined, cyclopenta[*cd*]-pyrene was not detected in three of them and varied considerably in concentration in the others. Of the four furnace blacks analyzed in this study, the organic composition of number 1 differed substantially from the other three, which were qualitatively quite similar to one another. Furnace black 1 was manufactured by a different process than 2 and 3, although furnace temperatures were the same. In addition, the higher furnace temperature used in the production of number 4 seemed to reduce the total amount of PAH by a factor of ten as compared to the others, although the qualitative distribution of PAH was still very similar to 2 and 3. The main difference in the manufacture of 2 and 3 was the nature of the feedstock used.

A high-resolution gas chromatogram of the extract of furnace black 1 is shown in Figure 3. Again, numbers refer to compounds identified and listed in Figure 1. In addition to the identification of a number of previously unresolved isomers and trace compounds, four sulfur-containing polycyclic aromatic compounds were detected. However, because of the unavailability of standard compounds, exact identification of only dibenzothiophene and benzo[*a*]dibenzothiophene could be made. On the other hand, proposed structures (see Figure 1) seem to be reasonable when compared to structures of PAH identified in the same mixture. For example, although there are a number of possible structures for $C_{14}H_8S$, the similarity in the structures of benzo[*def*]dibenzothiophene and pyrene and the closeness in chromatographic retention of both compounds give strength to the proposed assignment. Furthermore, in the pyrosynthesis of benzo[*def*]dibenzothiophene, a sulfur bridge could be added across the 4 and 5 positions in phenanthrene analogous to the addition of a methylene goup or an ethylene group to form 4-*H*-cyclopenta[*def*]phenanthene or pyrene, respectively.

Verification of the presence of these four sulfur polycyclics and detection of an additional three (Figure 1; numbers 29–31) were accomplished by high-resolution mass spectrometry as previously described. Again, proposed structures were derived from related hydrocarbons present in the fraction. The absence of sulfur compounds in the carbon black produced from natural gas (see Figure 2*B*) as compared to their detection in all carbon blacks produced from sulfur-containing feedstocks indicates that organic sulfur persists in the combustion of sulfur-containing petroleum feedstocks and appears as stable sulfur polycyclic compounds associated with the carbon black product.

The carcinogenic activity of a particular compound is very dependent on its structure. Shape, size, electronic, and steric factors all seem to be important. For example, the addition of alkyl substituent groups in different positions on the ring of certain PAH can either have an activating or deactivating influence (5, 6). Similarly, the substitution of a sulfur for an ethylene group in a ring may increase or decrease the carcinogenic activity of that particular compound (7, 8). These considerations, coupled with the recent identification of many sulfur-containing polycyclics in air particulate matter (9), clearly indicate that information about these compounds must be included in future studies concerning the environmental hazards of carbon black.

ACKNOWLEDGMENT

We thank Cabot Corporation, Boston, Mass., for supplying samples of various carbon blacks and for providing some of the information given in Table I.

LITERATURE CITED

(1) *Chem. Eng. News*, April 5, 1976, p 8.
(2) L. Wallcave, D. L. Nagel, J. W. Smith, and R. D. Waniska, *Environ. Sci. Technol.*, **9**, 143 (1975).
(3) A. Gold, *Anal. Chem.*, **47**, 1469 (1975).
(4) K. Biemann in "Application of Computer Techniques in Chemical Research", Institute of Petroleum, London, 1972, pp 5–19.
(5) R. Schoental, in "Polycyclic Hydrocarbons", E. Clar, Ed., Academic Press, London, 1964, p 133.
(6) D. Hoffmann, W. E. Bondinell, and E. L. Wynder, *Science*, **183**, 215 (1974).
(7) B. D. Tilak, *Tetrahedron*, **9**, 76 (1960).
(8) E. Campaigne, D. R. Knapp, E. S. Neiss, and T. R. Bosin, *Adv. Drug Res.*, **5**, 1 (1970).
(9) M. L. Lee, M. Novotny, and K. D. Bartle, *Anal. Chem.*, **48**, 1566 (1976).

RECEIVED for review May 26, 1976. Accepted July 19, 1976. This work was supported by Grant R803242 from the U.S. Environmental Protection Agency.

APPENDIX H

Cyano-Aromatic Compounds by the Combustion of Nitrogen Containing Fuels

NTIS is authorized to reproduce and sell this report. Permission for further reproduction must be obtained from the copyright proprietor.

Reprinted from ENVIRONMENT SCIENCE & TECHNOLOGY, Vol. 12, Page 965, August 1978
Copyright © 1978 by the American Chemical Society and reprinted by permission of the copyright owner

Cyano-arenes Produced by Combustion of Nitrogen-Containing Fuels

George R. Dubay and Ronald A. Hites*

Department of Chemical Engineering, Massachusetts Institute of Technology, Cambridge, Mass. 02139

■ Cyanonaphthalenes (both isomers) and cyanoacenaphthylenes (four isomers) were identified in the soot generated by the combustion of aromatic hydrocarbon fuels doped with 6–30% pyridine. These were by far the most abundant nitrogen-containing organic compounds in this combustion effluent; multiring, nitrogen heterocyclic compounds, such as those commonly observed in airborne particulate matter, were a minor component. These identifications were made by gas chromatographic mass spectrometry following a preliminary separation by alumina column chromatography. The environmental significance of these findings is discussed.

Certain organic compounds in soot cause cancer in man (*1*). Determining the structures of these compounds and understanding their biological activities have been the subjects of intense research over the last 50 years (*2*). It is now known that the major class of carcinogenic compounds associated with soot is the polycyclic aromatic hydrocarbons (PAH) (*3*). Nitrogen-containing aromatic compounds (aza-arenes) are also associated with soot (*4*), and some are known to be carcinogenic (*5*). However, because they are much less abundant than PAH, these compounds have received proportionately less attention. In the future, however, it is likely that the environmental abundance of aza-arenes will increase as fuels higher in organic nitrogen content are burned. We have, therefore, undertaken the identification of the major aza-arenes produced by the combustion of a model fuel containing 1–3% nitrogen.

Several researchers have developed methods for the analysis of aza-arenes in atmospheric particulate samples based on thin-layer, gas, paper, high-pressure liquid, and column chromatography and on electrophoresis (*6–10*). All of these techniques begin with a solvent-solvent extraction utilizing strong acid to partition the basic aza-arenes away from the PAH. This procedure obviously discriminates against neutral aza-arenes that might be present. To avoid this problem, we have separated the aza-arenes from the bulk of the PAH by alumina chromatography using gradient elution.

Once the compounds are separated from the PAH, the identification of the exact molecular structures of aza-arenes is still very difficult. Almost all assignments made in the literature are, to some degree, ambiguous. Assignments have been based on gas chromatographic retention information and on fluorescence, UV, or electron impact mass spectra (*6–10*). In these analyses, all the possible isomers of a particular molecular structure have not been available. Hence, by use of these techniques, there is no criterion by which the unavailable isomers can be ruled out.

To address the problem of determining the precise molecular structure of compounds produced by combustion, we have

developed a method based on charge exchange-chemical ionization mass spectrometry (CE/CIMS). We have established that isomeric PAH and aza-arenes have characteristic mass spectra when 5 or 10% methane in argon is employed as the reagent gas for CE/CIMS (*11, 12*). The two most prominent ions in the reacting plasma are $C_2H_5^+$ and Ar^+. A molecule reacts either with a strongly acidic $C_2H_5^+$ ion to give the protonated molecular ion (M + 1), or it reacts with an Ar^+ ion to give the molecular ion (M). The relative rates of these two reactions determine the intensity ratio of the two ions. A high, positive correlation was found between ionization potential and M + 1/M ratio (*11*). We have also established that this relationship holds for some aza-arenes and for some methylated PAH (*12*). Aza-arenes that have ionization potentials differing by more than 0.1 eV can be distinguished using this method.

The great potential of this technique lies in its predictive ability. The relationship between ionization potentials and M + 1/M intensity ratios can be established for all available isomers. Calculation of ionization potentials from molecular orbital theory will then allow prediction of the M + 1/M ratio for unavailable isomers.

Experimental

Combustion Conditions. Soot was obtained in two ways:

A solution of 32% pyridine in *o*-xylene (6% fuel nitrogen) was burned in a wick-fed, alcohol-lamp burner. Soot was collected on the exterior of a precleaned, water-cooled, filter flask. The soot was removed by scrubbing the flask with CH_2Cl_2-soaked glass wool. The soot, glass wool, and associated CH_2Cl_2 were put in a preextracted Soxhlet thimble and extracted with 200 mL CH_2Cl_2 overnight. The extract volume was reduced to 1 mL on a rotary evaporator operating at 30 °C and 15 torr. Samples were stored in the dark at 6 °C.

A Meker burner was modified by replacing the air inlets with oxygen feeds. The fuel inlet was attached to a stainless steel tube through which a benzene-methane mixture was passed. The fuel mixture was preheated to vaporize the benzene, and the plumbing was heated (300 °C) to prevent condensation. Methane and O_2 flows were maintained by critical orifices, and the benzene flow was measured before vaporization by passing the liquid through a capillary tube in which the upstream and downstream pressures were carefully measured. The liquid flows corresponded to Reynold's numbers of 800–1000 through the capillary tube. Thus, the flow was always laminar and proportional to the pressure drop through the tube. The benzene was doped with sufficient pyridine (5.3%) to give a fuel containing 1% nitrogen. Fuel equivalence ratios of 4.0 and 4.5 were used, the CH_4/C_6H_6 ratio was 1.5, and the cold gas velocity was 31.8 cm/s. Soot was collected by a water-cooled spray probe (*13*) and was trapped in glass wool packed filters. The organic compounds were extracted first with acetone and then with CH_2Cl_2.

Column Chromatography. To eliminate interferences caused by PAH and to obtain an enrichment of the nitrogen compounds, the soot extracts were fractionated as follows: The sample (1 mL) was added to 1 g of neutral alumina (activity grade 1, ICN Pharmaceuticals) in a 25-mL beaker, and the CH_2Cl_2 was allowed to evaporate at room temperature (15 min). This precoated alumina was added to the top of a column prepared from 5 g of alumina with hexane as the solvent. Six fractions were then eluted (Table I). These fractions were then concentrated on a rotary evaporator for analysis.

Instrumentation. A Hewlett-Packard 5730A gas chromatograph equipped with dual nitrogen–phosphorus flame ionization detectors (FID) was used for GC analyses. A Hewlett-Packard 5982A mass spectrometer interfaced to a 5933A data system was utilized for gas chromatographic mass spectrometry. Charge exchange-chemical ionization mass spectrometry was performed with 5% methane in argon (supplied by Matheson Gas Products). The flow of carrier gas was 10 mL/min, and the ion source temperature was 195 ± 2 °C. The ratios of the protonated molecular ion to the molecular ion were established by adding all spectra scanned within a given GC peak.

Results and Discussion

The two different combustion systems gave virtually identical results; therefore, they will not be distinguished in the following discussion. As indicated in Table I, all of the aza-arenes were collected in fractions 3 and 4. The gas chromatogram of fraction 4 was extremely complex. Because this fraction contained less than a third of the aza-arenes and because the identities of most of the components in this fraction corresponded to those reported elsewhere (*10*), further analyses of this fraction have not been pursued.

Fraction 3 contained most of the aza-arenes; gas chromatograms of this fraction are shown in Figure 1. The upper trace was obtained with a normal FID, and the lower with a nitrogen specific FID. Comparison of these two traces show that the nitrogen-FID and the normal FID respond equally to the early eluting peaks, indicating that nitrogen is present in all of these constituents. The later eluting peaks were detected only by the normal FID, indicating that they are probably PAH.

The electron impact and CE/CI mass spectra of peaks 1–7 are given in Table II. The spectra of peak 1 were interpreted as those of either 1- or 2-cyanonaphthalene, and authentic samples of these two compounds were obtained (K and K Laboratories). The exact retention time (by coinjection) and the electron impact and CE/CI mass spectra of 1-cyanonaphthalene were identical with those of peak 1. The identification of peak 2 as 2-cyanonaphthalene was proved in a similar fashion.

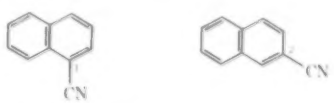

Peaks 3–6 all show molecular weights of 177 ($C_{13}H_7N$) (see Table II). Based on analogy and on the abundant presence of the parent hydrocarbon, these peaks have been tentatively identified as the four isomers of cyanoacenaphthylene.

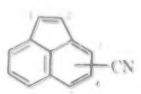

Table I. Fractionation of Soot Extracts

Fraction	Solvent	Vol (mL)	% PAH[a]	% Aza-arene[a]
1	Hexane	30	0	0
2	30% Benzene, 70% hexane	30	64	0
3	70% Benzene, 30% hexane	30	12	15
4	Benzene	30	2	7
5	Benzene	50	0	0
6	CH_2Cl_2	50	0	0
		Total	78	22

[a] Percent of total material in the various fractions as measured from the normal FID or nitrogen-specific FID responses, respectively.

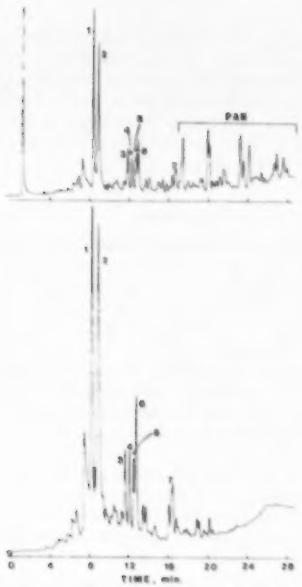

Figure 1. Gas chromatograms of fraction 3, isolated from organic compounds produced by combustion of solution of 32% pyridine in *o*-xylene

GC conditions: 1.8 m × 6.3 mm o.d. glass column packed with 3% OV-17 on 80/100 mesh Supelcoport, programmed from 100 to 310 °C at 8 °C/min. Upper trace obtained with normal FID, bottom trace with nitrogen specific FID

These are not available compounds, and proof of their structure must await their synthesis. Peak 7 has a molecular weight of 203 ($C_{15}H_9N$) and probably represents several unresolved cyanophenanthrene isomers.

Based on the GC data, we estimate that 80% of the azaarenes in fraction 3 are cyanonaphthalenes, cyanoacenaphthylenes, and cyanophenanthrenes. These compounds are the most abundant class of organic nitrogen compounds in the effluent from these flames. Multiring, nitrogen heterocyclic compounds (such as acridine or phenanthridine) that have been commonly observed in airborne particulate matter (*10*) are a minor component (<7%) in these effluents.

Cyanonaphthalenes have not been found in combustion effluents before. They have, however, been found at trace levels in cigarette smoke tar (*14, 15*), in petroleum (*16*), in tar from the low-temperature pyrolysis of coal (*17*), and in anthracene oil (*18*). In all of these cases, it is presumed that cyanonaphthalenes are formed from the pyrolysis of other nitrogen compounds (*19*). The biological activity of these compounds is not clear. There have been reports that cyanonaphthalenes cause irregular mitoses and chromosomal aberrations (*14, 20*), that they have insecticidal properties (*21, 22*), and that they are toxic to the eggs of body lice (*23*). On the other hand, testing by a quantitative forward mutation assay using 8-azaguanine resistance in *Salmonella typhimurium* (*24*) indicates that these compounds have less than 1% of the activity of benzo[*a*]pyrene on a molar basis (*25*).

The environmental significance of our results is twofold. (*a*) The relative amount of cyano-arenes being produced by the combustion of a nitrogen containing fuel is significant (see Table I), and some of these compounds *may* be biologically active. Emission of large amounts of such compounds into the environment would seem to be undesirable. (*b*) Although several cyano-arenes are being produced in flames, it is not known if they are environmentally persistent. Nitrogen functional group analyses by ESCA have indicated the presence of the cyano functionality in certain urban air particulate samples (*26*), but specific cyano-arenes have not been found in the atmospheric environment. Cyano-arenes may well be present in air particulates, but because of the analytical limitations outlined above, they have not yet been detected. We suggest that the quantity (if any) of cyano-arenes in the ambient air environment should be measured using techniques designed for these compounds. Cyano-arenes may be more prevalent than the multiring, nitrogen heterocyclic compounds studied in the past, and their environmental chemistry and toxicity may warrant at least equal attention.

Table II. Mass Spectra of Peaks 1–7 in EI (Top) and CE/CI (Bottom) Modes

	Peak 1		2		3		4		5		6		7	
	m/e	Int	m/e	Int	m/e	Int	m/e	Int	m/e	Int	m/e	Int	m/e	Int
M + 1	154	13	154	13	178	15	178	16	178	18	178	19	204	22
M	153	100	153	100	177	100	177	100	177	100	177	100	203	100
M − H	152	7	152	8	176	15	176	8	176	11	176	11	202	13
M − CN	127	5	127	5	151	9	151	6	151	4	151	4	177	6
M − HCN	126	17	126	15	150	18	150	15	150	13	150	18	176	10
Others	125	4	125	3	179	5	179	7	179	4	179	4	201	13
					175	6	175	4	175	7	175	6	175	7
					149	4	149	6	149	7	149	3	151	6
M	153	38	153	40	177	41	177	45	177	38	177	42	203	46
M + H	154	100	154	100	178	100	178	100	178	100	178	100	204	100
M + 2	155	15	155	14	179	25	179	18	179	17	179	16	205	17
M + CH_3	168	9	168	9	192	6	192	8	192	13	192	16	218	11
M + C_2H_5	182	35	182	37	206	34	206	40	206	45	206	44	232	41
M + 30	183	6	183	5	207	14	207	8	207	11	207	11	233	9
Others	156	6	156	3	180	14	180	9	180	10	180	8	206	10
					208	6	208	6	208	3	208	5	234	5
M + 1/M[a]	2.63		2.37		2.33		2.10		2.49		2.27		2.01	

[a] Corrected for ^{13}C.

Acknowledgment

The authors thank Jack B. Howard and William J. Kausch, Jr., for the design and operation of the second burner system.

Literature Cited

(1) Pott, P., "Chirugical Observations", p 63, Hawkes, Clarke, and Collins, London, England, 1775.
(2) National Academy of Sciences, "Particulate Polycyclic Organic Matter", Washington, D.C., 1972.
(3) Hoffmann, D., Wynder, E. L., in "Chemical Carcinogens", C. E. Searle, Ed., pp 324–65, Amer. Chem. Soc. Monograph 173, Washington, D.C., 1976.
(4) Sawicki, E., McPherson, S. P., Stanley, T. W., Meeker, J., Elbert, W. C., *Int. J. Air Water Pollut.*, **9**, 515 (1965).
(5) Dipple, A., in "Chemical Carcinogens", C. E. Searle, Ed., pp 245–314, Amer. Chem. Soc. Monograph 173, Washington, D.C., 1976.
(6) Sawicki, E., Stanley, T. W., McPherson, S., Morgan, M., *Talanta*, **13**, 619 (1966).
(7) Sawicki, E., Guyer, M., Engel, C. R., *J. Chromatogr.*, **30**, 522 (1967).
(8) Engel, C. R., Sawicki, E., *ibid.*, **31**, 109 (1967).
(9) Cautreells, W., van Cauwenberghe, K., *Atmos. Environ.*, **10**, 447 (1976).
(10) Dong, M. W., Locke, D. C., Hoffmann, D., *Environ. Sci. Technol.*, **11**, 612 (1977).
(11) Lee, M. L., Hites, R. A., *J. Am. Chem. Soc.*, **99**, 2008 (1977).
(12) Hites, R. A., Dubay, G. R., in "Carcinogenesis", P. W. Jones, Ed., Vol III, pp 85–7, Raven Press, New York, N.Y., 1978.
(13) Prado, G. P., Lee, M. L., Hites, R. A., Hoult, D. P., Howard, J. B., Sixteenth (Int.) Symp. on Combustion, pp 649–61, Combustion Institute, Pittsburgh, Pa. 1977.
(14) Izard, C., Moree-Testa, P., *CR Acad. Sci., Ser. D*, **272**, 2581 (1971); *Chem. Abstr.*, **75**, 61573j.
(15) Benner, J., Keene, C. K., Holt, T. W., in 4th Tobacco and Health Workshop Conf. Proc., pp 408–20, Univ. of Kentucky, Lexington, Ky., 1973; *Chem. Abstr.*, **79**, 89669b.
(16) Hartung, G. K., Jewell, D. M., *Anal. Chem. Acta*, **27**, 219 (1962).
(17) Andre, J., Dath, P., Mahieu, J., Grand'Ry, E. H., *Brennst. Chem.*, **48**, 369 (1967); *Chem. Abstr.*, **68**, 31869y.
(18) Proksch, E., *Oesterr. Chem. Ztg.*, **67**, 105 (1966); *Chem. Abstr.*, **64**, 19251g.
(19) Patterson, J. M., Haidar, N. F., Smith, Jr., W. T., *Chem. Ind.* (London), **1975**, p 128.
(20) Bhalla, P. R., Arnold, R. C., Sabharwal, P. S., *J. Hered.*, **65**, 311 (1974).
(21) Swingle, M. C., Mayer, E. L., Gahan, J. B., *J. Econ. Entomol.*, **37**, 672 (1944); *Chem. Abstr.*, **39**, 764(6).
(22) Mayer, E. L., Robertson, C., Nelson, R. H., Woodward, C. F., *Bur. Entomol. Plant Quarantine*, E-836 (1952); *Chem. Abstr.*, **46**, 5251a.
(23) Eddy, G. W., Carson, N. B., *J. Econ. Entomol.*, **41**, 31 (1948); *Chem. Abstr.*, **42**, 5156g.
(24) Skopek, T. R., Liber, H. L., Krolewski, J. J., Thilly, W. G., *Proc. Nat. Acad. Sci.*, **75**, 410 (1978).
(25) Kaden, D. A., Thilly, W. G., Massachusetts Institute of Technology, Cambridge, Mass., private communication, 1977.
(26) Chang, S. G., Novakov, T., *Atmos. Environ.*, **9**, 495 (1975).

Received for review November 23, 1977. Accepted February 24, 1978. Work supported by the Environmental Protection Agency (Grant R803242) and the Department of Energy (Grant EE-77-S-02-4267).